DECIMATION TESTING OF HIGH DENSITY SEISMIC DATA FOR THE WICHITA MOUNTAIN FRONT AREA

By

ERIC MATTHEW GERDING

Bachelor of Science in Geology

Wright State University

Dayton, Ohio

2004

Submitted to the Faculty of the
Graduate College of the
Oklahoma State University
in partial fulfillment of
the requirements for
the Degree of
MASTER OF SCIENCE
May, 2007

DECIMATION TESTING OF HIGH DENSITY SEISMIC

DATA FOR THE WICHITA MOUNTAIN FRONT AREA

Thesis Approved:

Dr. Surinder Sahai

Thesis Adviser

Dr. William Coffey

Dr. Anna Cruse

Dr. Alexander Simms

Dr. A. Gordon Emslie

Dean of the Graduate College

ACKNOWLEDMENTS

This section could not express the amount of gratitude that I have for all those who dedicated their time, energy, and talents to this thesis.

I wish to first thank my advisor Dr. Surinder Sahai. He managed to always clear up any confusion that I may have had with a clean sheet of paper and willingness to teach. His passion for the science and confidence in me supplied the perfect foundation. I also want to thank the rest of my committee, Dr. Bill Coffey, Dr. Anna Cruse, and Dr. Alexander Simms because their timing, support, and encouragement were impeccable. Their general overview on this project and life always seemed to put things in perspective.

I would like to than Petroleum Geosciences for their permission to present the seismic data used.

I wish to thank Devon Energy Corporation for the availability to the data and resources that made this project possible. Many thanks go to the people within Devon who have also played a vital role in the completion of this thesis. To Dr. Bill Coffey, Dale Fritz, and David O'Bright for their persuasive and persistent encouragement (demand!) to finish this project. I feel fortunate for the time that is spent with them to not only learn how to do something but why we do it. To Rick Coleman, Priscella Eddy, John Spaid, William Talley, and Jim White who all willingly provided assistance whenever it was needed. To David Deering who saved me from what could only be described as a Pandora's Box of formatting issues.

I would like to give special thanks to Patrick Kamann and Jim Hager. Patrick provided his outstanding guidance and friendship throughout the project. While Jim gave an incredible amount of time and effort that insured the study would be a success. His energy, passion, and positive attitude made the project enjoyable on a daily basis.

Finally to my remarkable family who provided me with every opportunity a son, little brother, and husband could ask for. I feel incredibly blessed to have each of them in my life. To my parents who made countless sacrifices to make my life better. Our relationship is exactly what I want with Amy and my future children. To my siblings, Veronica, Angie, Brad, and Andy thank you for the amazing support you have given me. They have always made me feel like an athlete with home field advantage because I hear their cheers at my triumph and boo's at anything that would oppose my victory. Then to my wife, Amy, who is my perfect complement. Every hole is filled with her by my side.

TABLE OF CONTENTS

Chapter Page

I. INTRODUCTION 1

Location 2
Purpose and Scope 2
Background Geology 8
Methods 10
Previous Investigations 13

II. SEISMIC PARAMETERS 17

Recorded Seismic 17
Decimated Seismic 18
Synthetic Seismogram 20

III. COMPARING THE PROCESSING OF DECIMATED VOLUMES 23

Survey Layout 24
Fold 26
Statics 42
Velocity Analysis 48

IV. COMPARISONS OF FINAL DECIMATED IMAGES 62

Empirical Observations – Cross Sections 62
Flex Binning 68
Empirical Observations – Time Slices 78
Difference Volumes 86
Amplitude Maps 93
Synthetic Tie 104

V. CONCLUSION 115

Future Investigations 117

REFERENCES 119

LIST OF FIGURES

Figure Page

1. Location map of study area 3
2. Generalized comparison of 2D to 3D data 5
3. Geologic provinces and basement map 6
4. Isopach of Timbered Hills/Arbuckle Groups and Oklahoma Basin Outline 7
5. Stratigraphic column 11
6. Acquisition geometry 25
7. Reference volume fold plot with all offsets 27
8. Reference volume fold plot with offset up to 5000' 29
9. Reference volume fold plot with offset up to 15000' 30
10. Decimated receiver fold plot with all offsets 32
11. Decimated shot fold plot with alls offsets 33
12. Decimated receiver fold plot with offset up to 5000' 35
13. Decimated shot fold plot with offset up to 5000' 36
14. Decimated receiver fold plot with offset up to 15000' 37
15. Decimated shot fold plot with offset up to 15000' 38
16. Decimated shot and receiver fold plot with all offsets 39
17. Decimated shot and receiver fold plot with offset up to 5000' 40
18. Decimated shot and receiver fold plot with offset up to 15000' 41

19. General static model 43
20. Static solution 46
21. Decimated receiver volume with different static corrections 47
22. Reference semblance plot with gathers 52
23. Decimated receiver semblance plot with gathers 53
24. Decimated shot semblance plot with gathers 54
25. Decimated shot and receiver semblance with gathers 55
26. Reference constant velocity stacks 57
27. Decimated receiver constant velocity stacks 58
28. Decimated shot constant velocity stacks 59
29. Decimated shot and receiver constant velocity stacks 60
30. Seismic line location map 63
31. In line shallow section extract for all volumes 65
32. In line medium section extract for all volumes 66
33. In line deep section extract for all volumes 67
34. In line deepest section extract for all volumes 69
35. Cross line shallow section extract for all volumes 70
36. In line section before flex binning on decimated receiver 71
37. In line section after flex binning on decimated receiver 72
38. Cross line section before flex binning on decimated receiver 74
39. Cross line section after flex binning on decimated receiver 75
40. Time slice before and after flex binning 76
41. Arbitrary line through feature of interest 77

42. Time slice at 1000 ms for all volumes 79
43. Time slice at 1000 ms for all volumes with interpretation 80
44. Time slice at 3500 ms for all volumes 82
45. Time slice at 3500 ms for all volumes with interpretation 83
46. Time slice at 4800 ms for all volumes 84
47. Time slice at 4800 ms for all volumes with interpretation 85
48. Difference volume (reference – decimated receiver) in line section 88
49. Difference volume (reference – decimated receiver) cross line section 89
50. Difference volume (reference – decimated shot) in line section 91
51. Difference volume (reference – decimated shot) cross line section 92
52. Difference volume (shot – decimated receiver) in line section 94
53. Difference volume (shot – decimated receiver) cross line section 95
54. Difference volume (reference – decimated shot and receiver) in line section 96
55. Difference volume (reference – decimated shot and receiver) cross line section . 97
56. Amplitude maps of Horizon 1 all volumes 100
57. Amplitude maps of Horizon 2 all volumes 101
58. Amplitude maps of Horizon 3 all volumes 102
59. Synthetic tie in line section (reference) 106
60. Synthetic tie in line section (decimated receiver) 107
61. Synthetic tie in line section (decimated shot) 108
62. Synthetic tie in line section (decimated shot and receiver) 109
63. Synthetic tie cross line section (reference) 110
64. Synthetic tie cross line section (decimated receiver) 111

65. Synthetic tie cross line section (decimated shot)..... 112

66. Synthetic tie cross line section (decimated shot and receiver)..... 113

67. Synthetic tie enlargement with electric logs 114

LIST OF PLATES

Plate Page

1. In-line cross-section for all volumes ..... In Pocket

2. Cross-line cross-section for all volumes ..... In Pocket

CHAPTER I

INTRODUCTION

Oklahoma has a rich history of oil and gas exploration and production. In 2004, production rankings placed Oklahoma 6th in crude oil and 2nd in natural gas (EIA, 2006). A large portion of natural gas production comes from the Anadarko Basin and associated shelf area. Several fields in this area have produced over one trillion cubic feet of natural gas. These fields, as well as many others were discovered in the early 20th century but were underappreciated at that time due to the low demand for natural gas. It wasn't until the establishment of roads, pipeline, and the deregulation of natural gas in the mid-1970s that these fields would draw much interest. In the Anadarko Basin, sediments range from Cambrian to Permian in age and account for well over 30,000 feet thick in the basinal axis. Due to these very large accumulations of sediment, plays are being made in stratigraphic and structural traps as well as in some unconventional plays. Here in this thesis in particular the term unconventional refers mainly to low permeability (tight) sandstone reservoirs. Though the area has been explored for decades, there remains a large potential in the deeper sediments below 15,000 feet. Along with the potential for these deeper reservoirs is the continued development of the "wash" plays directly related to orogeny and erosion of the Wichita Mountains.

Location

This study is focuses on a 3D seismic reflection survey on the north side of the Amarillo-Wichita Uplift where it merges with the Anadarko Basin in southwest Oklahoma (Figure 1). Due to the proprietary nature of the data, the exact location of the study is not indicated in the figure. Seismic interest in the Wichita Mountain Front area has been ongoing for many years. Covering the area from Grady and Stephens counties in the south to Roger Mills and Beckham counties in the west. The mountain front region as a whole as well as all seismic data, extends beyond these limits, but the limits of this study are within this region (Figure 1).

Purpose and Scope

This study is primarily concerned with mountain front development and investigates the quality of seismic data available to geoscientists. The main objective of this study is to evaluate the effect of decimation on a previously collected high trace density survey. Decimation is the practice of systematically resampling the data to reduce the number of samples used (Sheriff, 2002). The method of removing traces is done so in a manner to simulate different acquisition parameters, such as in this case source and/or receiver intervals. As is usually the case, decimation is being conducted to prevent over sampling of receiver and source effort, or field effort, in future acquisitions. Since much of the cost results from the amount of receivers and sources deployed during collection this inherently prevents over spending as well. Thus several decimated volumes were created to simulate reduced shots, reduced receivers, and a combination of

Figure 1 – The yellow outline indicates the study area. Background image downloaded from Google Earth (2007)

these. In the case of land 3D surveys sources cost significantly more than the receivers. To observe the effect of reducing field effort a series of tests are run to show a comparative analysis of the data quality and determine what information is lost. It is hypothesized that the amount of degradation and difficulties in processing will be the same for the decimated receiver and the decimated shot volumes. The decimated shot and receiver is expected to exhibit the poorest quality in each of the performed tests.

Decimation is a very cost effective method to determine minimum field effort for multiple reasons. First decimated volumes can be created at a fraction of the cost and time that it would take to actually recollect the data with slightly differing parameters. This eliminates the search for an available seismic crew as well as re-permitting the area. Additionally, decimation establishes better control on the comparison because field conditions remain constant, where weather or the exact location of stations could vary with separate collection dates.

The mountain front region of the Anadarko Basin is known for its complex structure and deep targets. Therefore, seismic imaging in this complex area has been challenging. Due to advances in seismic acquisition and processing in the last two decades, the quality of seismic data has improved considerably. However, due to the increased sampling of data, the cost of acquiring data has also increased tremendously. The first major increase in cost results from the collection of 3D rather than 2D data. In areas such as the Anadarko Basin that have been worked for many decades, the industry demands more information from seismic to unravel the less obvious reservoirs. Figure 2

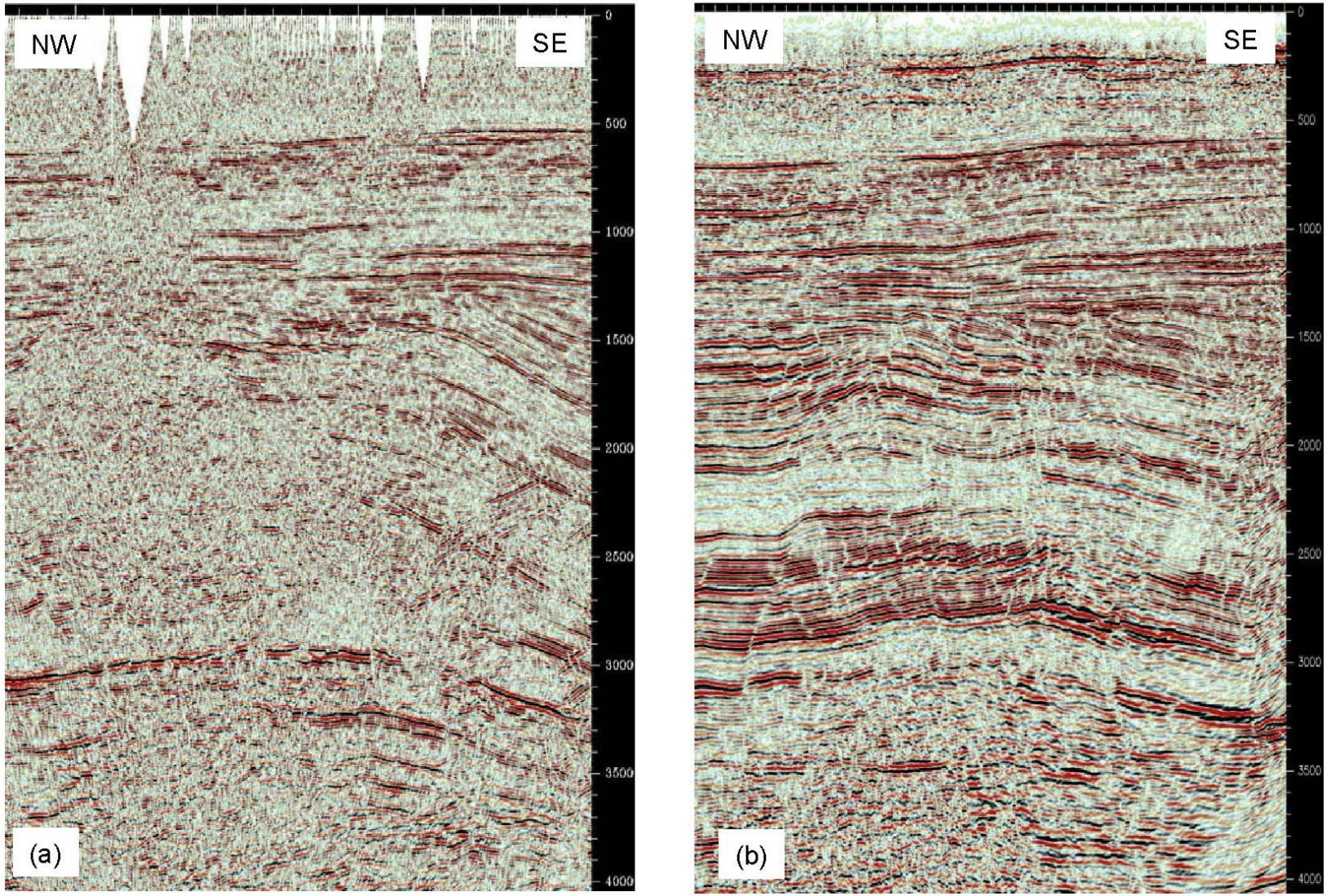

Figure 2 – A 2D line (a) is compared to the same line in 3D (b) to show the improvements in image quality over the past two decades.

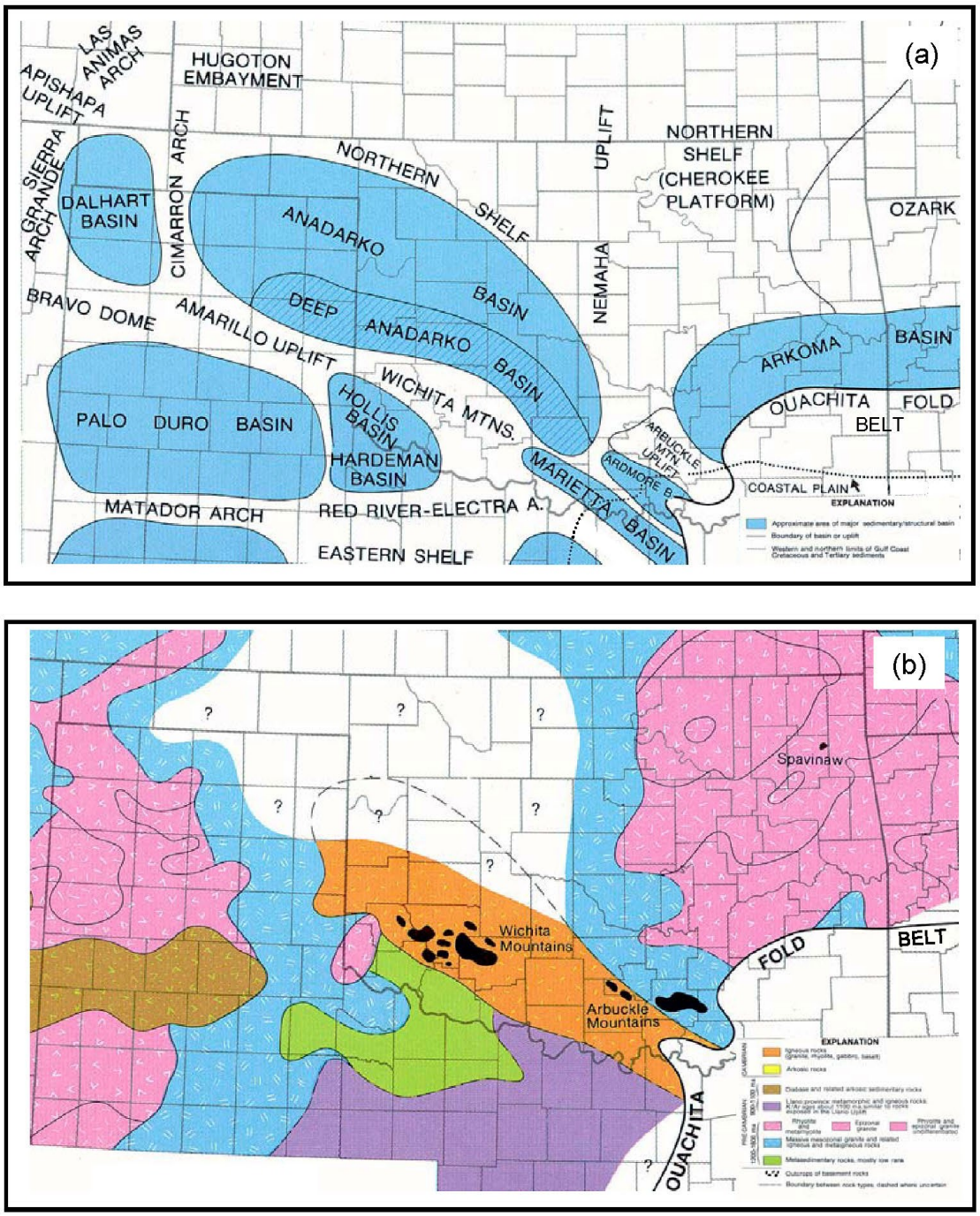

Figure 3 – (a) The major physiographic regions, and (b) generalized basement geology of the southern mid-continent. Figure 3a is from Johnson (1989), and Figure 3b is from Denison (1989).

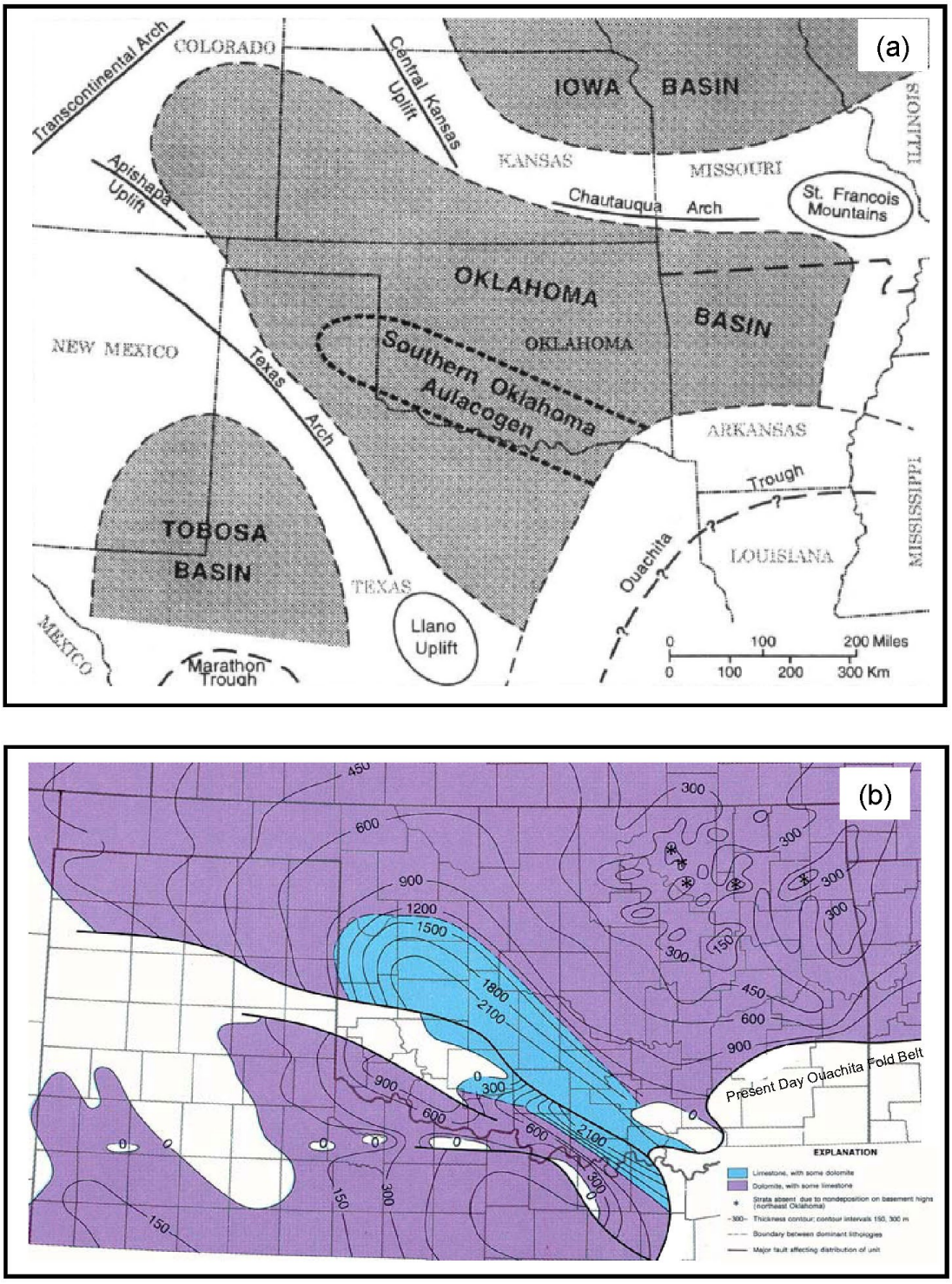

Figure 4 – (a) Map of southwestern United States showing outline of Oklahoma basin and major features that existed in Early and Middle Paleozoic time. (b) Isopach map of the Timbered Hills and Arbuckle Groups. Figure 4a is take from Johnson (1989); Figure 4b is taken from Denison (1989)

llustrates the advantages of 3D and why it is preferred over 2D seismic data. These lines are nearly identical in location but are drastically different in their quality. The ability of 3D to properly place diffracted energy, seen in the 2D image from 2000 – 3000 ms, has resulted in increased resolution which is critical in areas with high fault concentrations such as the mountain front region. Not only does this increase confidence in the structural interpretation, but also allows for a better stratigraphic interpretation. This has become very important in today's understanding for the deposition of the sediments shed from the mountain front known as the "Granite Wash."

Background Geology

The Anadarko Basin, specifically the deeper section adjacent to the Wichita Mountain Front (Figure 3a), contains an extensive geologic record with over 30,000 ft of sediments (Boyd, 2002). The geologic history of the area can be summarized into four tectonic phases; (1) rifting, (2) epeirogenic movement/subsidence, (3) orogenic, and (4) eperiogenic movement/subsidence. These same set of tectonic phases were experienced in many nearby basins where stratigraphies greatly resemble one another.

Rifting began at the end of the Proterozoic Eon and continued into the Early Cambrian with the formation of a triple junction. Two spreading centers of the triple junction successfully opened into the Iapetus Ocean while one arm failed and became the Southern Oklahoma Aulacogen. Part of the aulacogen can be seen on the basement map in Figure 3b by the area representing the Cambrian age igneous rocks. During the Middle Cambrian, the area entered the second phase of major subsidence as the aulacogen cooled causing eperiogenic movements. This broad subsidence allowed an epicontinental sea to flood the area. Massive deposition of siliciclastics and carbonates occurred throughout

the region during this phase. The Anadarko Basin area was part of a larger system called the Oklahoma Basin (Figure 4a). Figure 4b shows the widespread nature of the Timbered Hills and Arbuckle Groups in an isopach, with the thickest accumulations occuring over the Aulacogen during this time. Clastic deposits, such as the Woodford Shale, would also have a chance to be regionally supplied to the basin.

During the Early Devonian to Late Mississippian, the area began its third tectonic phase, of which intense orogenic pulses dominated. These pulses were caused by the closure of the proto-Atlantic Ocean from the southeast. Orogenic activity was limited to folding, faulting, and uplift, and was not accompanied by igneous or metamorphic activity (Johnson et al 1988). Clastics were shed from the uplifted areas, infilling the rapidly subsiding basins. Two principal movements were associated with the deformation: 1) narrow vertical displacement, followed by 2) left lateral strike slip (Evans, 1979). Figure 5 shows the approximate timing of the orogenic movements and age of sediments supplied by the Wichita Mountains referred to as "Granite Wash." Nearly 7,500 meters of Pennsylvanian and Permian sediment accumulated by the end of this phase.

The final phase experienced in the Anadarko Basin is somewhat of tectonic stability with broad subsidence and epeirogenic movements dominating the area. The epicontinental sea remained for some time but large fluctuations in sea level occurred until the Cretaceous when the last marine inundation took place. Low relief in the surrounding area provided little sediment input allowing for increased carbonate deposition compared to orogenic times. Eventually the sea receded and continental sediments became the primary deposition with few exceptions.

Methods

3D seismic reflection data was collected to assess the economic potential of the reservoirs along the mountain front. Well data, seismic data, and advanced software were all provided courtesy of Devon Energy Corporation. The 3D volume was collected using the High Density 3D (HD3D) trademark of Petroleum Geoservices (PGS). High density refers to the tight spacing of source and receiver intervals relative to other 3D surveys collected recently. To understand the value in the increased field effort, a series of decimation tests were used to compare this new collection to traditional 3D standards. Again, decimation in this study refers to the reprocessing of HD3D data to simulate that of a conventionally collected 3D surveys. Decimation will have a direct affect on the either fold or bin size since it is removing the number of traces within the originally defined bin. If the bin size follows the natural bin size then the fold will remain constant. However, if the bin size remains unchanged then the fold will be sacrificed by fifty percent. A variety of methods is used to compare these datasets during and after processing to assess the ease of which the data can be processed and the quality of the image produced.

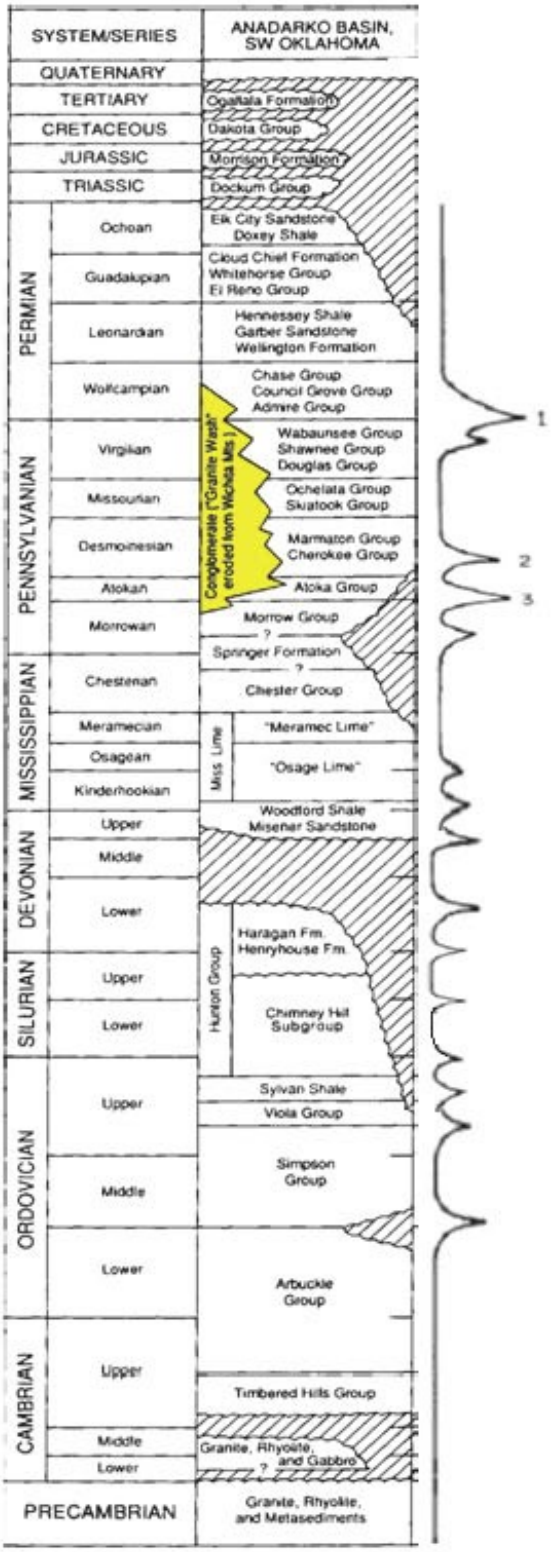

Figure 5 – Stratigraphic column with tectonic pulses from the Anadarko and Wichita Mountain area. (Column modified from Johnson and Cardott, 1992 and pulses modified from Ham and Wilson, 1967)

Creation of the decimated volumes was based off the original volume collected by PGS. A decimated receiver volume simulating acquisition with every other receiver group was created. A decimated shot volume was constructed by removing every other shot point. The last decimated volume was a combination of every other shot point and receiver group removed and called the decimated shot and receiver volume. Finally a reference volume that maintained all shot points and receivers was created. This was done because migration, due to it added expense, was not performed on the decimated volumes. Additionally this volume was needed to compare the ease of processing.

Processing comparisons begin with the reassignment of the field geometry. Using the geometry, an assessment can be made on the fold in each design. Then the correction of residual statics and velocity analysis will be closely monitored. Specifically, the velocity analysis will be compared by velocity spectra, gathers, and constant velocity stacks, to observe if the velocity model changes and/or the difficultly at which the model is built.

Next, tests that relate to the interpretation capability of each dataset will be used to describe there differences. First visual observation of cross sections and time slices are used to evaluate changes in signal characteristics not quantified by software. Then, difference volumes created by subtracting amplitudes of one volume from another are created to quantify changes resulting from the data reduction. Amplitude maps extracted from horizons are also compared between the simulated volumes to specifically observe if anomalous locations shift spatially. Finally a comparison is made evaluating the ability of the seismic to match the geology using a synthetic seismogram. Using these practices

it will be possible to determine which decimated seismic volume allows for the best interpretation of geology.

Collecting high density data can increase acquisition costs by approximately 12 percent. An increase in processing can also be expected due to the quadrupling of traces that would be collected in a traditional layout. In this study these financial concerns are ignored to determine the volume with the best quality image maintained through decimation. This is contrary to real world applications that require a balance between the budget and ideal acquisition parameters to be used.

Previous Investigations

Fold is often regarded as a measure of the data quality but Lansley (2004) took the approach of leaving the fold constant and dramatically reducing the bin size to increase the image quality. The report suggests that using only fold to compare data quality between surveys is not valid unless the bin size is specified. Instead Lansley (2004) proposes using trace density or traces per mile/kilometer as an adequate measure of the data quality. This is done by reducing the source and receiver interval by roughly half in each direction while the fold remains constant. In turn a natural bin size is created that is also halved in both dimensions. The bin size used to be calculated once the survey or the line spacing required to allow ample coverage for shallow reflectors has been determined, many seismic designs relied on Nyquist sampling to decide interval spacing. This is calculated with the highest frequency of interest on the steepest measured reflector dips without any reference to adequate spatial sampling of coherent noise trains, fault planes, and diffraction energy (Lansley 2004). Thus the nyquist sampling interval cannot be relied upon and increased density is believed to improve image quality.

Krey (1987) attempted to determine the required fold for a 3D survey from the analysis of 2D data. This study showed that the same high degree of common depth coverage was not required to achieve the same signal to noise ratio after migration. His calculations were based on the theory that signal within the Fresnel zone is imaged properly during migration and random noises are attenuated. This discussion provides supporting arguments for the importance of trace density mentioned by Lansley (2004). The first point is that fold was calculated for a certain bin size. Thus the fold required is controlled by the number of traces per unit area. Next, signal frequency is directly proportional to the fold. Finally the trace density needs to be calculated for all depths of interest. This will affect the source and receiver line spacings as well as the far offset. As a precaution from using the Krey (1987) investigation to solely determine fold needed, one must consider that the attenuation discussed dealt merely with random noise. Krey (1987) states that the concepts can probably be used on weakly correlated noise but it is believed by others that the noise that we are concerned with is source generated and not random.

Lansley (2004) study compared identical seismic sections with constant fold and different bin sizes using decimation. Again the basic idea of decimation is to degrade a higher sampled dataset by restricting inputs to prevent over sampling in future acquistions. A common way to do this is to remove strategic shot points and/or receiver groups to simulate a new bin size or fold. One of the first decimation tests to be reported was that of Bouska (1995, 1996). Bouska (1996) used decimation to insure the most cost effective means of collecting Sparse 3D. Sparse 3D is a name given by Amoco to a 3D survey that is lower priced than the collection of a comparable 2D line. The goals of

Sparse 3D were to cut costs thereby allowing for greatly increased survey size to assist in exploration. Due to the success of this approach in earlier studies, decimation tests became more popular and are commonly used in the industry today.

While the most common use of decimation tests are in 4D surveys, there is still some use for exploration. Bouska et al (2005) report its cost effectiveness in Azerbaijan, Nolte et al (2004) used it in the North Sea, and Wombell et al (1999) conducted their tests on a United Kingdom survey. Though the results varied for acceptable field effort, the information gained was substantial. These studies contributed methods for which they analyzed the comparison of multiple volumes. Assuming that proprietary reasons restricted publication, these studies still mentioned several methods that are used in this study such as; amplitude maps, difference volumes, S/N estimates, variation with depth, and comparison to well ties.

Commonly in marine 3D collection the fold distribution becomes irregular across the overall survey. In marine surveys trace distribution is easily affected by inclement weather, currents, and obstructions that do not allow for the streamers to cooperate. Although, even land 3D collection in structurally complex regions can experience uneven fold distributions. In the early 1990's work was being done to correct for this irregularity which results in missing data. One method that persists today is a cost effective method referred to as 'flex binning.' In flex binning if a bin is found devoid of a trace it is then expanded until it reaches the optimal number of traces or a maximum expansion is reached. The trace bin interval remains the same but has been populated by outside traces. This results in a slight amount of data smearing. Lu et al. (1996) reported the successful use of this technique on a land and marine example of 3D data. Spitzer et al.

(1998) took this technique further by qualifying its ability to not only redistribute incorrectly placed traces but to duplicate traces. They found a cost effective way of collecting high resolution 3D with the use of 'flex binning.' Instead of using so much source effort to meet fold requirements, the same trace would be allow to contribute to multiple bins.

CHAPTER II

SEISMIC PARAMETERS

In an area that has been as heavily explored and developed as the Anadarko Basin the potential for new plays becomes increasingly difficult to find through time. Seismic data in this area has always played an integral role in assisting geological interpretations. Seismic quality has evolved with improved acquisition and processing methods.

Recorded Seismic

The originally acquired volume is one of many High Density (HD3D) surveys collected by Petroleum Geoservices (PGS) along the Wichita Mountain Front. Collection was done with a Remote Seismic Recorder (RSR) – Telemetry System using primarily a Vibroseis source. Eight vibrators provided frequencies ranging from 8-80 Hz over 20 seconds. Shot and receiver lines were spaced 1320 ft. apart with a station interval spacing of 165 ft. Receiver groups consisted of 12 geophones and the nominal number of channels was roughly 1800. Shot lines were laid out parallel to the mountain front, while receiver lines were perpendicular. Target depth for the project was estimated at approximately 15,000 ft with full fold ranging from 56 to 84. Source and receiver intervals were set at 165 feet to allow a bin size of 82.5x82.5 ft. Some of the early stage processing was also conducted by PGS. These steps were imbedded in the input data for decimation, therefore this portion of processing remains the same for all volumes. The processing sequence for this data is as follows:

Pre-processing Steps

1. Reformat tapes to internal format
2. Verify first break pick and geometry
3. Trace editing
4. Write final field processed data
5. Minimum phase conversion filter
6. Resample to 4ms
7. Spherical divergence compensation
8. Surface consistent scale compensation
9. Refraction statics
   - Replacement velocity: 9500 ft/s
   - Final datum: 1700 ft
10. Surface consistent deconvolution
    - Operator length: 220 ms
    - Gap: spike
    - White noise: 0.01 percent

Decimated Seismic

Costs can be reduced significantly in the acquisition and processing of 3D land seismic data by removing receiver groups and shot points from the survey. In order to understand how much signal will be lost by reducing field effort, decimation is conducted similar to the procedure used by Bouska (1995). By systematically removing traces from the original volume we can simulate the dataset that would be expected from a specific set of acquisition parameters. In this study traces were removed at the earliest data processing stage available which was immediately following the deconvolution performed by PGS (Step 10 above). Thus the refraction static solution could not be altered. This only allowed for the recalculation of residual static solutions and velocity analysis on the decimated data. The results of these tests are discussed in detail in the following chapter. Approximately 25 mi^2 of the original volume was extracted to perform decimation and is believed to provide enough of a sample to exhibit the effect of decimation on data quality. The area was selected for varying structural complexity and

a known well location that would tie the data into the geology. Decimation volumes were created in a fashion to replicate acquisition layouts in the following scenarios:

1. Every other receiver was removed from the original dataset to create a volume referred to as decimated receiver. A process known as flex binning was performed due to the irregular distribution of fold that was created by removing half the receivers. Flex binning allows a bin to duplicate a trace from a neighboring gather. Specifically, when a certain offset range is missing the computer will search nearby gathers for that same offset and copy the trace if found.
2. Every other shot was removed from the original dataset to create a decimated shot volume. Flex binning was again required to even the distribution of fold.
3. A decimated shot and receiver volume was created by removing every other shot and every other receiver from the original volume. Flex binning was also performed in this scenario. This was conducted for the same reasons as previous volumes to evenly distribute fold.

Synthetic Seismograms

The correlation of seismic data to well data is an important aspect of geological interpretation of seismic surveys, and is accomplished by constructing a synthetic

seismogram from the sonic log. The synthetic seismic is then tied to the surface seismic data.

A sonic log records interval transit time of a formation which is usually designated as Δt. This interval transit time is the reciprocal of velocity, and has the units of μs / ft. The interval transit time typically has a range of 140 – 40 μs / ft, which is equivalent to velocities of ~7100 – 25000 ft/s. The sonic tool is more sensitive to porosity changes rather than lithology changes (Rider, 2002), and is primarily used to quantify porosity. The sonic log is also used to calculate the acoustic impedance log, which is subsequently used to create a synthetic seismogram. Before the synthetic seismogram can be tied to the seismic data the difference in the frequency content between the two must be considered. Since a seismic trace usually exhibits frequencies on the order of 10 – 50 Hz, the synthetic trace must be filtered so that it has similar frequency content. This is because the sonic tool will record frequencies in the kHz scale which is higher frequency than would be expected in the seismic data. Moreover, check shot corrections may need to be applied to the synthetic seismogram to correct for borehole effects. After collection of the logs the first step to synthetic seismogram creation is to calculate an acoustic impedance log.

Acoustic impedance is calculated by:

$$Z = \rho v \tag{1}$$

where,

Z = acoustic impedance [Mass / Length^2 * Time]
ρ = density [Mass/Volume]
v = P-wave velocity [Length/Time]

Real world application doesn't always provide a complete sonic and density log. It is common to omit the density log as it has minimal control in the equation relative to the

velocity input. Next the impedance log is used to create a reflection coefficient log and converted from depth to time. The reflection coefficient is calculated with the assumption that the incident wave is vertical, via (Yilmaz, 2004),

$$R = \frac{Z_{n+1} - Z_n}{Z_{n+1} + Z_n} \tag{2}$$

where,

R = reflection coefficient [dimensionless]

Z_n = acoustic impedance [Mass / Length^2 * Time]

Z_{n+1} = acoustic impedance for a lower stratigraphic layer [Mass / Length^2 * Time]

Finally to the complete the synthetic seismogram a wavelet selected by the user is convolved with the reflection coefficient log to create a synthetic trace. Additionally at this point the geologic formations are usually displayed from the well picks. This allows the interpreter to determine which reflector is of interest and relate the seismic to geology.

Though bulk density logs are typically collected in this region, in this study they were not used due to the large number of corrections that would need to be applied to the log data. Commonly density logs are run on a limestone matrix which can later be corrected for with some degree of ease. However in the mountain front region where large number lithologies are mixed together it requires more effort to make the corrections. Even though these corrections can be made the density values were omitted from the acoustic impedance log calculation because its affect on the equation is minimal.

The ideal situation to tie seismic would involve migrated seismic data and a complete sonic log without washouts. However, in this study only one well was available that contained a sonic log of considerable length and could tie to the unmigrated data. Even within this well there were depths where the sonic log was incomplete or too erroneous to use without correction. Thus, to compensate for erroneous or incomplete

sonic readings, the deep resistivity curve was used to estimate the missing sonic sections through the use of Faust's equation. This equation states that:

$$V_P = \gamma(ZF)^{1/6} \tag{3}$$

where,

V_p = P-wave velocity [Length / Time]
γ = constant [dimensionless]
Z = depth [Length]
F = formation factor (R_t / R_w) [dimensionless]

After the estimated sonic log (from the resistivity log) is merged with the original sonic log, the construction of the synthetic seismogram can resume its normal workflow.

CHAPTER III

PROCESSING OF DECIMATED VOLUMES

The ultimate goal of any seismic dataset is to yield an accurate interpretation of geology. While the requirements to meet this goal may vary greatly with respect to field effort, the overall goal is to obtain the best image the data can produce. It is through the difficult step of processing that the data is transformed into an interpretable final image. Though the steps involved in the processing sequence are not necessarily the same for every decimation test conducted, they are grossly similar. While observing the difference in image quality from different collection methods, the ease with which the data could be processed was also assessed.

Decimation began immediately after the traces had deconvolution, elevation statics, and refraction statics applied as well as had been common mid-point (CMP) gathered (Chapter II). Only residual statics, velocity analysis, and migration remained as major processing steps. Since prestack seismic migration is expensive and time consuming to perform on 3D datasets, only residual statics and velocity analyses were repeated on the various decimated volumes. This study was conducted with the intent to image a 25 mi^2 area within a larger collected volume. The area was chosen due to the combination of simple and complex structures in the shallow and deep sections respectively as well as potential well tie locations.

In order to compare each decimated volume to the originally collected data, a reference volume was created. This volume maintained all sources and receiver groups. The same tests were conducted on it as the decimated volumes. Additionally, the fact that migration had not been performed on the decimated volumes, made the creation of this reference volume vital to the study. This is because the originally licensed dataset had been migrated it would not be a valuable comparison to unmigrated data.

Survey Layout

Using the trace header information from the traces, the survey layout was established and reconstructed for each volume. Figure 6 illustrates the layout of sources in pink and receivers in blue. Receiver lines were laid out parallel to dip while shot lines were approximately parallel to strike along the mountain front.

Figure 6 also shows the shot and receiver layout represented by a box, which is the area bounded by two adjacent source lines and two adjacent receiver lines, for each of the decimated volumes. The dense band at the center of the layout of sources and receivers results from the merger of two independent surveys. One of these surveys (to the North) was acquired with a slant design where the source lines are at a constant angle to the receiver lines. The second survey (to the south) was acquired with a modified brick pattern.

Also within Figure 6 restrictions to source point and receiver group locations are shown. Since the planting of receiver groups is quite passive and typically restricted by access, large empty patches on the map indicate missing source/receiver locations.

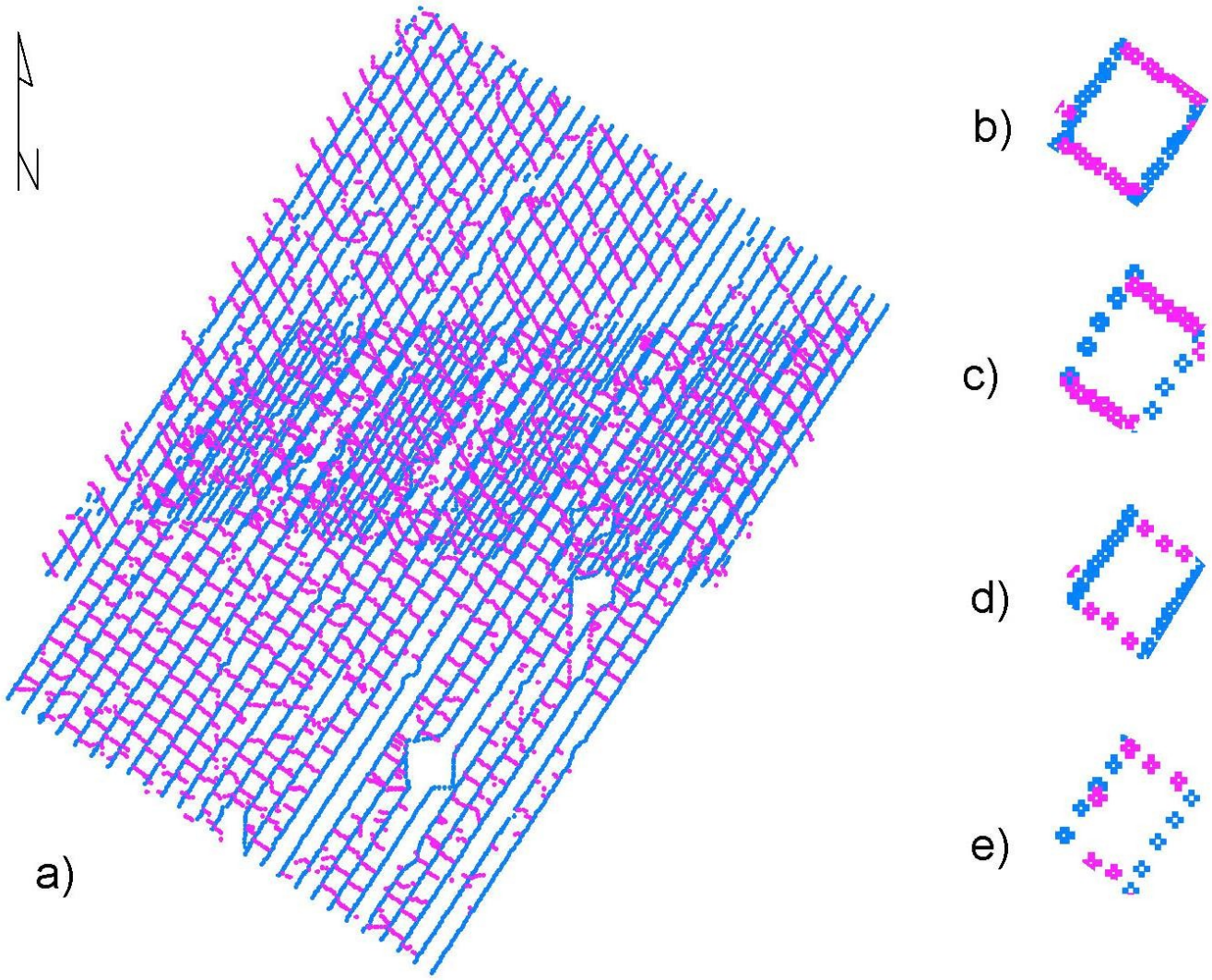

Figure 6 – (a) The acquisition geometry for the decimated volumes. Receiver lines are represented in blue while shot point are pink. (b) – (e) show enlargements of a box for each individual volume. The full volume (b) is followed by decimated receiver volume (c), decimated shot volume (d), and decimated shot and receiver volume (e).

Fold

A fold plot can be generated from the acquisition geometry. The fold plots were generated before the flex binning had occurred, so this is not the true fold that is stacked later to provide the final image comparisons discussed in Chapter IV. Again, flex binning is used to evenly distribute the fold since deviations to trace placement result from irregular dipping layers and ray bending in the subsurface.

The fold plots that are generated are used to detect any major patterns or deficiencies that exist within the survey. These are important as they will influence the interpreted image. Patterns that result from fold distribution may mislead the interpreter from observing valuable geologic influence on the data. Additionally fold plots generated for different offsets can help to understand the offset distribution within the survey. Offset distribution is important because it is believed to assist with static solutions as well as provide a better velocity analysis (Cordsen 2000).

The maximum fold for the reference volume ranges from the mid-50's to just below 200 (Figure 7). This would result in a signal to noise (S/N) ratio of just over 7 to 14. Though the main goal of fold is to improve the S/N ratio, it should also be evenly distributed throughout the survey. Uneven distribution can lead to artifacts of acquisition such as foot printing or other non-geological changes in the interpreted image. The variation in fold coverage seen in Figure 7 results from the merger of two surveys. The northern survey has nominal fold of approximately 85. The nominal fold of the southern survey is about 50. This overlap would then result in a fold of about 135+. Additional

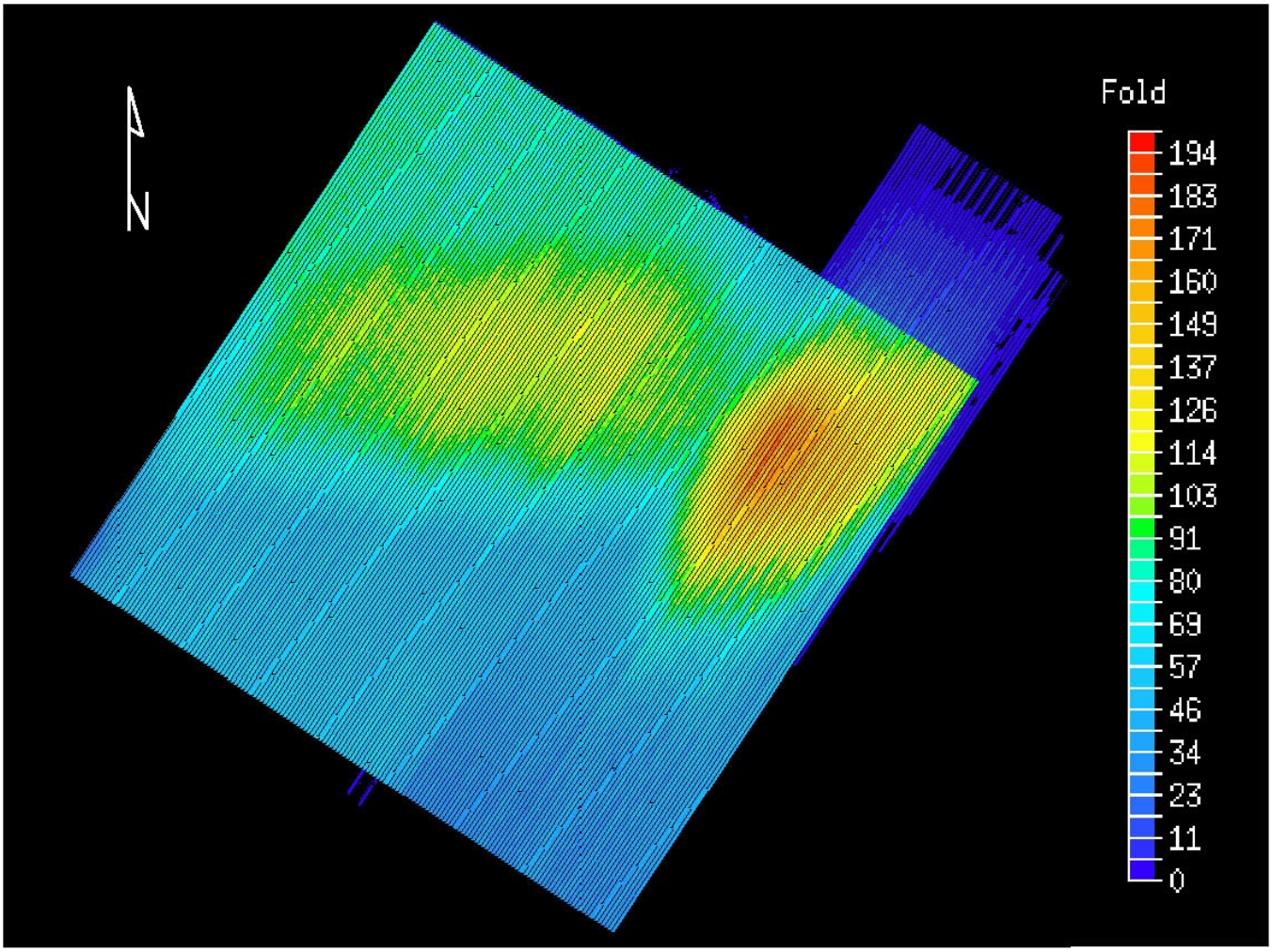

Figure 7 – Fold plot for the reference volume with a full range of offsets. High fold indicated by the hot colors is a result of the merged surveys.

fold plots were generated for the 5000' and 15000' offsets. These displays help show the even distribution to fold contribution. To acquire this even distribution the aspect ratio of the patch, which is defined by the source length divided by the receiver length of the recording patch, would approach one or the shape of a square rather than a rectangle.

The fold plot for an offset distance zero through 5000' is illustrated in Figure 8. As before there is a band of higher fold present across the middle of the survey. This effect will be observed throughout all of the generated fold maps. Another effect that will persist in most of the displays is the difference in fold between the northern and southern surveys. The highest fold obtained in the 5000' offset plot is roughly 45, while the lowest is approximately 6 (Figure 8). This region of very low fold is likely due to either potential permitting issues or terrain restrictions which created the empty block of shot and receivers in the south (Figure 6). The more convincing explanation would be terrain restrictions such as bodies of water, severe topography changes, and overgrowth of vegetation since receiver groups were deployed in most of these areas but sources were not.

When the offset of 15000' (Figure 9) is considered the region of high fold and geographic differences in fold are again observed. However the low fold area is not as pronounced as it was in the 5000' offset (Figure 8). This is likely caused by two things; (1) the dynamic range of the color bar was increased thus aliasing small changes in fold and (2) longer offsets are created by source points that are out of the obstacle-ridden area. The overlay band at this offset produced fold of approximately 135. In areas where

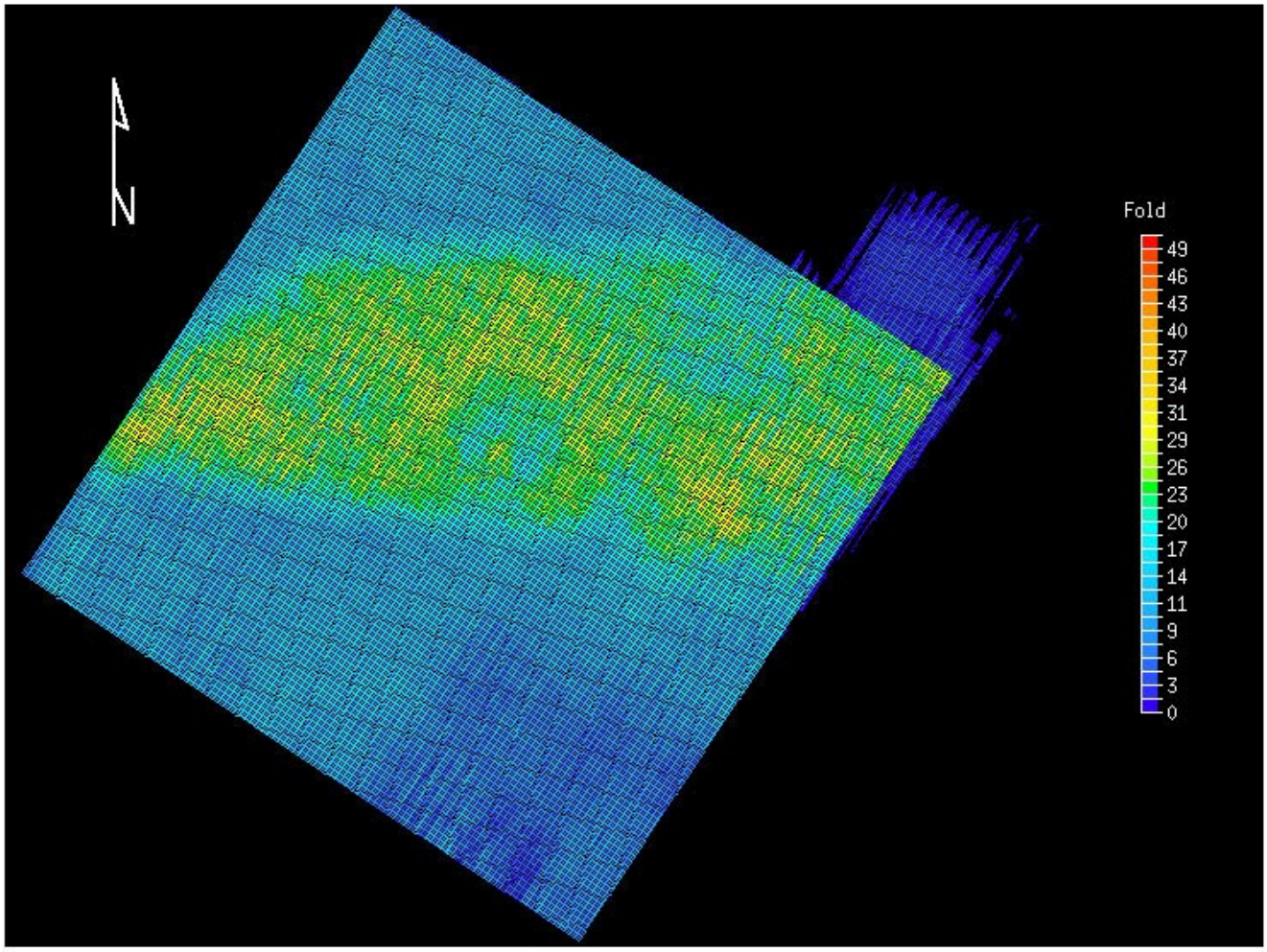

Figure 8 – Fold plot for the reference volume with an offset range up to 5000'. High fold is observed where surveys are merged.

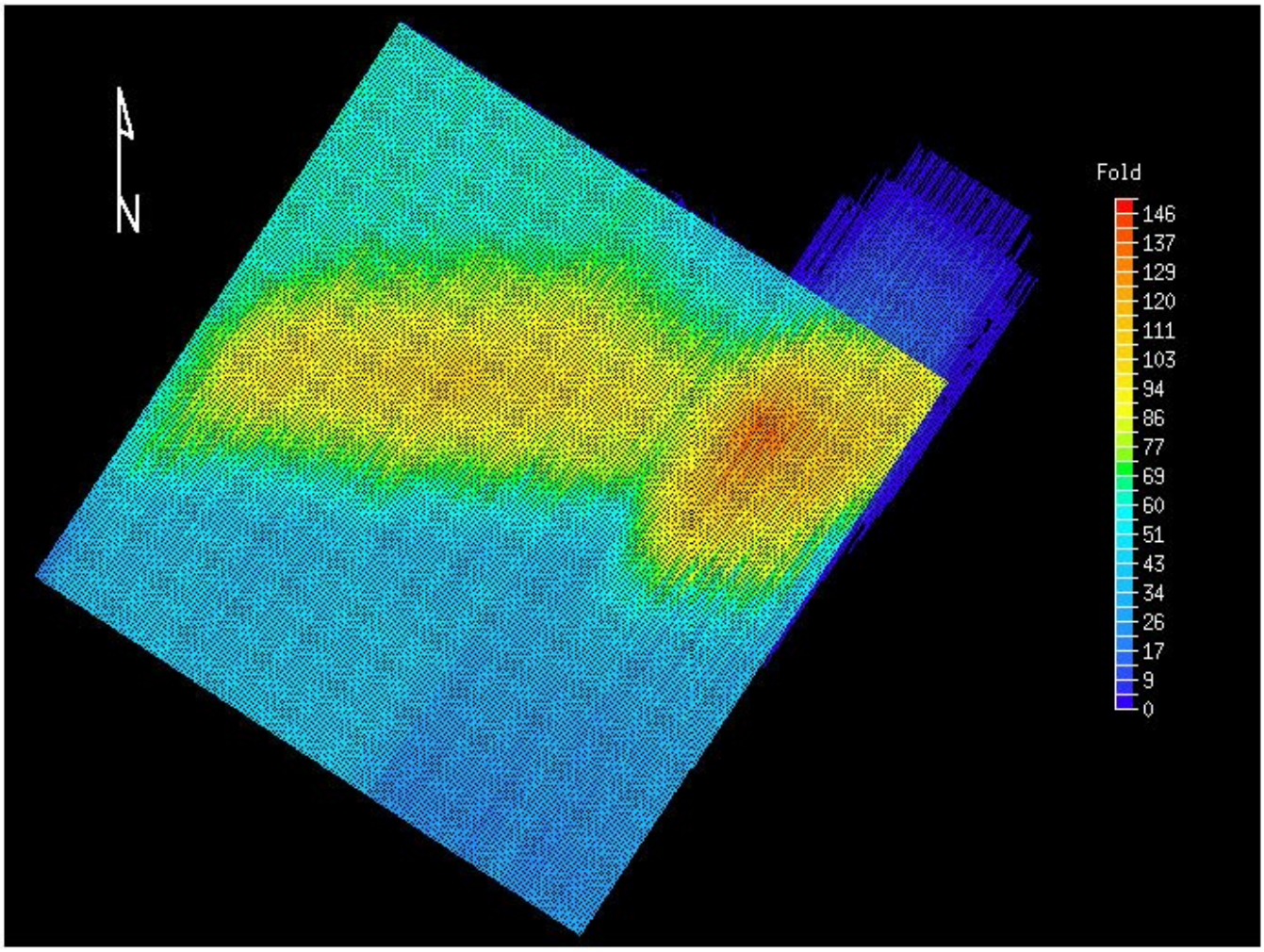

Figure 9 – Fold plot for the reference volume with an offset range up to 15000'. High fold is observed where surveys are merged.

source points were not restricted, which is essentially everywhere except the southern portion, the fold is three times higher in the zero to 5000' offset range. Also in comparing the 0 – 15000' offset range to the full range of offsets, the band of high fold increases from 135 to roughly 180 respectively. This demonstrates that sampling was evenly distributed to allow for an increase of roughly 45 fold every 5000' of offset.

In continuing to understand how fold was affected by decimation, fold plots were created for the decimated shot and decimated receiver volumes which appear very similar to each other. The fold plots with the full range of offsets were generated for the decimated receiver (Figure 10) and decimated shot volume (Figure 11). There are two displays for each fold offset on both figures. One of the displays (Figure 10a & 11a) used the same color bar as the reference volume (Figure 7) to allow easy comparisons. However, this sacrificed the dynamic range of the color bar so a second display was created (Figure 10b & 11b) that adjusted the scales to provide better contrast across the survey.

Comparing the quantitative differences in the fold for the full range of offsets in the decimated receiver (Figure 10a) and decimated shot (Figure 11a) to the reference volume (Figure 7) illustrates that the fold in both decimated volumes reduced by one half. This reduction is not predicted by the 3D total fold equation because the equation makes the assumption that the bin size used is one half the source interval by one half the receiver interval. In our study bin size remained constant at 82.5 x 82.5 ft therefore reducing the fold with decimation of shots and/or receivers. Changing the bin size would

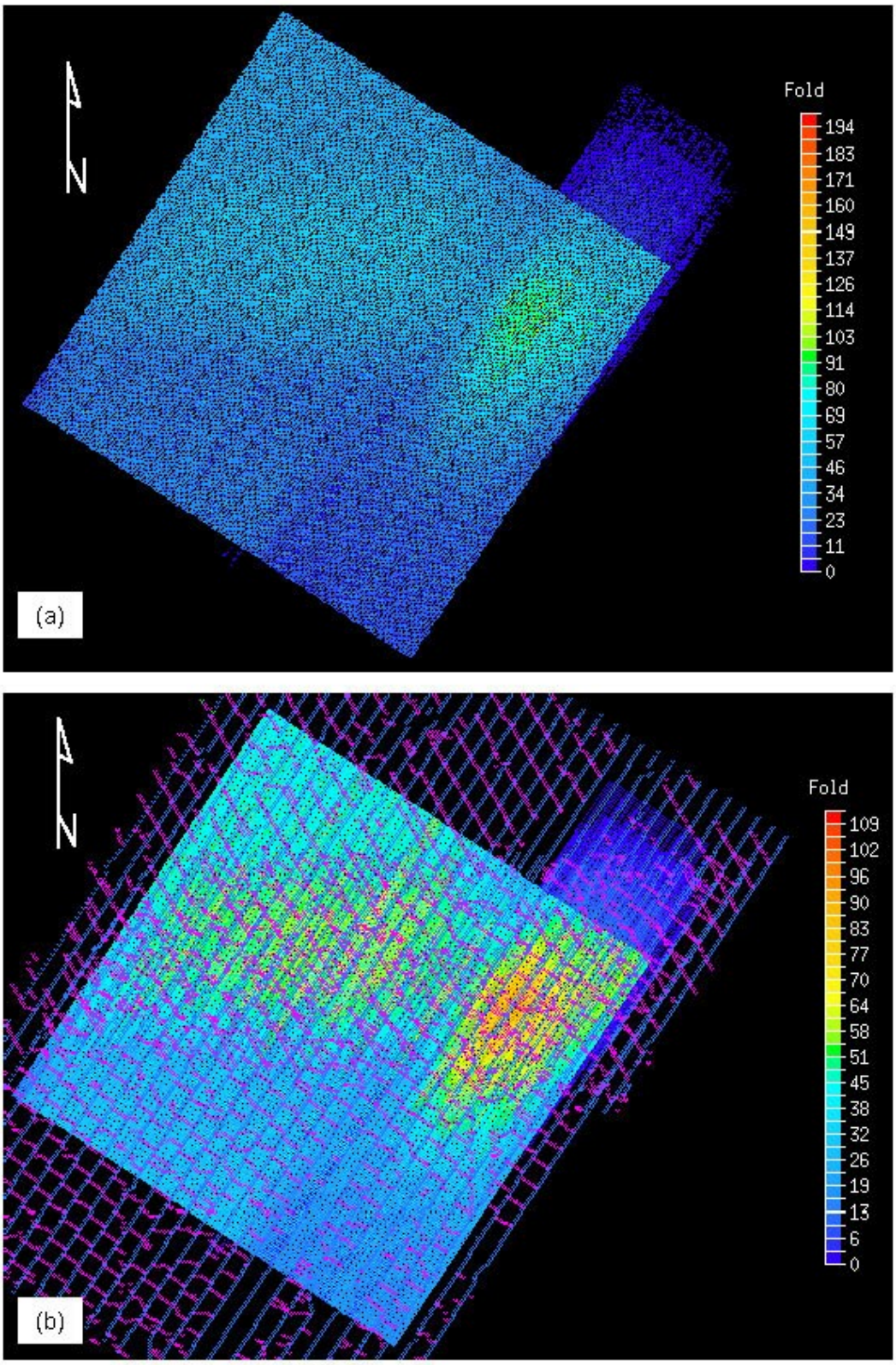

Figure 10 – Fold plots for the decimated receiver volume with a full range of offsets. The scale in (a) is the same as the reference volume. The scale in (b) shows the same variation in fold where increased fold is related to the merged surveys, additionally there is a geometry overlay.

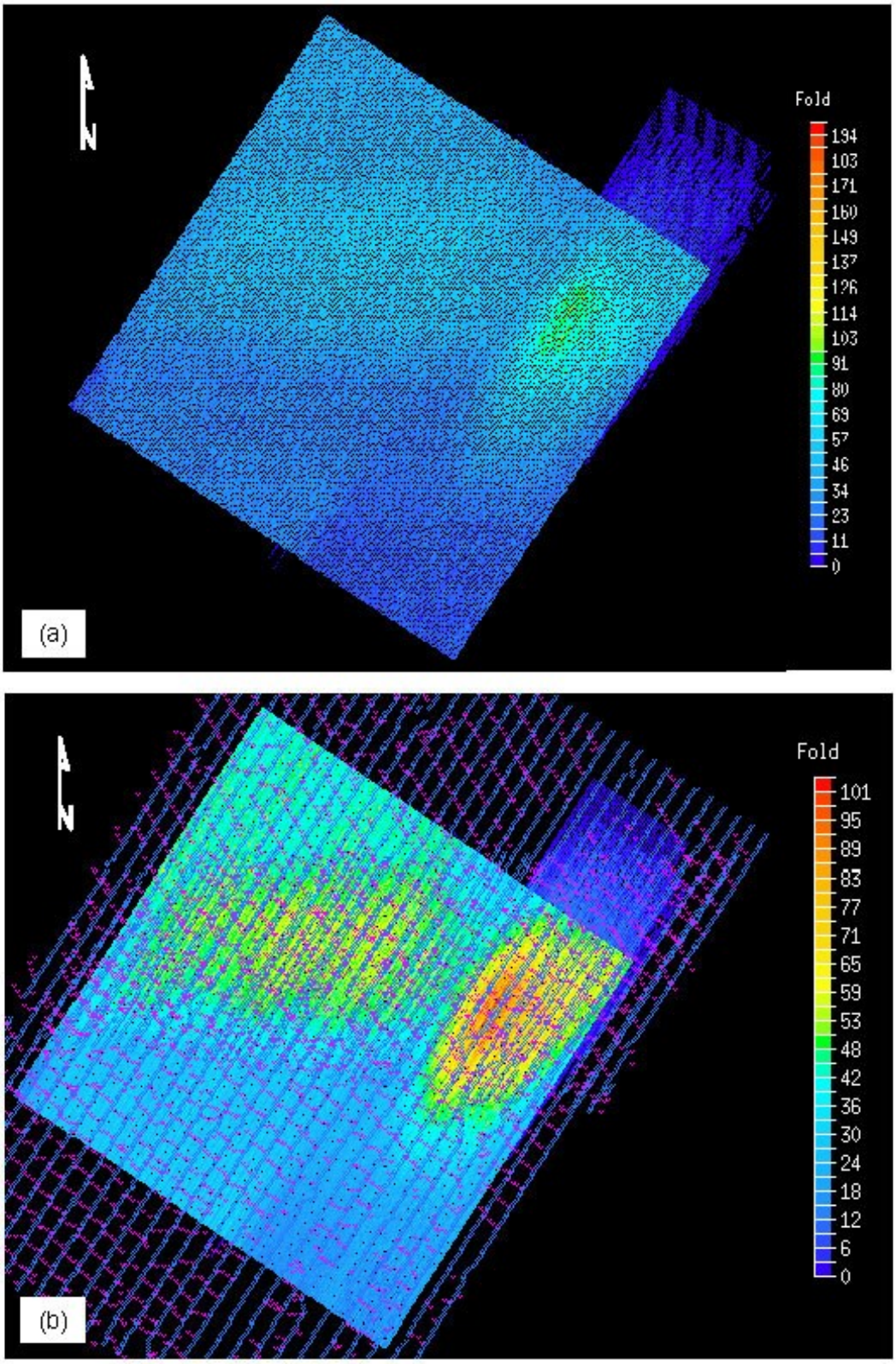

Figure 11 – Fold plots for the decimated shot volume with a full range of offsets. The scale in (a) is the same as the reference volume. The scale in (b) shows the same variation in fold where increased fold is related to the merged surveys, additionally there is a geometry overlay.

also have changed the number of traces that represent the survey. Bin size was chosen to remain constant so that comparisons could be made with the method of volume differences, discussed later. The method requires an equal number of traces in both volumes to create a valuable comparison. This reduction results in a decreased S/N ratio compared to the reference volume. When using the fold values of approximately 180 and 45 with the full range of offsets for the reference volume and decimated shot and receiver volume the S/N ratio is lower by roughly fifty percent.

The second display for each offset (Figure 10b & 11b) better represents the fold distribution across the survey. The fold obtained with the full range of offsets on both volumes is roughly 25 to 45 fold for the southern and northern sections, respectively, while the maximum is actually near values in the upper 90's. On the 5000' offset for both the decimated receiver (Figure 12) and decimated shot (Figure 13) the low fold section in the southern portion is again very apparent. The majority of the merge section in both volumes is approximately 18 fold. In the 15000' offset fold plots for both scenarios (Figure 14 and 15) fold increased nearly three times the 5000' offset in areas other than the low fold section.

Finally comparing the decimated shot and receiver volume in Figure 16a it is incredibly difficult to make any inferences from the displays with the same color bar as the reference volume. Once again the fold has been greatly reduced since the bin size has not changed with decimation. In Figure 16b, where the scale bar is reset to a different range of values the eastern corner has fold in the mid 40's. This is approximately one

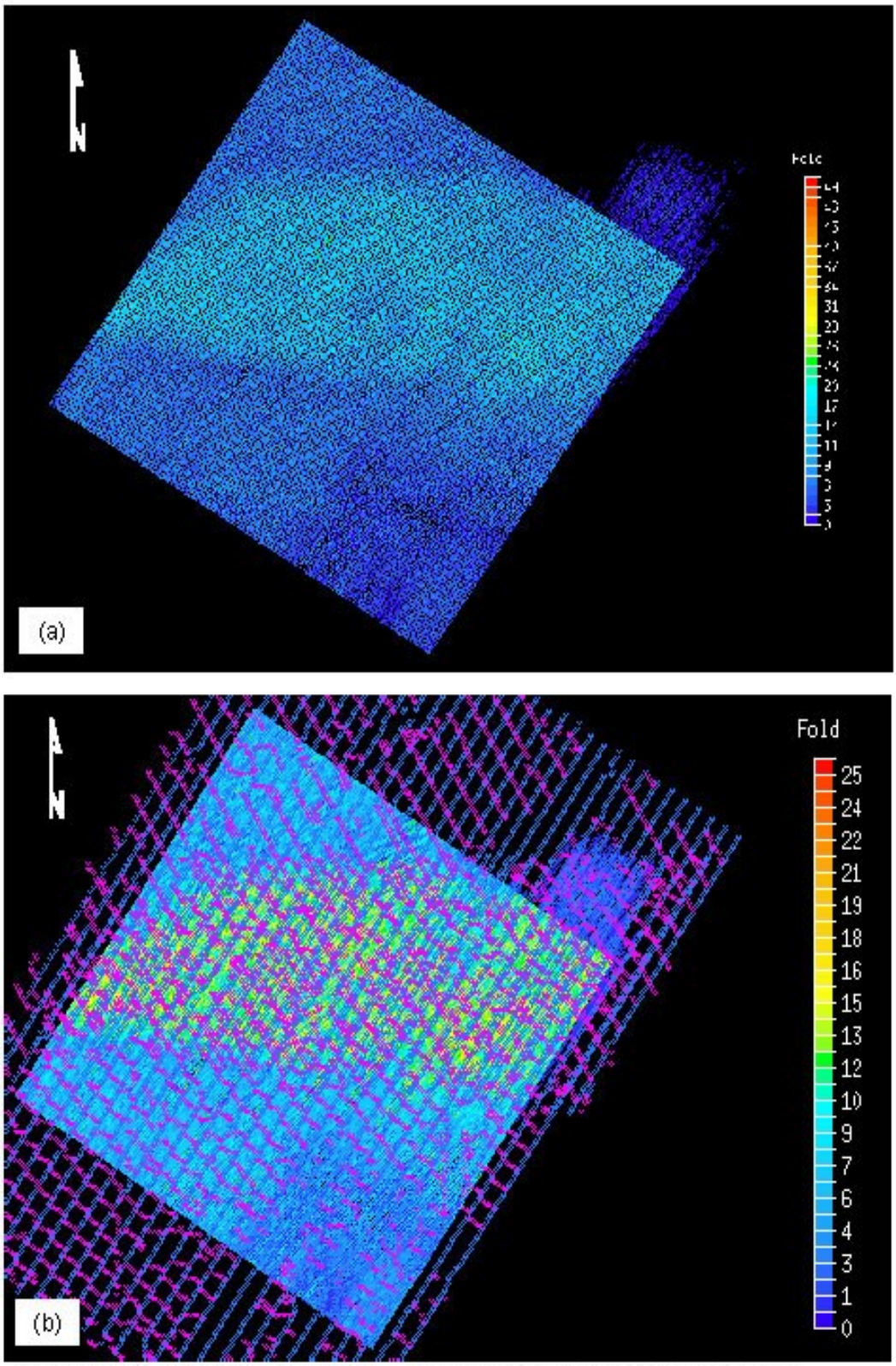

Figure 12 – Fold plots for the decimated receiver volume with a offset range up to 5000'. The scale in (a) is the same as the reference volume. The scale in (b) shows the same variation in fold where increased fold is related to the merged surveys, additionally there is a geometry overlay.

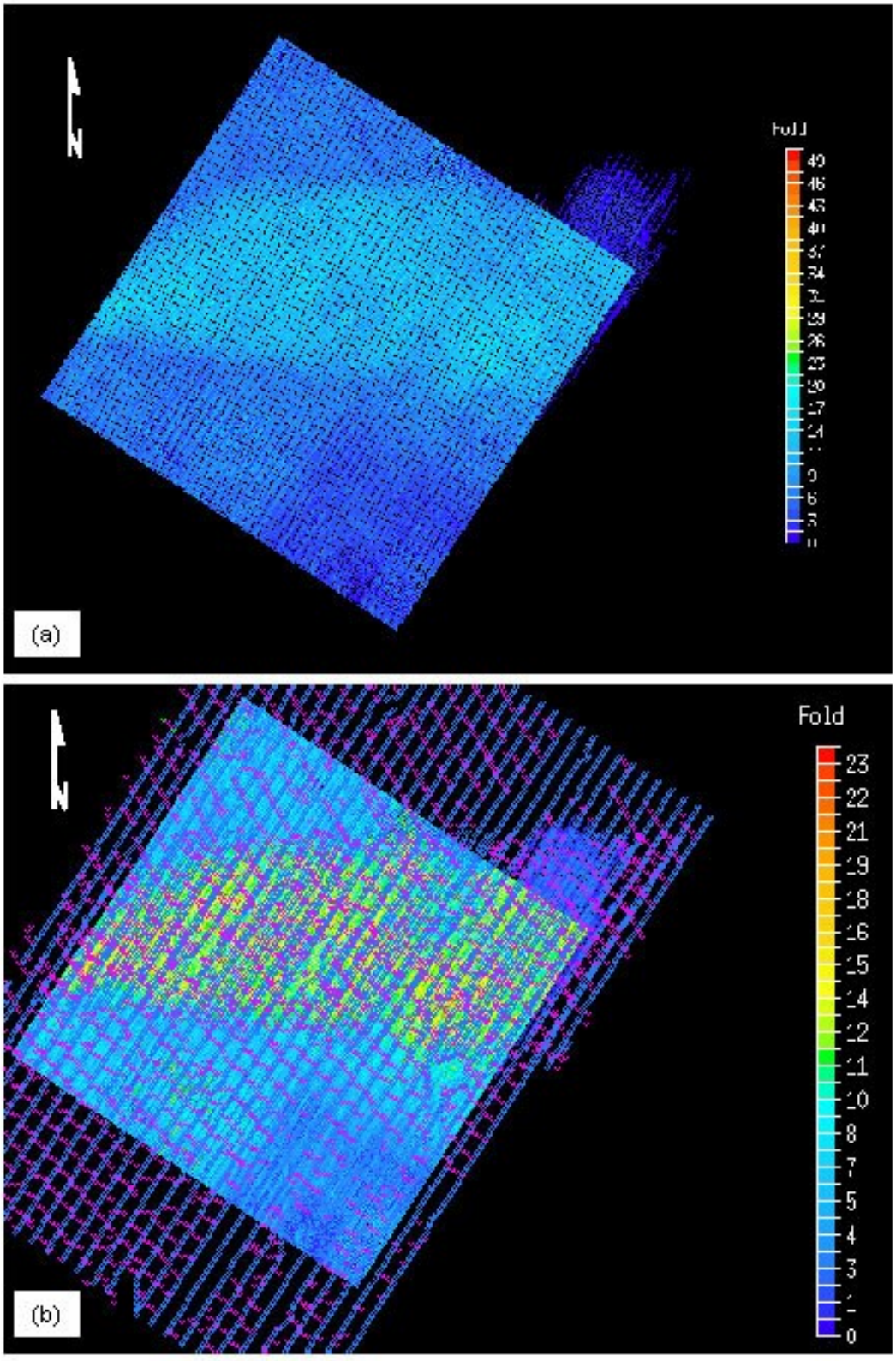

Figure 13 – Fold plots for the decimated shot volume with a offset range up to 5000'. The scale in (a) is the same as the reference volume. The scale in (b) shows the same variation in fold where increased fold is related to the merged surveys, additionally there is a geometry overlay.

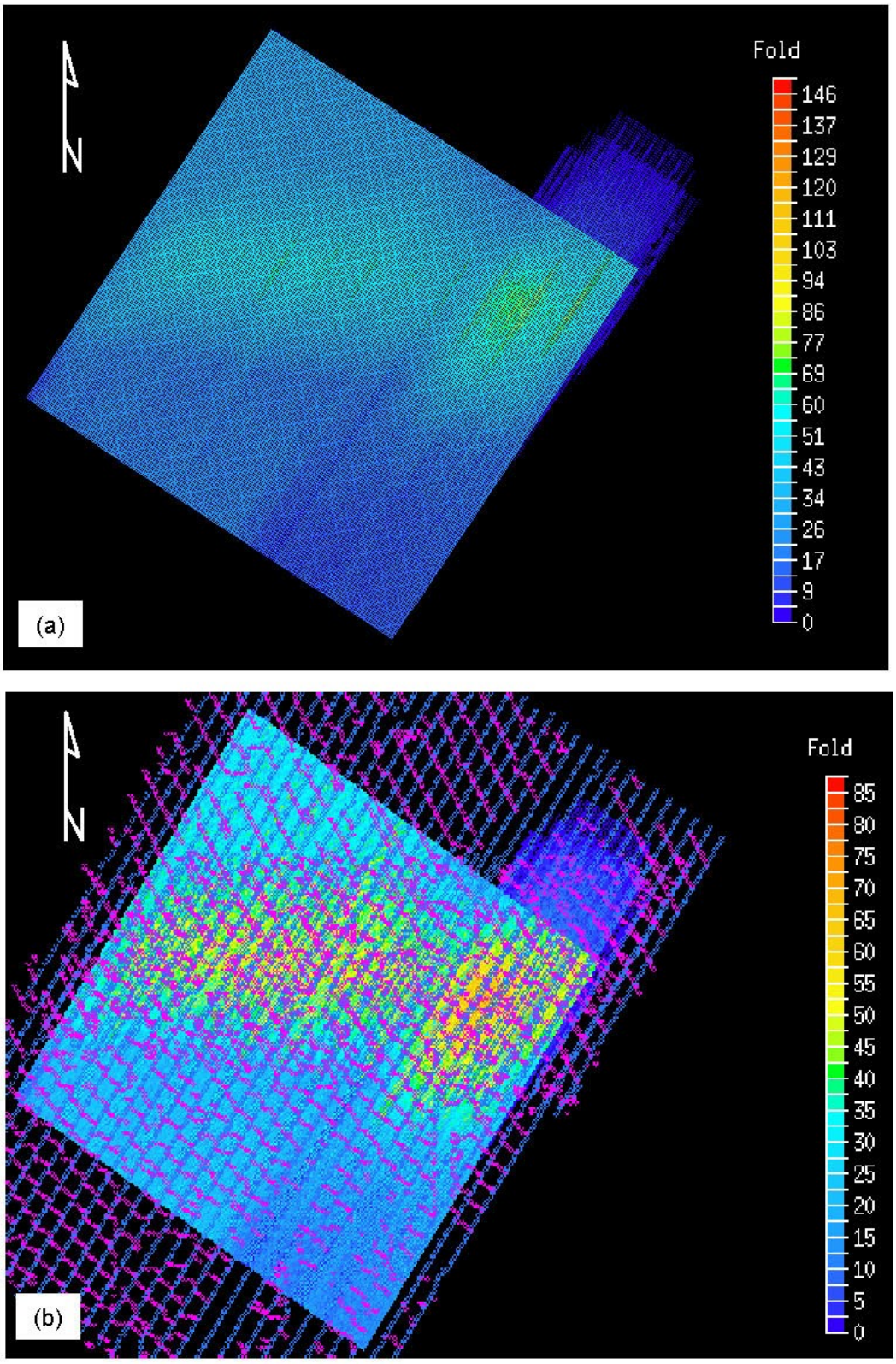

Figure 14 – Fold plots for the decimated receiver volume with a offset range up to 15000'. The scale in (a) is the same as the reference volume. The scale in (b) shows the same variation in fold where increased fold is related to the merged surveys, additionally there is a geometry overlay.

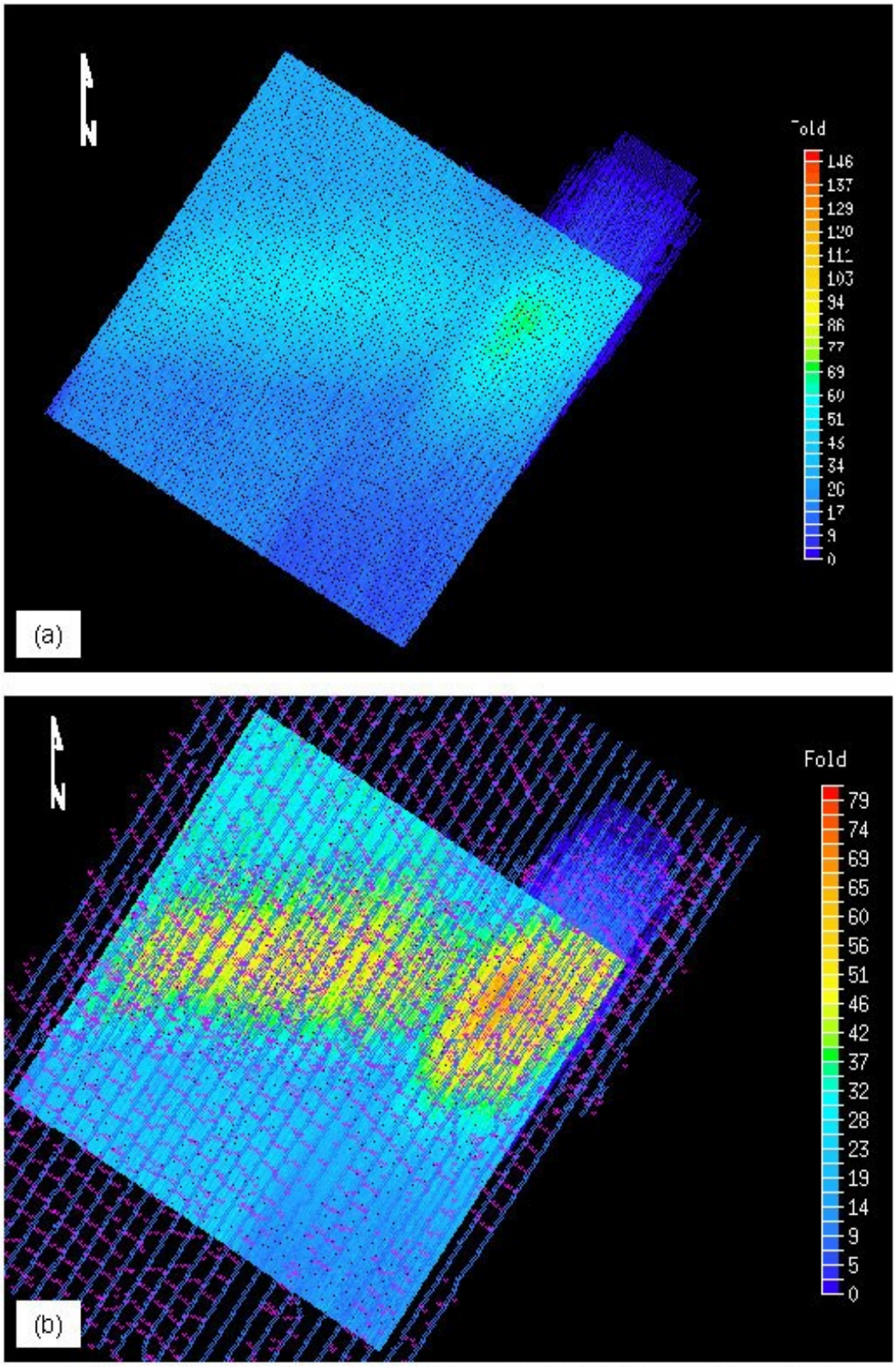

Figure 15 – Fold plots for the decimated shot volume with a offset range up to 15000'. The scale in (a) is the same as the reference volume. The scale in (b) shows the same variation in fold where increased fold is related to the merged surveys, additionally there is a geometry overlay.

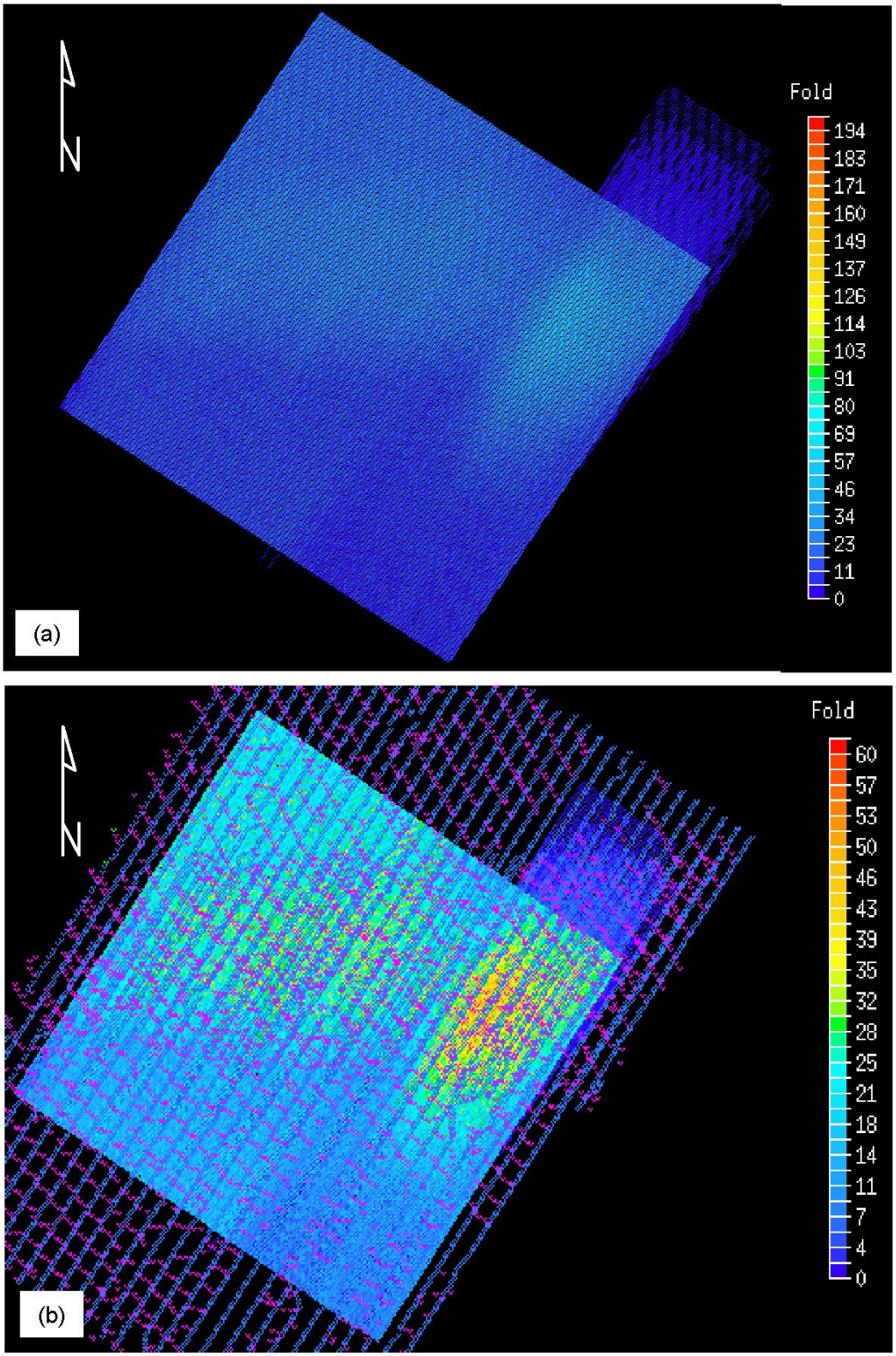

Figure 16 – Fold plots for the decimated shot and receiver volume with a full range of offsets. The scale in (a) is the same as the reference volume. The scale in (b) shows the same variation in fold where increased fold is related to the merged surveys, additionally there is a geometry overlay.

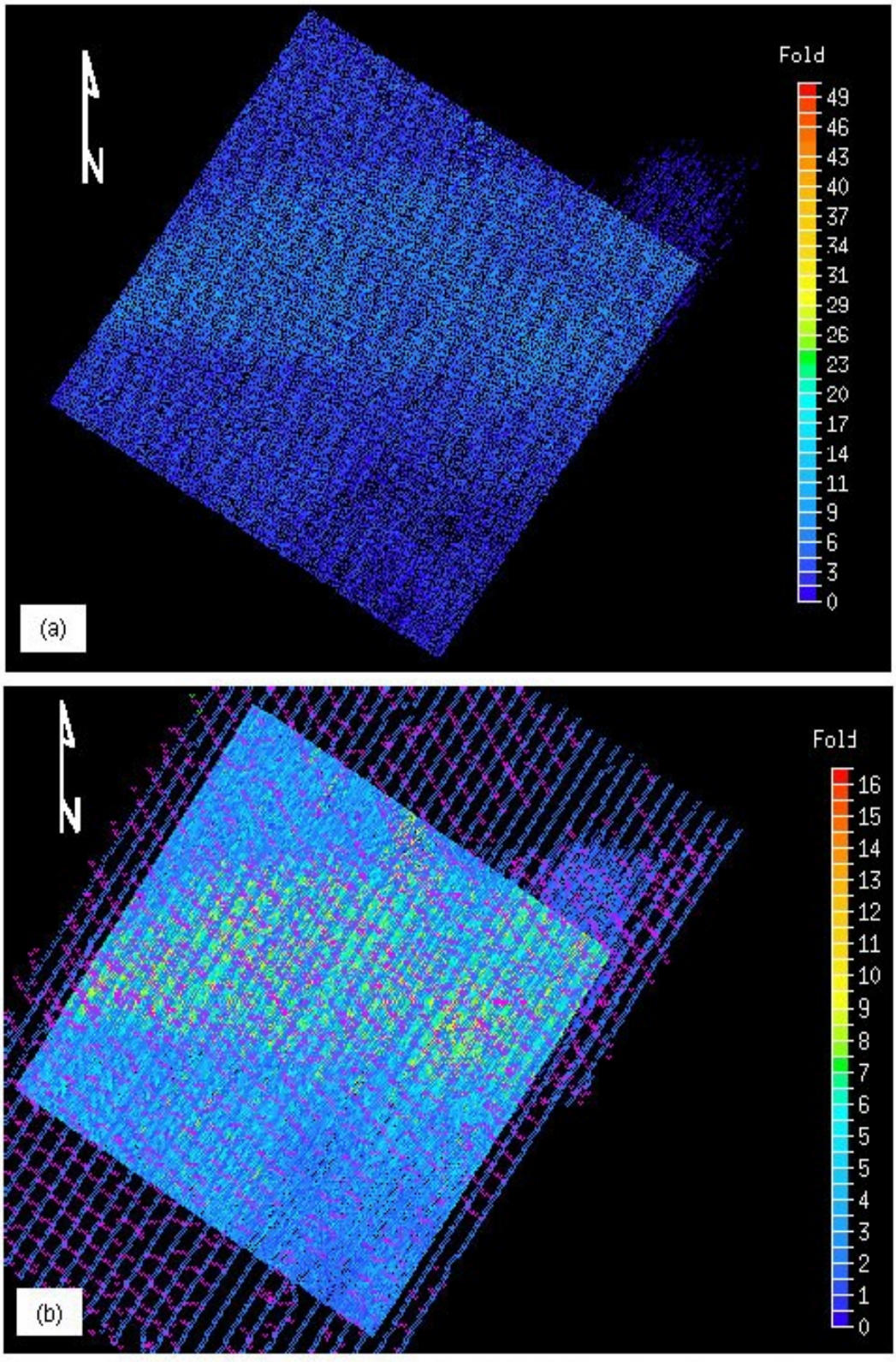

Figure 17 – Fold plots for the decimated shot and receiver volume with a offset range up to 5000'. The scale in (a) is the same as the reference volume. The scale in (b) shows the same variation in fold where increased fold is related to the merged surveys, additionally there is a geometry overlay.

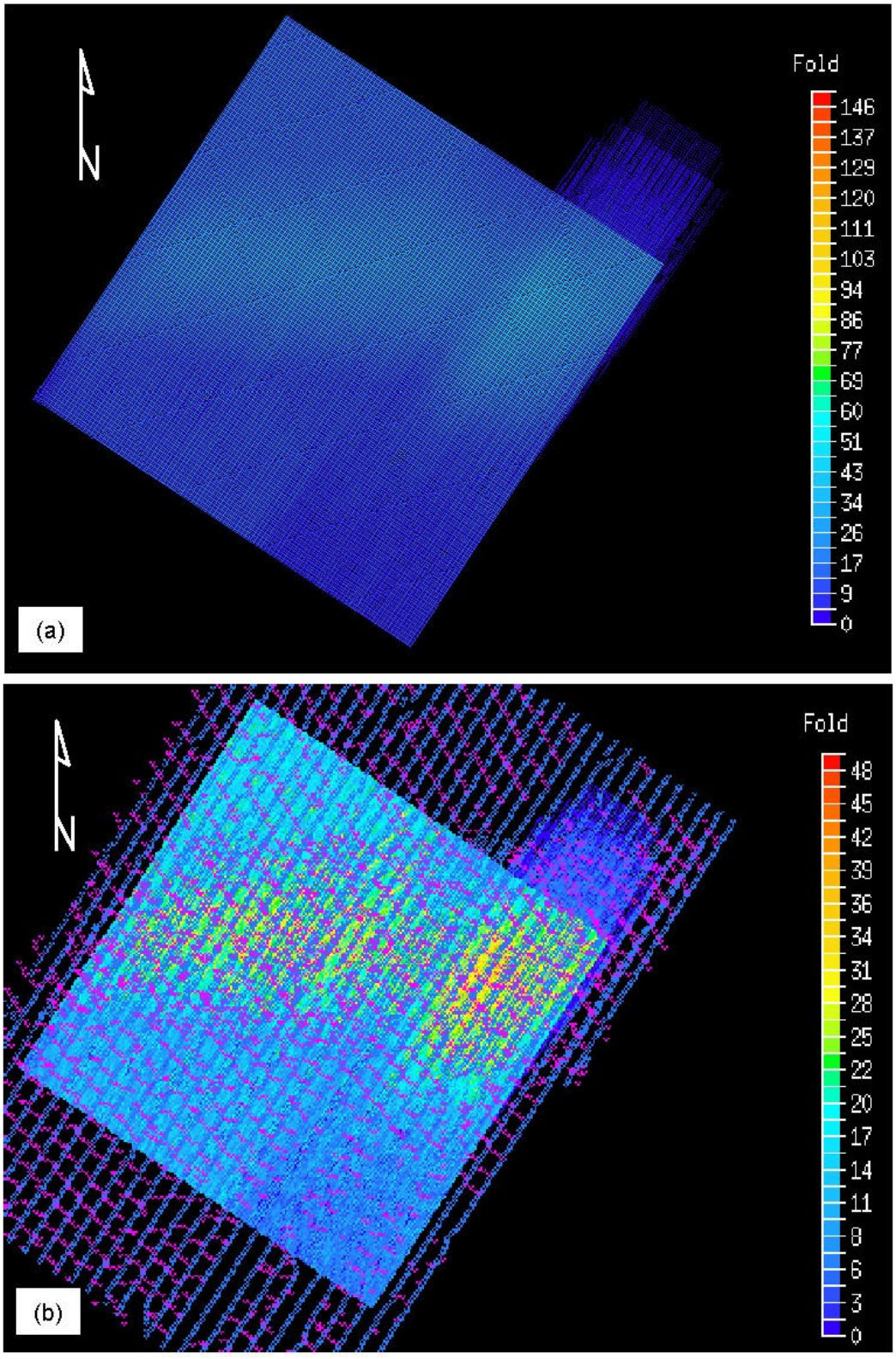

Figure 18 – Fold plots for the decimated shot and receiver volume with a offset range up to 15000'. The scale in (a) is the same as the reference volume. The scale in (b) shows the same variation in fold where increased fold is related to the merged surveys, additionally there is a geometry overlay.

fourth the estimated 180 fold that is seen on the reference volume in the same area (Figure 7). The 5000' and 15000' offset fold plots (Figure 17 and 18 respectively) for the decimated shot and receiver volume still record the merged section in the middle but it becomes increasingly complex to observe other features.

Statics

When raw data is collected in the field, multiple affects are encoded by the near-surface geology of the region on the data that can lead to a severely compromised image if neglected. These effects result from topographic variations and what is commonly referred to as the "weathered zone." The "weathered zone" refers to a low velocity layer that is usually near the surface, and which varies spatially and with elevation. If the layer were consistent in its velocity and/or dip it would not be problematic, since it could easily be modeled. However, because the variation is not easily parameterized or predicted, it is quite problematic. The goal in static correction is to align the data on the same datum which should also allow for the alignment of the same reflectors. These corrections are of the utmost importance because the goal of summing multifold data is to enhance primary reflections at the expense of noise or unwanted signal (Marsden, 1993). Figure 19a-b shows the fundamental need for a static correction where part b) shows the problem of unresolved corrections. The representation of the geology is not well captured unless these issues are corrected. Elevation and refraction static corrections are two methods applied in preprocessing. The elevation corrections account for added ray path travel time that results only from changing source and/or receiver elevations. Time

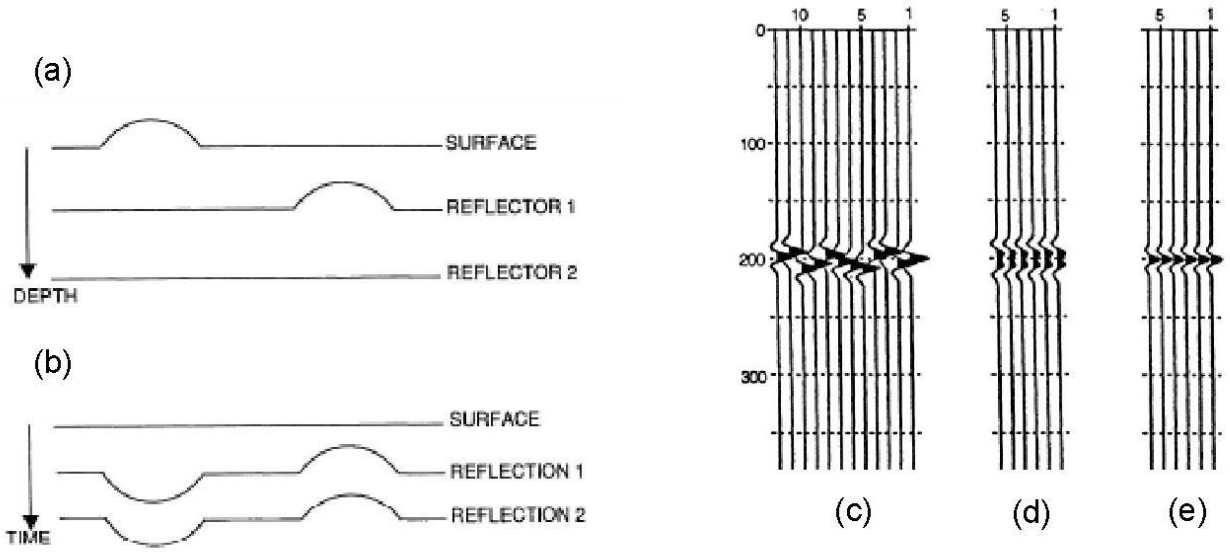

Figure 19 – The overall need for a static solution is shown by representing the depth model (a) in time (b). If traces that have been normal moveout (NMO) corrected (c) do not undergo residual static correction and are stacked an incorrect reflection response can be created (d). If the traces in (c) have residual static corrections applied then the intended single reflector can be represented. Figure from Marsden (1993) and B.H. Russell (1998).

differences caused by the low velocity layer are corrected by refraction statics. Both will bring the data very close to the datum but typically oversimplify the geology. Thus further refinement is required as shown in Figure 19c-e. Residual statics help make the final smaller time shifts required to provide the best stack. Because field statics (i.e. elevation and refraction statics) were previously applied to the recorded tapes, residual statics are the focus of this discussion. Multiple iterations are usually required to refine the static solution, but only the final solution is shown with source and receiver statics combined.

The total (elevation, refraction, and residual) static solution for all four volumes is shown in Figure 20. The cool colors are negative shifts meaning that the trace was moved up in the time domain. The hot colors signify that the trace had time added to it in order to move it down in the time domain, with yellow representing almost zero time shifting. The correlation window used to correct for residual statics varied with each volume. The reference and decimated shot volumes used a window from 300 – 3900 ms. The decimated receiver and decimated shot and receiver volume used a window of 600 – 3900 ms. Total static solution maps were created for each volume but the dynamic range of the shifting, controlled largely by the elevation statics, did not allow for differences in the residual static solution to be observed. No other method was available to represent the different residual static solutions in a map. Though the resulting solution maps were very similar it is important to note the difference in the correlation window used for each volume.

Yilmaz (2001) indicated that a correlation window must be picked in an area where there is as much signal as possible and it should be outside the mute zone. The

'mute zone' is referring to the part of the trace that must be zeroed due to excessive stretching after normal moveout (NMO) corrections. While the same window could be used in the decimated shot scenario as the reference volume, this was not the case for the other decimated volumes. The altered window length for the decimated receiver volume is consistent with the results of Yilmaz (2001) concerning high signal and muted areas. When the muted low fold section of 300 – 600 ms was included in the correlation window, there were large problems with the decimated receiver and decimated shot and receiver volumes (Figure 21). A comparison of the decimated receiver volume (Figure 21a), where a 600 – 3900 ms correlation window was used, and Figure 21b, where a 300 – 3900 ms correlation window was used, show the false time structure and low resolution created by a poor residual solution. This stresses the point made by Marsden (1993) which states the two goals of a static solution are to (1) obtain the correct structural interpretation and (2) obtain the highest resolution section available within the data. These goals are exemplified by Figure 21a, where the time structure is correct and the resolution is increased compared to Figure 21b.

The similarity between static solutions for all volumes could be predicted because the same rapidly changing near surface effects, from elevation and low velocity layer, are present regardless of the survey layout. The banded pattern across the survey on the static map (Figure 20) was compared to a topographic map, confirming that the static

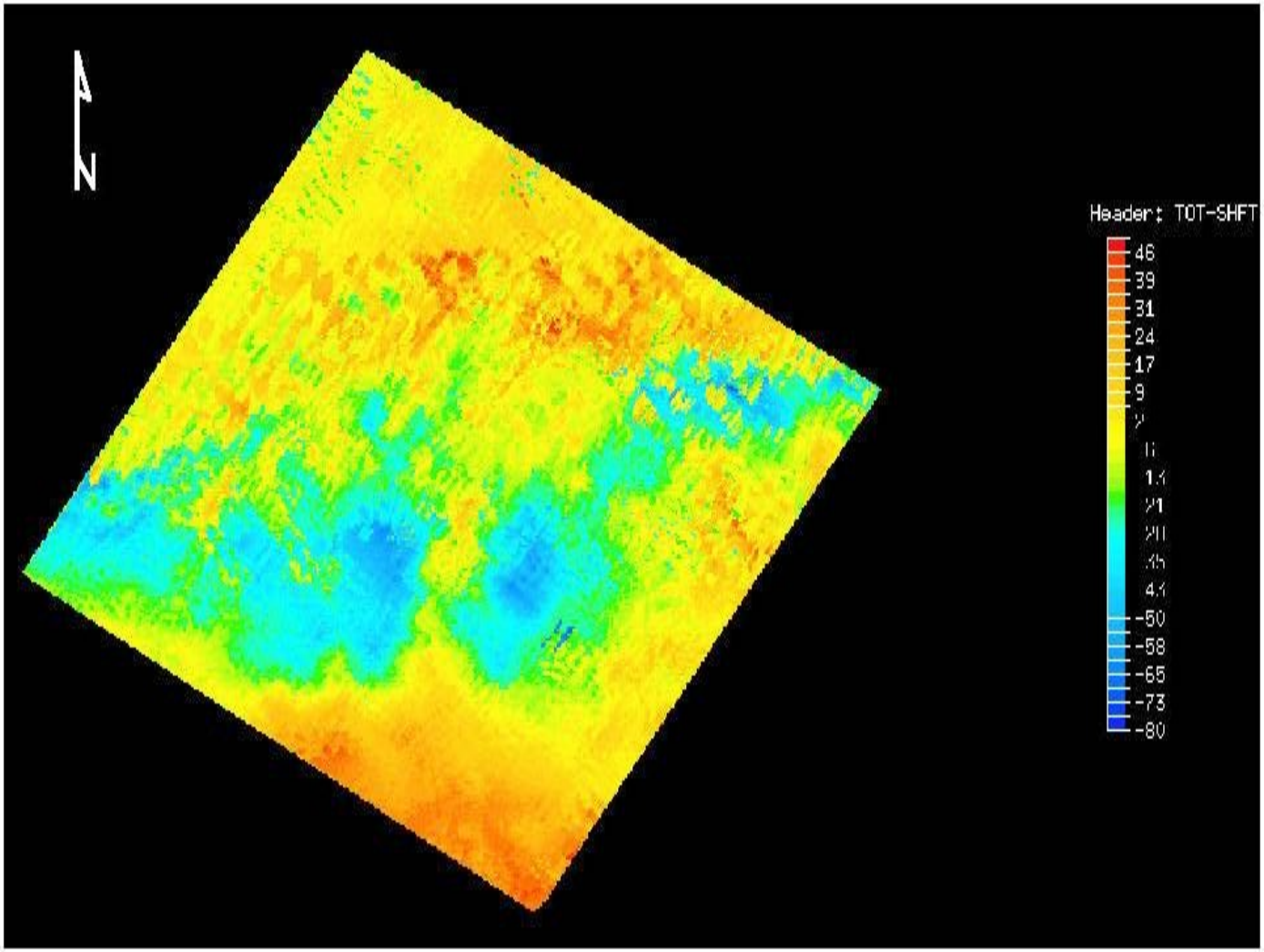

Figure 20 - The final static solution used on all volumes. This solution includes refraction, elevation, and residual static corrections. Residual statics did change for each volume but are too small to be recognized on this map.

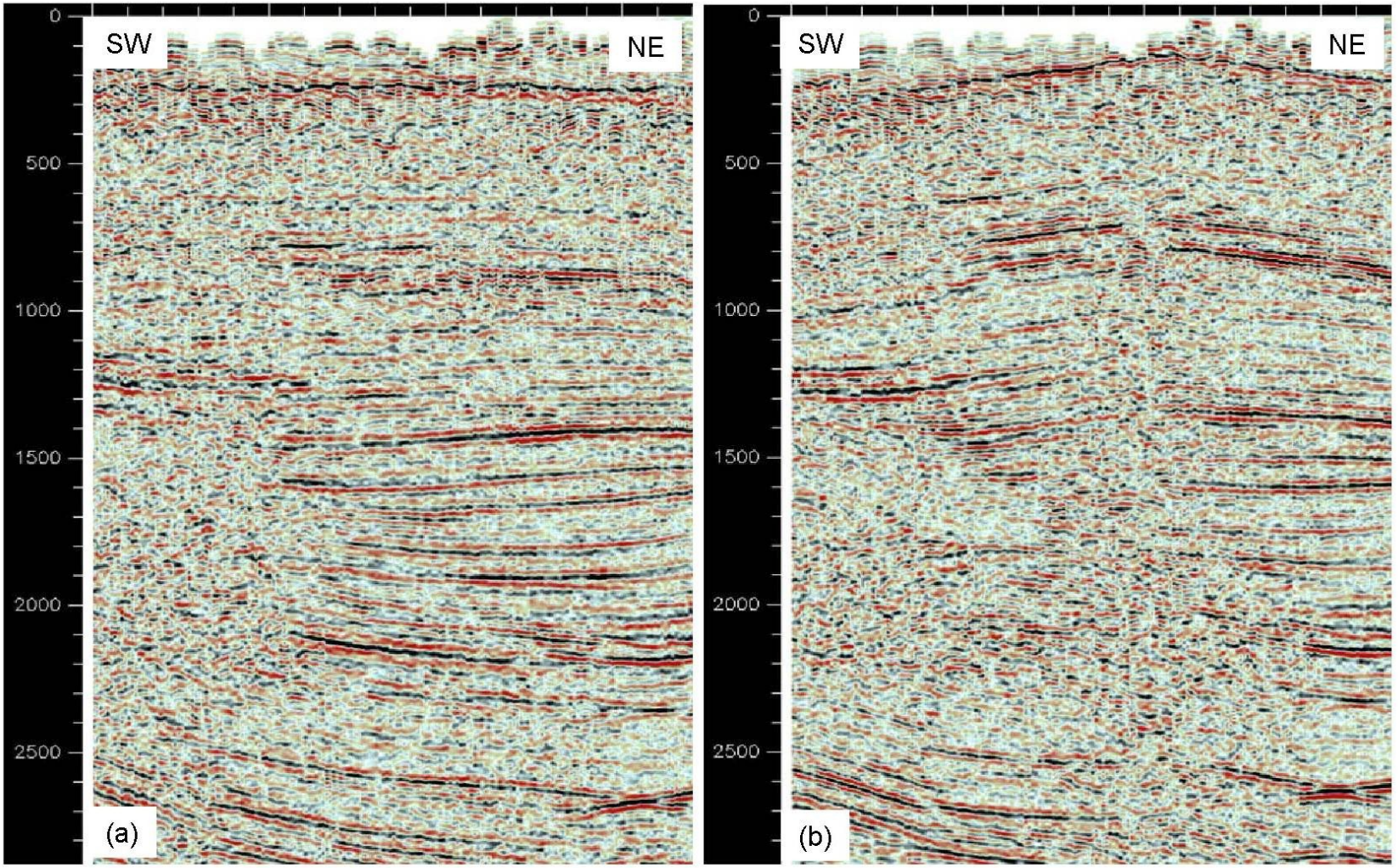

Figure 21 – The decimated receiver volume is shown after residual static corrections have been made. A correlation window of 600 – 3900 ms was used in (a), while 300 – 3900 ms was used in (b). False time structures are created in (b).

map aligned with elevation. In regions of higher elevations, the trace recorded more time prior to interaction with primary reflectors. Thus time had to be removed or subtracted in order to align events. Yilmaz (2001) also indicates the majority of static corrections in many other studies are related to changing topography just as they were for this study.

Though the residual static solution could not be displayed through the use of a map, a few observations are noted. The correlation window required to correct for residual statics changed for individual decimated volumes. However, with the different correlation window, the temporal placement of reflectors in the decimated volumes completely matched the reference volume.

Velocity Analysis

Many different velocities must be considered during processing, the most important being the stacking velocity estimated by the normal moveout (NMO) velocity. Yilmaz (2001) provides a review of these as follows. In a layered media, a stacking velocity is related to normal moveout velocity. These become related to the root mean squared velocity from which the average and interval velocities can then be calculated. The interval velocity is the average velocity over a specified interval. Thus, interval velocities in reference to geologic horizons are dependent on factors such as lithology, pore fluid, pressure, shape, and temperature. These variables will not change due to the acquisition techniques. However the interval velocities that are seismically derived will vary considerably due to changes in the ability to sample them. Stacking velocity is simply the velocity that yields the best stack. It is typically approximated by the normal moveout velocity given by the equation (Yilmaz, 2001):

$$t^2 = t_0^2 + \frac{x^2}{v_{NMO}^2} \tag{4}$$

where,

t = zero offset travel time [Time]
t_0 = measured travel time for x [Time]
x = offset [Length]
v_{NMO} = approximate velocity of medium above reflector [Length/Time]

This estimates the velocity required to flatten a reflector with hyperbolic moveout in order to create the best stack. When a small spread approximation is made the root mean squared velocity can be estimated from equation by replacing the v_{NMO}^2 term with v_{RMS}^2.

In order to approximate the stacking velocity several methods are used in interactively with one another. The velocity spectrum is one method by which stacking velocities can be estimated. This method is usually combined with another technique of comparing common mid-point (CMP) gathers side by side to observe flatness. The other method is referred to as constant velocity stacks (CVS). Each method has pros and cons, however when used together interactively a more confident set of velocities are found.

The use of velocity spectra with common mid-point (CMP) gathers usually allows for a reasonable approximation of stacking velocity. A velocity spectrum is constructed with a graph of velocity vs. time. The input data for each spectrum can be a single CMP or a group of selected CMP's. Next the input data is essentially corrected for normal moveout (NMO) and stacked repeatedly over a constant range of velocities. This converts the data from offset vs. two-way time to the stack velocity vs. two way zero offset time. When the spectrum is displayed the highest amplitude will appear at the velocity that should be chosen to stack the data. It is important to realize that the higher amplitude will appear with the contribution of the full range of offsets. Thus for detailed resolution of the spectrum long offsets are advised (Yilmaz, 2001). Stacked amplitude graphs can quickly become distorted and in practice are not the displays of choice to

represent velocity spectrum. Instead, coherency measured by semblance is typically used, hence semblance plots. The resulting graph shows a system of hot and cold colors that represent the coherency after cross correlation. The hot colors represent the velocities that should be used to obtain the NMO corrected data, or best stack. On the CMP gathers that are placed side by side this velocity should result in a flat reflector which can be used to verify the pick on the semblance plot.

Because the goal of a valid velocity model is to create the best stack, the CVS method allows us to empirically derive the best velocity. Constant velocity stacks use a designated number of CMP gathers stacked with one velocity throughout the recorded time and displayed as a panel. The panel is then repeated using a different velocity each time. Just as the case for the semblance plots the velocity resolution seems to decrease with increasing depth. This occurs for multiple reasons. First the offsets become smaller in relation to the depth. Second as the higher frequencies are attenuated the wavelet becomes less compact, thus the less accurate the velocity pick becomes (Yilmaz, 2001).

The major benefit of CVS is that the user can visualize the most important result in real time, namely the quality of the stack. However in a case where coherent noise is present, such as multiples, CVS are unbiased and unsuitable. In this case a velocity spectrum will be more useful to discriminate the multiple. The problem with velocity spectra alone only allow for the observation of a graph and not data unless used with CMP gathers, although CMP gathers are difficult to use in structurally complex regions. Thus, all three methods must be used together to obtain the best results.

In this study super gathers, which are multiple adjacent bin combined for processing, were used to construct velocity spectra with semblance used as the coherency

measure (Figure 22 – 25). All of the spectra use a purple line, pink line, and green crosses to show the results of the processors velocity picks. The specific picks are indicated by the crosses while the purple line merely shows the slope. Chosen picks do not necessarily indicate key geologic horizons, but were strategically placed to honor the changes in vertical velocity trends. However if picks are made too closely in time anomalous interval velocities could be created. The pink lines are interval velocities for the areas between picks.

The velocity spectrum with a set CMP gathers for the reference volume is shown in Figure 22. The spectrum indicates the high measure of coherency from the shallow section down to approximately 4 seconds. The CMP gathers also exhibit flattened horizons that validate the velocities used. The velocity spectra and CMP gathers for the decimated receiver and decimated shot volumes are shown in Figure 23 and 24, respectively. Again, the semblance appears very tight until roughly 4 seconds. The shape and the location of the hot spots are similar to the reference volume with a few

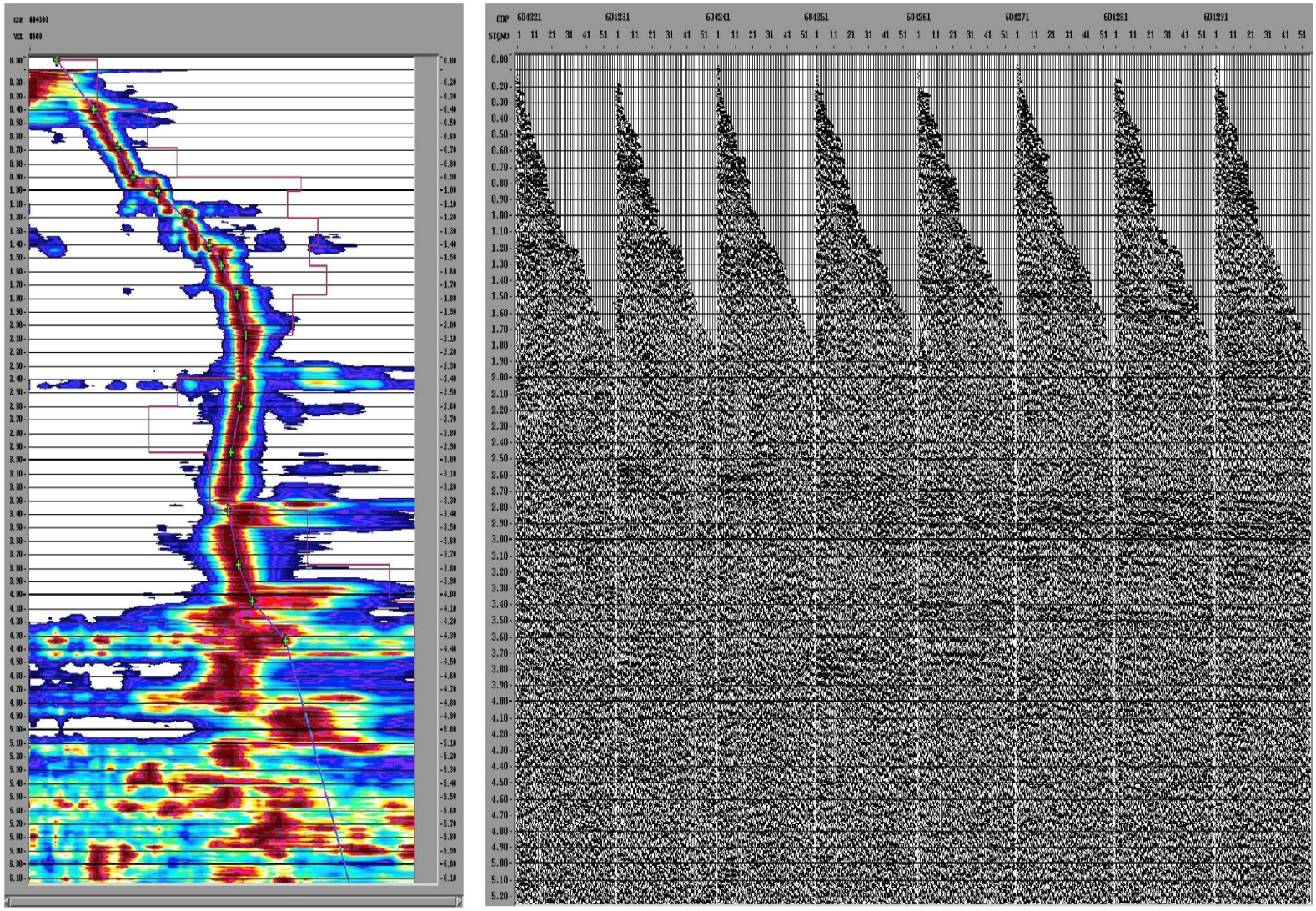

Figure 22 – Semblance plots and gathers for the reference volume. The semblance plot (left) shows the strength of coherency. Hot colors indicate strong agreement. Green "+" indicate the processors pick while the blocky pink line shows interval velocities between picks. The gathers (right) shows flattened reflectors on multiple CMP's with the correct velocity pick.

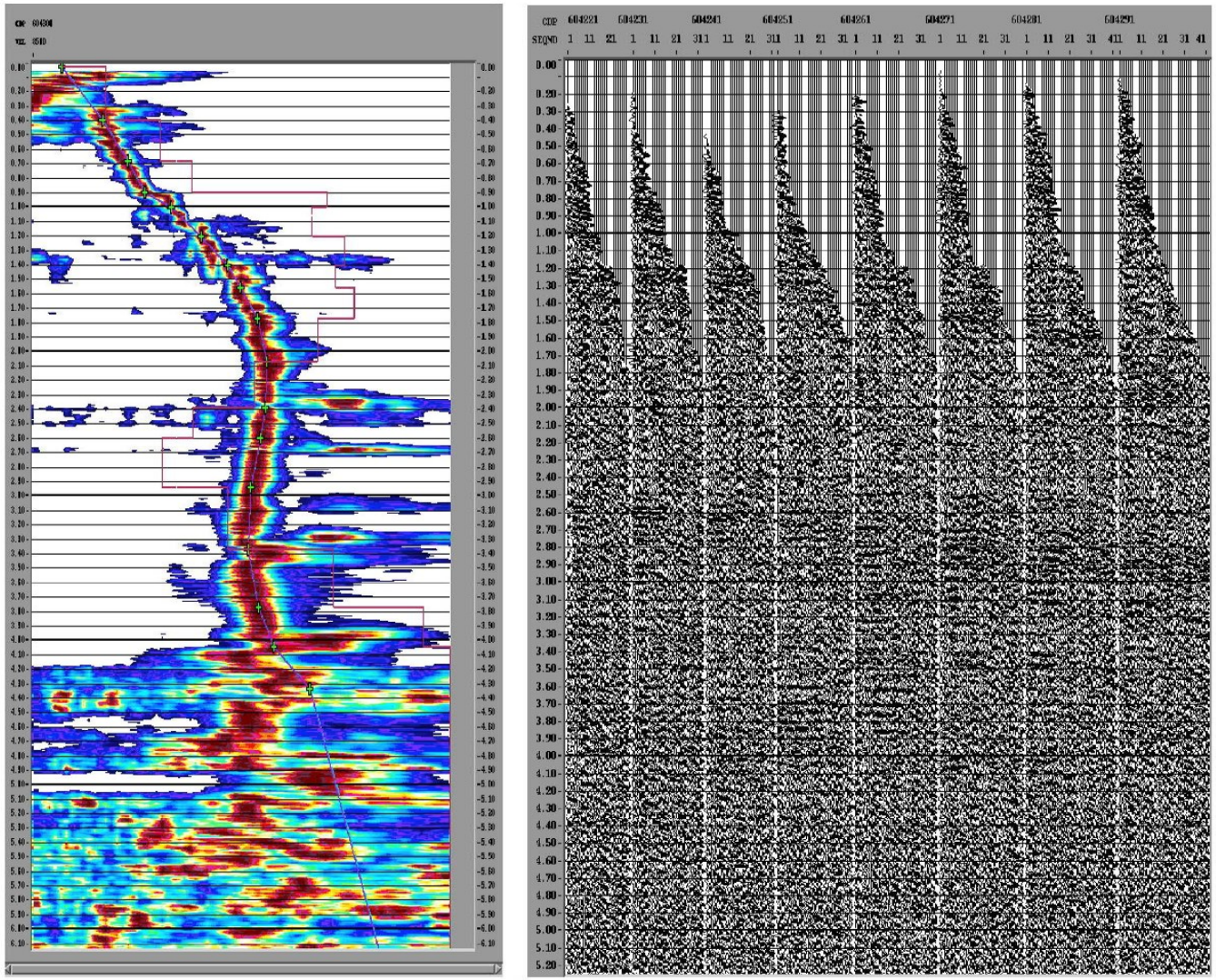

Figure 23 – Semblance plots and gathers for the decimated receiver volume. The semblance plot (left) shows the strength of coherency. Hot colors indicate strong agreement. Green "+" indicate the processors pick while the blocky pink line shows interval velocities between picks. The gathers (right) shows flattened reflectors on multiple CMP's with the correct velocity pick.

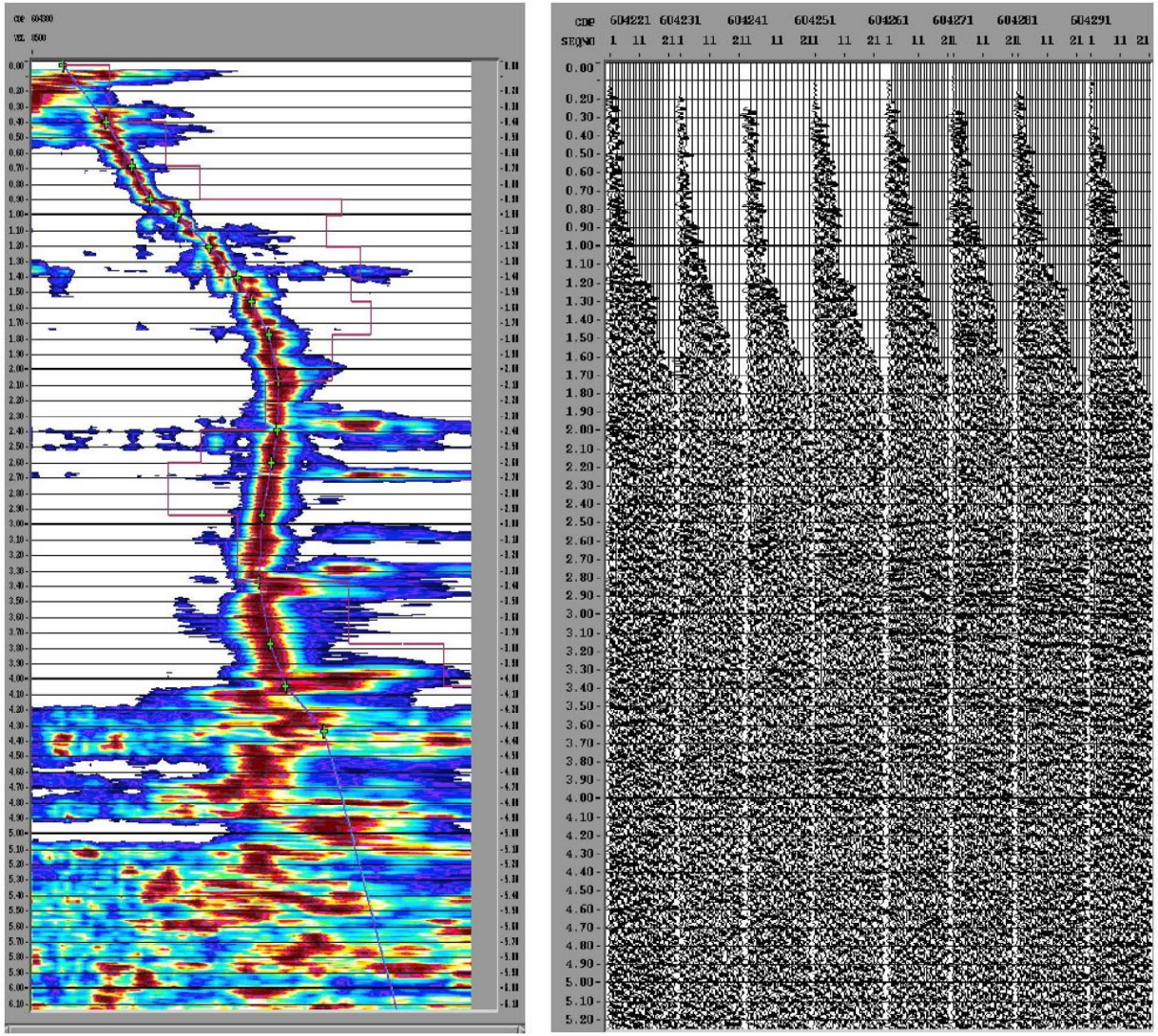

Figure 24 – Semblance plots and gathers for the decimated shot volume. The semblance plot (left) shows the strength of coherency. Hot colors indicate strong agreement. Green "+" indicate the processors pick while the blocky pink line shows interval velocities between picks. The gathers (right) shows flattened reflectors on multiple CMP's with the correct velocity pick.

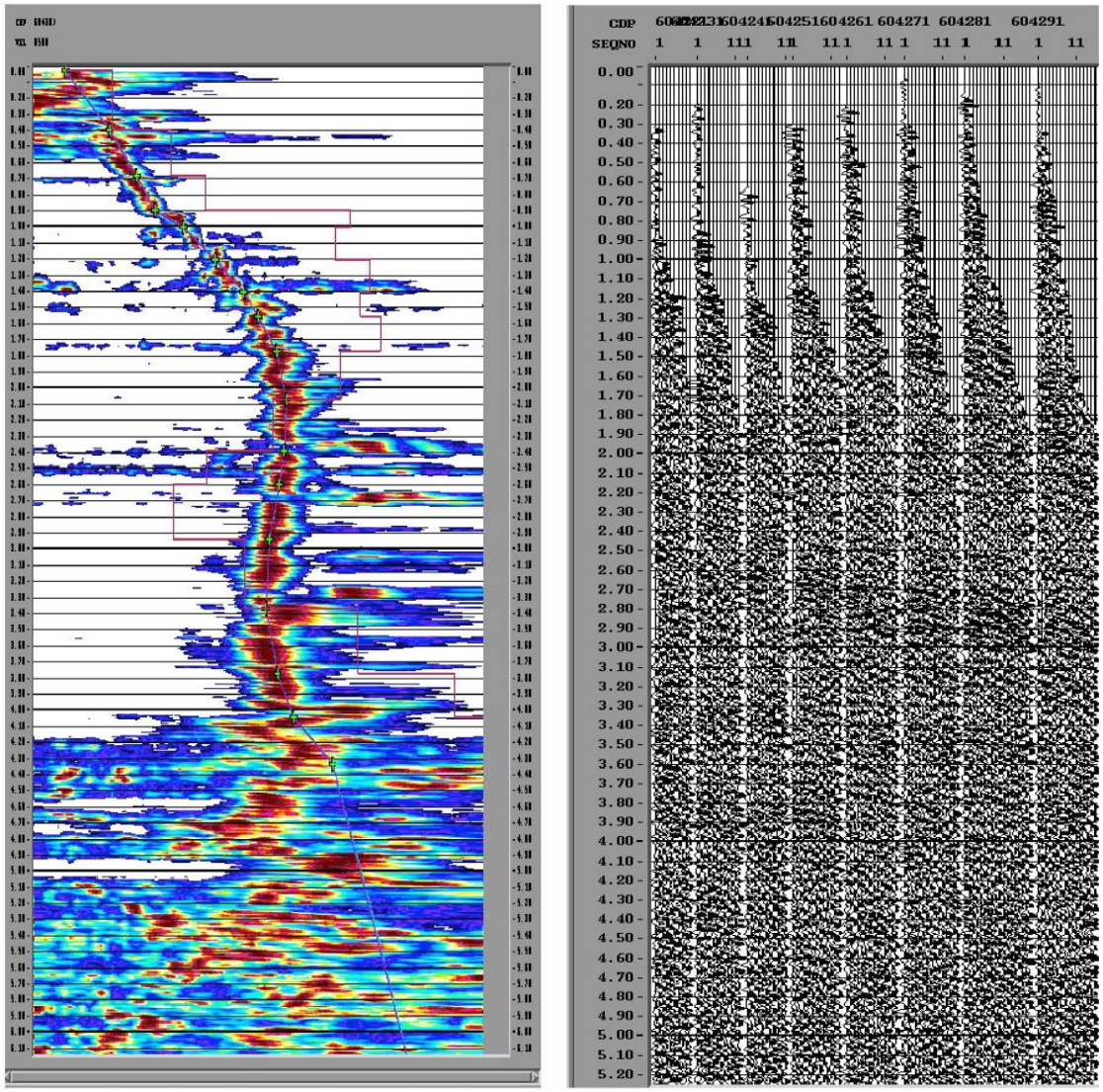

Figure 25 – Semblance plots and gathers for the decimated shot and receiver volume. The semblance plot (left) shows the strength of coherency. Hot colors indicate strong agreement. Green "+" indicate the processors pick while the blocky pink line shows interval velocities between picks. The gathers (right) shows flattened reflectors on multiple CMP's with the correct velocity pick.

minor exceptions. Just as for the reference volume, the gathers appear to agree with the velocities that have been chosen to flatten reflectors. Figure 23 – 26 also demonstrate the difference in fold for the same CMP in all four volumes. At these particular locations the decimated receiver seems to maintain 30 to 40+ fold compared to the 55+ fold exhibited by the reference volume. The decimated shot only has approximately 22 fold at these locations. However, regardless of the fold, all the CMP gathers show the difficulty in observing flatten reflectors in complex structural areas.

In the final volume of decimated shot and receiver (Figure 25), the coherency still remains concentrated, though much more distorted, down to 4 seconds. The gathers in this region are at very low fold of approximately 13, which makes it very difficult to determine the attitude of the reflectors. Yilmaz (2001) presents that the resolution within velocity spectra are strongly affected by the range of offsets. This supports the results that are shown in this study. The velocity spectra of the decimated volumes still represent the velocity trend very well compared to the reference volume. Since only the fold decreased and not the range of offsets this allowed for accurate velocity spectra.

The constant velocity stacks in this study used a line of 32 CMP gathers and were migrated. Migration provided a better stack to evaluate for the best stacking velocity. The display panels for the CVS remains the same in time but reveals the velocity used at the very top in increments of roughly 150 ft/s. Again the processor's picks are indicated by green crosses and the slope drawn by the purple line. The picks are interactive between the CVS and velocity spectrum. Comparing the constant velocity stacks in

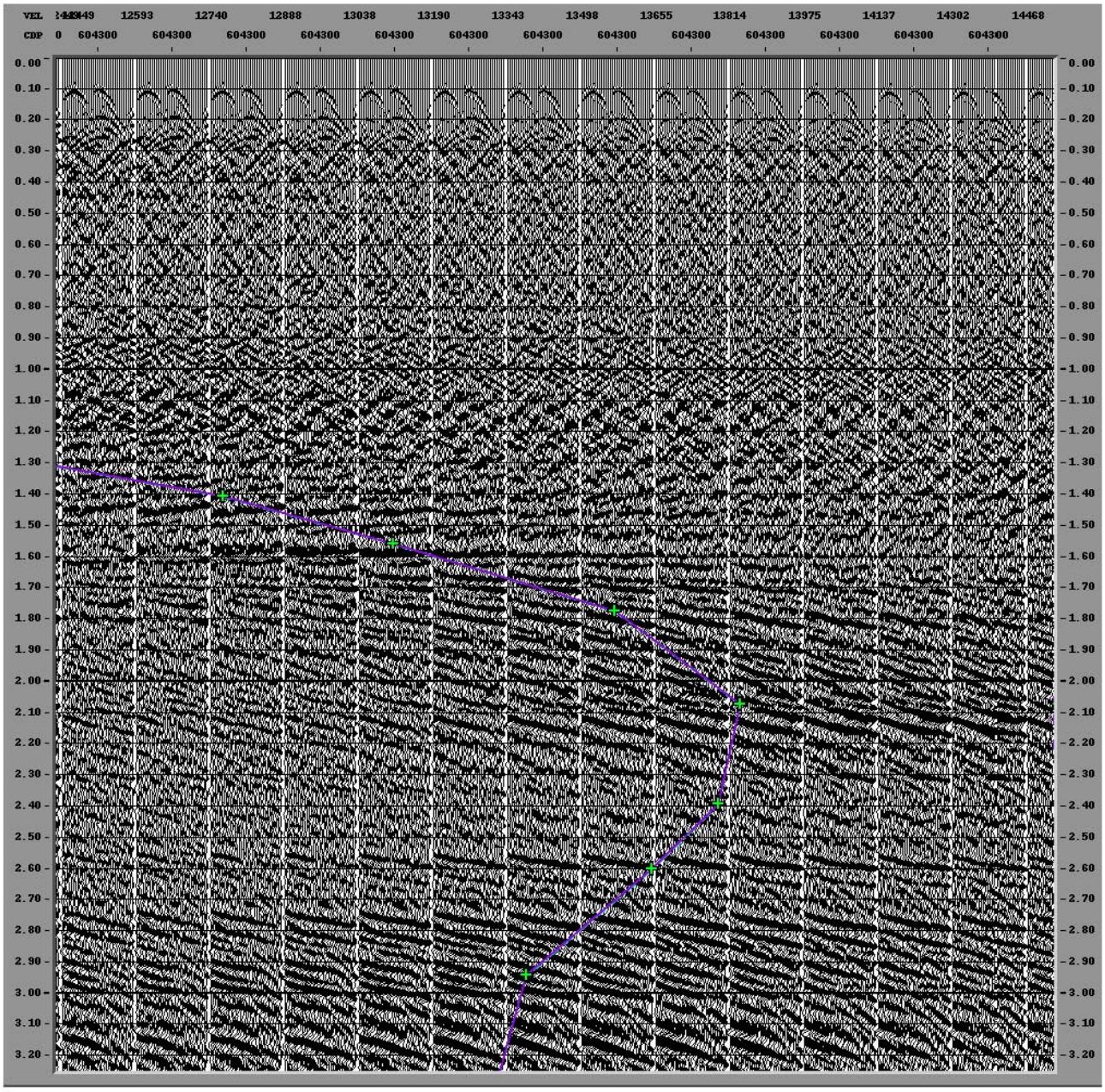

Figure 26 – Constant velocity stack for the reference volume. The processor's picks are indicated by the green "+."

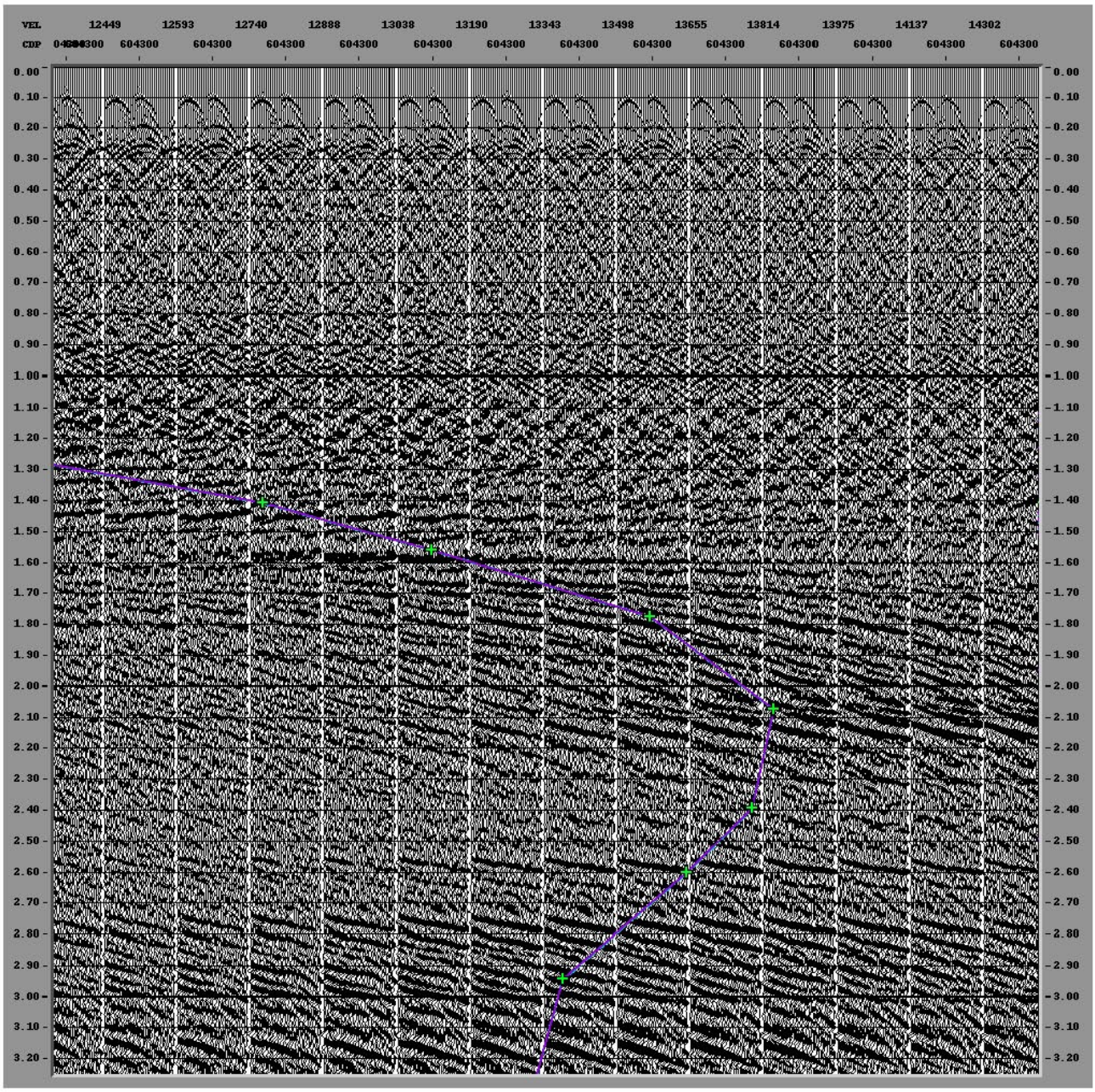

Figure 27 – Constant velocity stack for the decimated receiver volume. The processor's picks are indicated by the green "+."

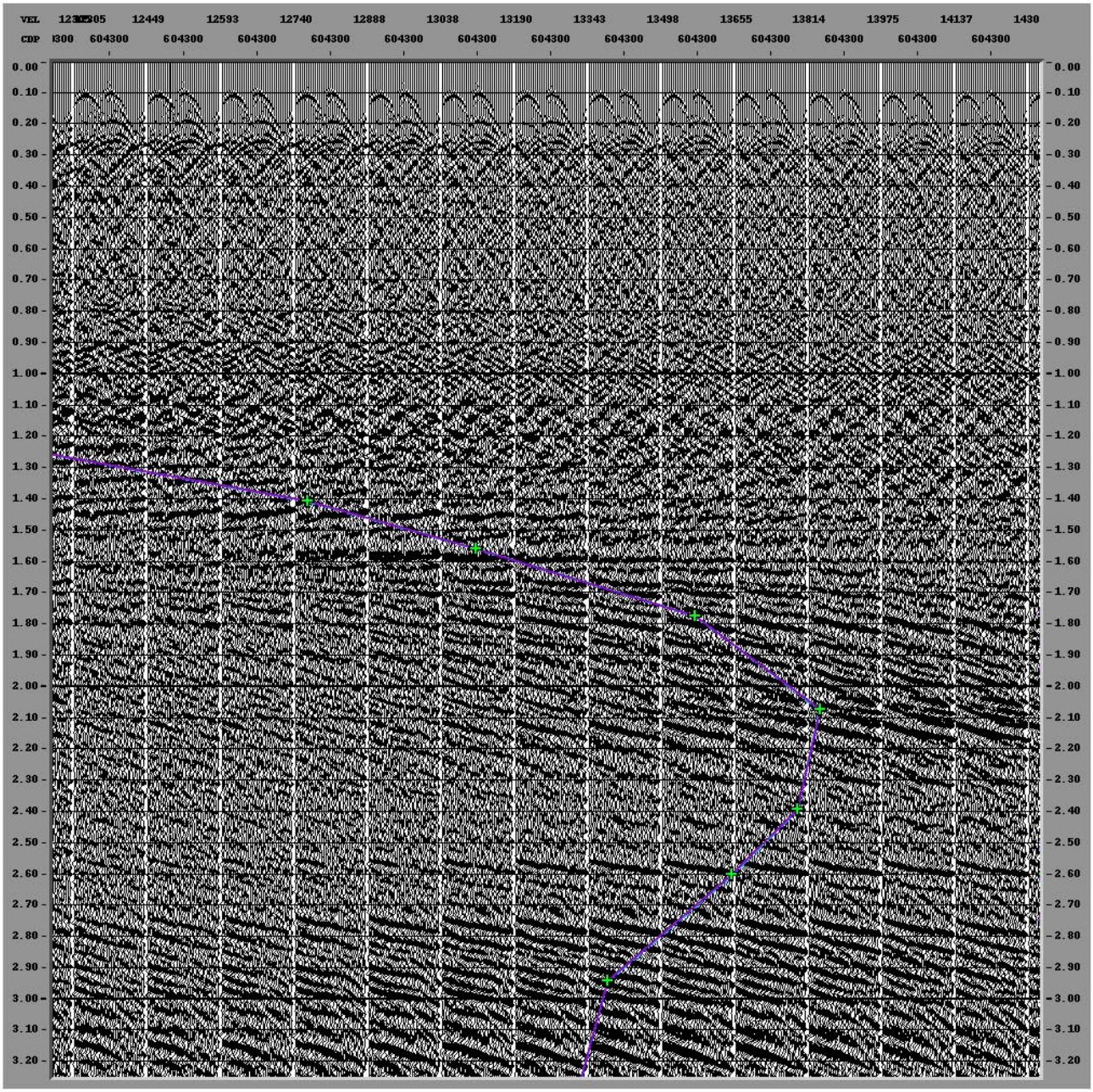

Figure 28 – Constant velocity stack for the decimated shot volume. The processor's picks are indicated by the green "+."

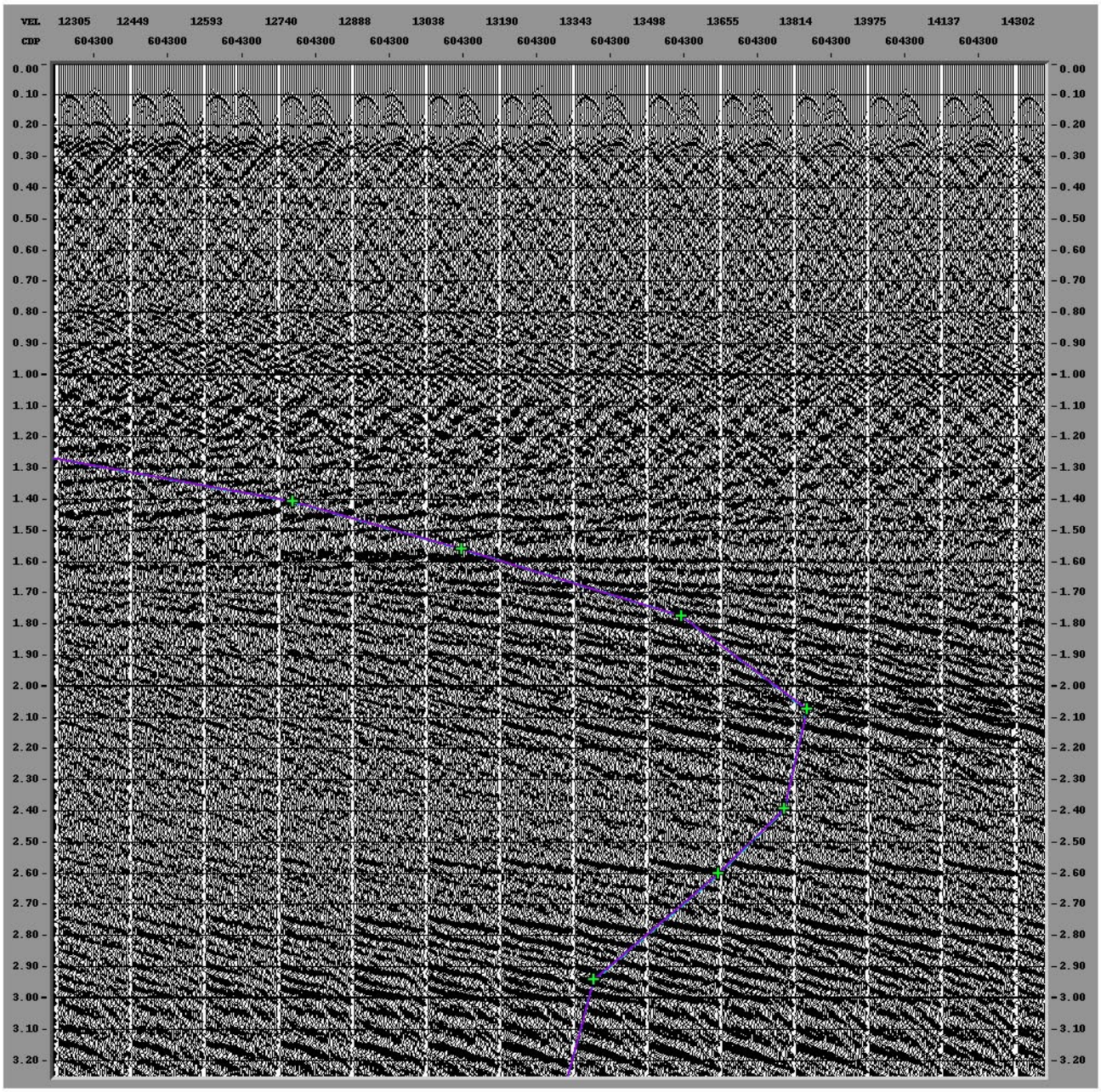

Figure 29 – Constant velocity stack for the decimated shot and receiver volume. The processor's picks are indicated by the green "+."

Figure 26 – 29, the stacking quality appears identical. This better explains why the processor's picks did not change in the velocity spectra (Figure 22 – 25). Though the spectra had little spatial disagreement the distortion may have caused the picks to change if CVS were not incorporated into the analysis.

Through the assistance of the CVS the velocity model was accurately recreated with each decimated volume. Thus CVS proved its value for velocity selections in a structurally complex region and allowed the velocity analysis overall to be minimally affected.

CHAPTER V

COMPARISON OF FINAL DECIMATED IMAGES

Following the analysis of the effects of decimation on processing, this study progressed to the interpretation stage. With regards to processing, the decimation volumes actually performed very well compared to the reference volume. However based on the decrease of fold observed in the fold plots the final product was expected to show considerable degradation with lowering signal to noise (S/N) ratios. In order to compare the reference and decimated datasets several approaches were used. An in line, cross line, and set of time slices was taken from each volume as shown in Figure 30. These lines and slices were selected based on the well location to compare the image quality. Well A is known to have a sonic log that can tie the seismic data from the originally licensed migrated dataset with the geology. The synthetic seismogram from the well was used to compare the ability of the seismic data from each volume to tie into the geology. Additionally, difference volumes and amplitude maps were used to compare each volume.

Empirical Observations – Cross-sections

First, comparisons were made using visual observations because these images have the largest affect on an interpreter's ability to pick horizons. Interpretation capability is influenced by the character of the reflector such as the continuity and coherency of the signal. These observations will be made on four in lines (Plate 1) and

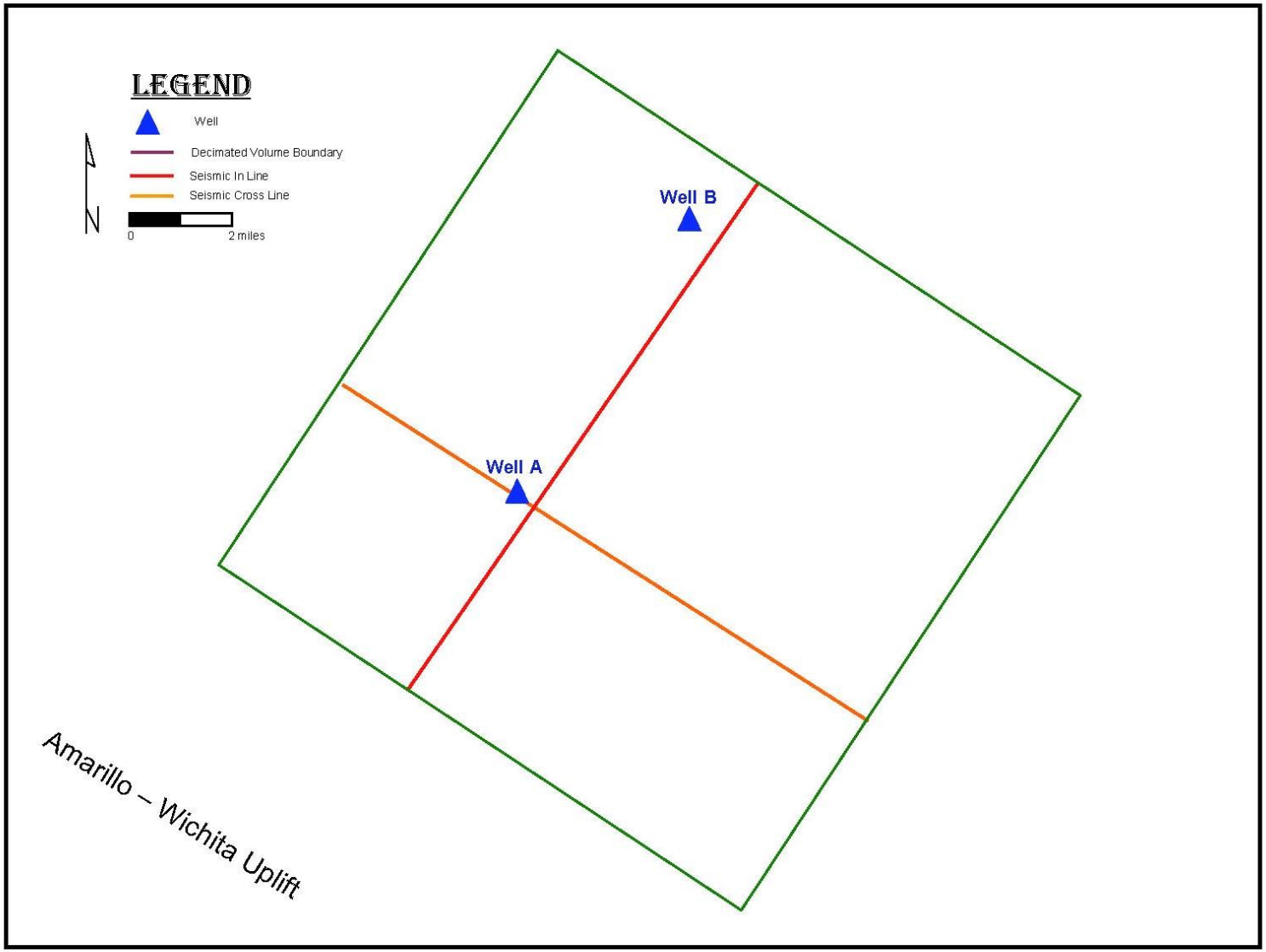

Figure 30 – Layout of the 25 mi^2 extraction near the Amarillo – Wichita Uplift.

four cross lines (Plate 2) that are all unmigrated. For specific comparisons sections of the plates have been enlarged and shown in subsequent figures.

Enlargements were extracted from the plates for ease of comparison. Each enlargement displays a significant difference in the quality of the image compared to the reference volume. The first expanded section in Figure 31 shows the changes of two shallow horizons at approximately 250 ms and 600 ms in each volume. Both horizons are strongly affected by the low fold caused by the muted zone which is displayed by the common mid-point gathers in Figures 22 - 25. While all decimated volumes failed to fully image the upper horizon as compared to the reference volume but the decimated shot volume best captures the lower reflector at 600ms (Figure 31c). The area in between horizon 1 and 2 is enlarged in Figure 32. The images of the decimated volumes are all degraded relative to the reference volume. In this case, it is not as obvious which decimated volume provides the most accurate image. However, the decimated receiver image may be easier to interpret because the right half of the section shows more continuity of the signals. The decimated shot and receiver volume failed to extensively image the reflections compared to the decimated shot and decimated receiver.

Deeper in the section (Figure 33) between horizons 2 and 3, the area is characterized in the left and right portions of the cross-sections by structural complexity which displays as noise. This area seems to have maintained its integrity in all of the decimated volumes. The last enlargement figure on the in line direction is located in an area known to contain a fault in the left half of the section (Figure 34). This area also

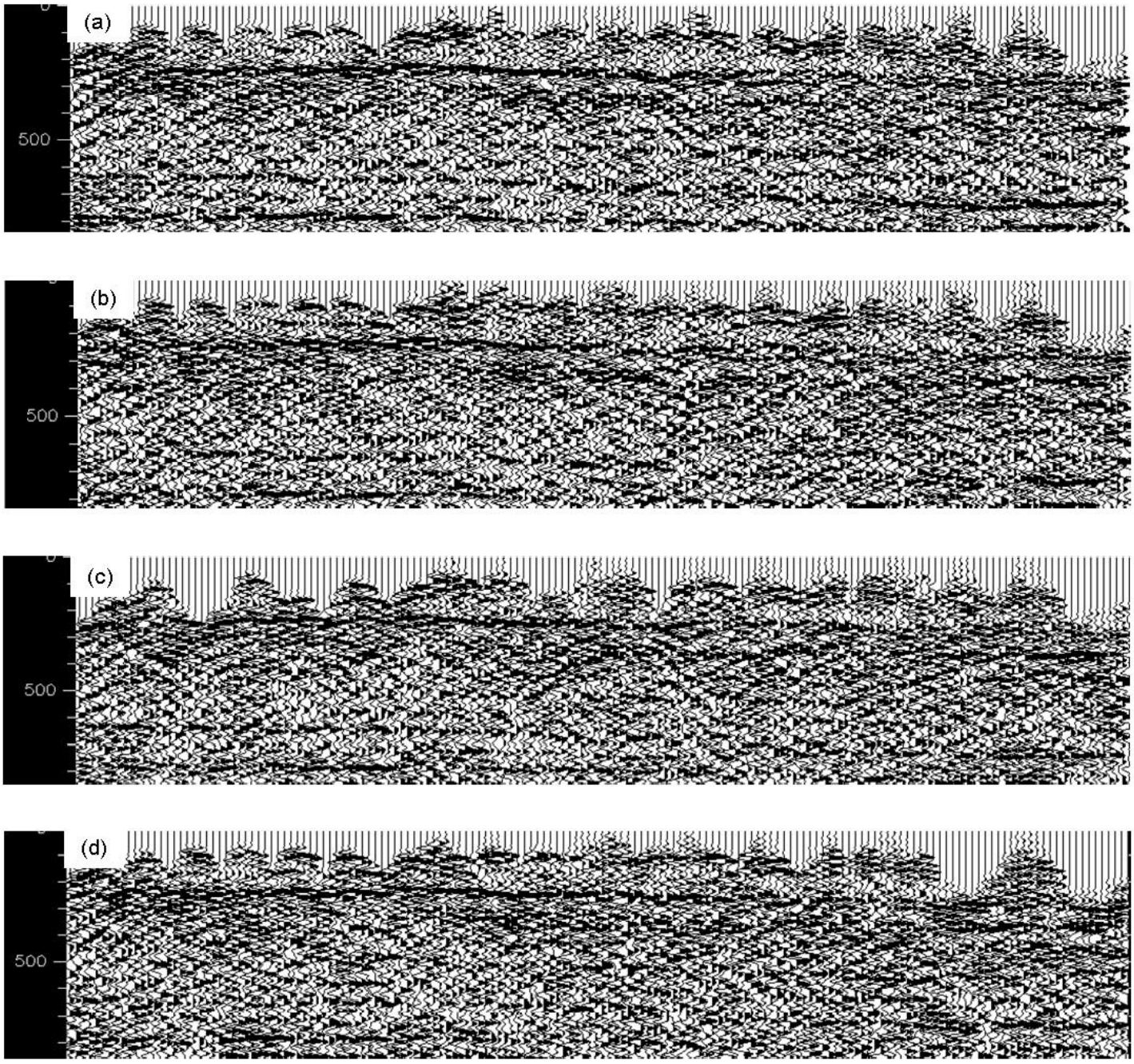

Figure 31 – These specific areas of interest show the difference in image quality for the (a) reference, (b) decimated receiver, (c) decimated shot, and (d) decimated shot and receiver. These enlargements were taken from Plate 1 (in line sections).

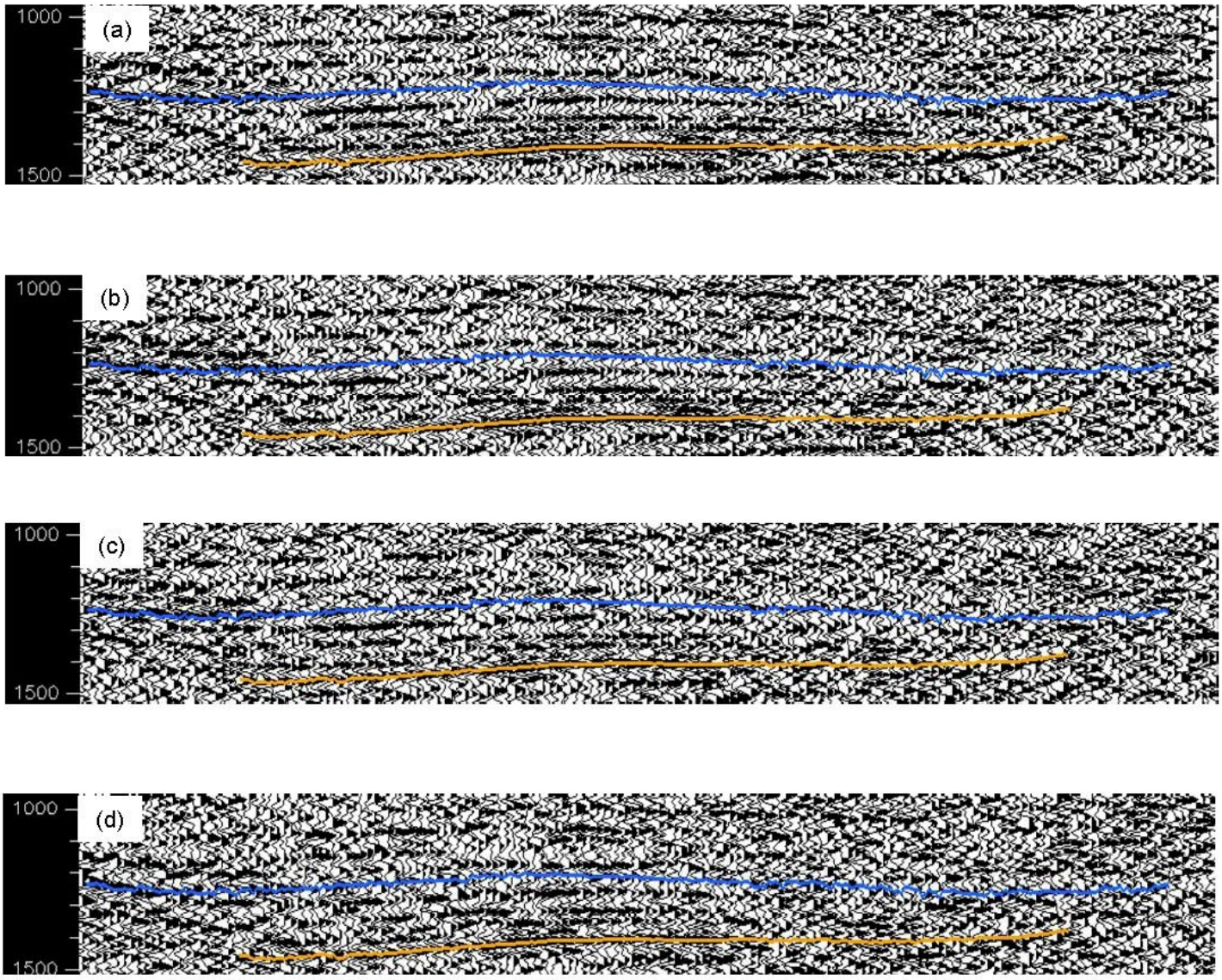

Figure 32 – These specific areas of interest show the difference in image quality for the (a) reference, (b) decimated receiver, (c) decimated shot, and (d) decimated shot and receiver. These enlargements were taken from Plate 1 (in line sections). Horizon 1 is indicated by the blue line while horizon 2 is denoted by the orange line.

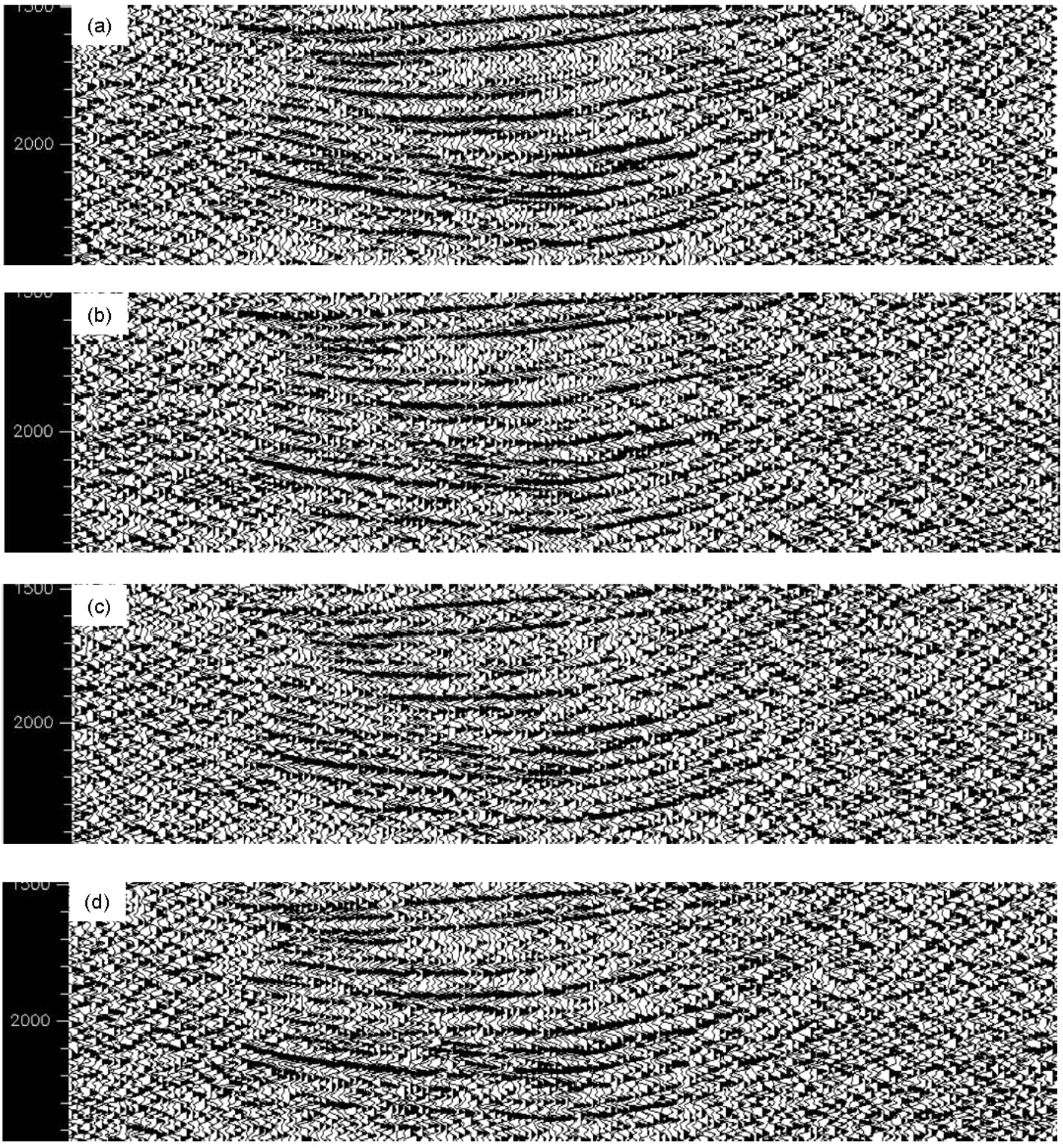

Figure 33 – These specific areas of interest show the difference in image quality for the (a) reference, (b) decimated receiver, (c) decimated shot, and (d) decimated shot and receiver. These enlargements were taken from Plate 1 (in line sections).

demonstrates the "bow tie effect," which is when waves dipping in opposite directions intersect one another located above an anticlinal structure and results from the lack of migration over synclines. In each decimated volume, noise has aliased a considerable amount of reflectors that were visible in the reference volume. The decimated shot volume (Figure 34c) produces the worst image of all the decimated volumes. For example the decimated shot and receiver volume (Figure 34d) and decimated receiver volume (Figure 34b) captures the diffraction energy on the right-side. These reflectors are absent in the decimated shot image (34c).

Comparing the volumes in the cross line direction did not yield the same obvious differences as the in-line direction. An enlarged section from around 600 ms is shown in Figure 35. The effect of low fold still remains evident in each decimated volume by the degraded image quality in Figure 35. Although, the rest of the image seems to be well represented by each of the decimated versions. There are some amplitude differences, represented by varying strengths of signal, that can be seen but this issue will further be tested and discussed later.

Flex binning

Flex binning is a common technique, in processing, that allows a bin, when found devoid of a certain offset, to expand in all directions in search of a trace with the required offset to duplicate. Though the bin size expands, the bin interval does not change. Overall, flex binning resulted in cleaner images for all of the decimated versions (Plates 1 and 2), as compared to images where it was not employed (data not shown). In

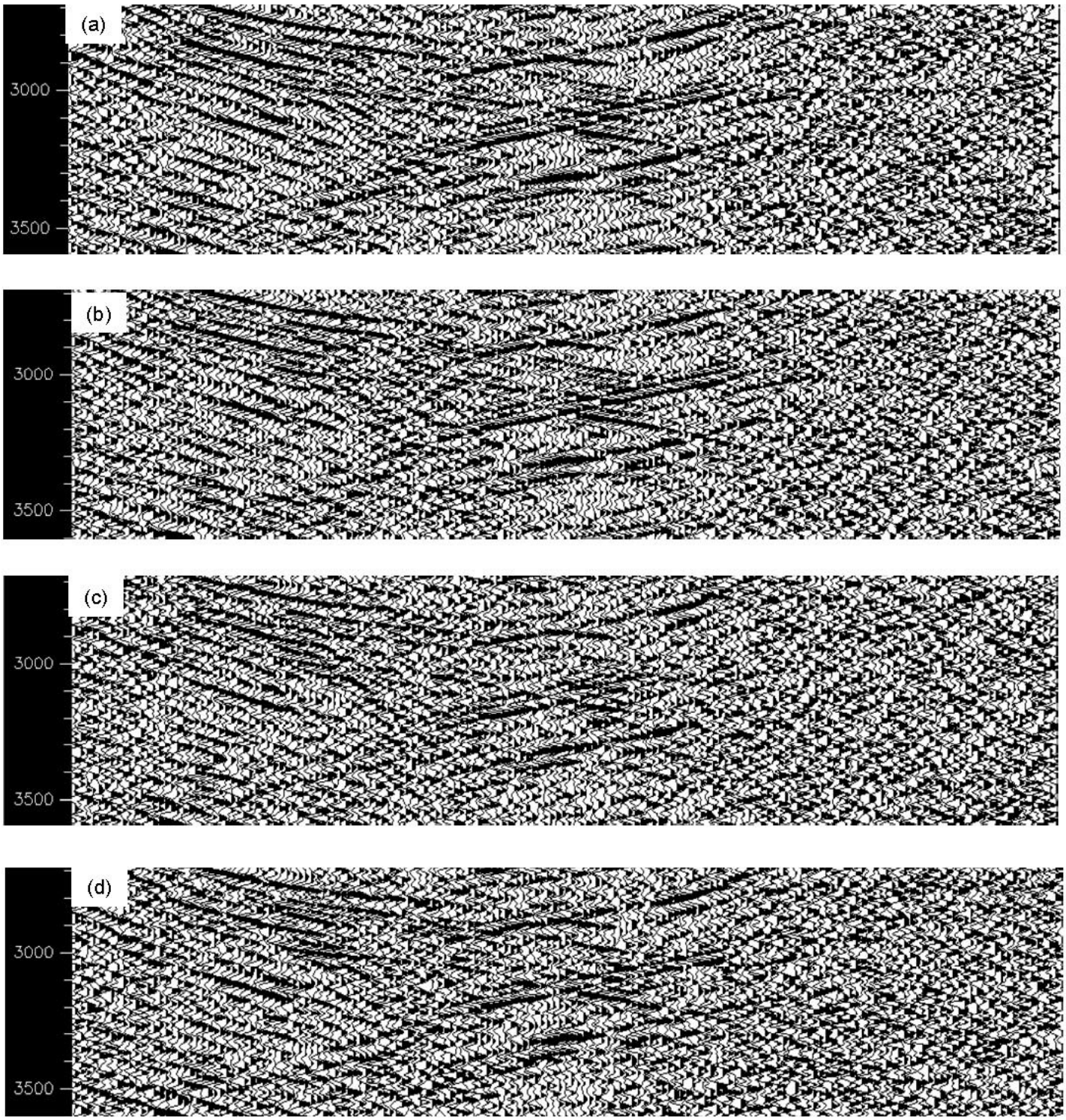

Figure 34 – These specific areas of interest show the difference in image quality for the (a) reference, (b) decimated receiver, (c) decimated shot, and (d) decimated shot and receiver. These enlargements were taken from Plate 1 (in line sections).

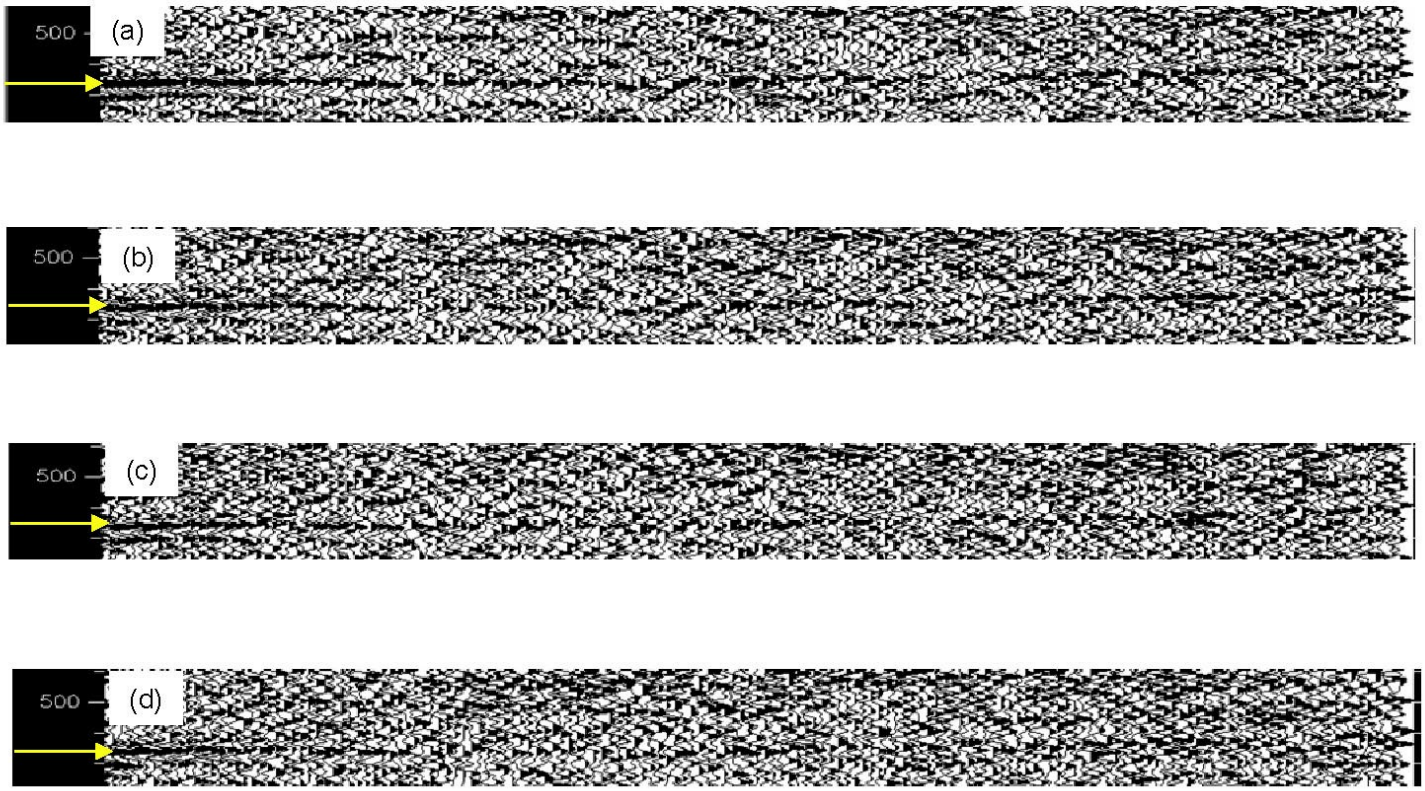

Figure 35 – These specific areas of interest show the difference in image quality for the (a) reference, (b) decimated receiver, (c) decimated shot, and (d) decimated shot and receiver. These enlargements were taken from Plate 2 (cross line sections).

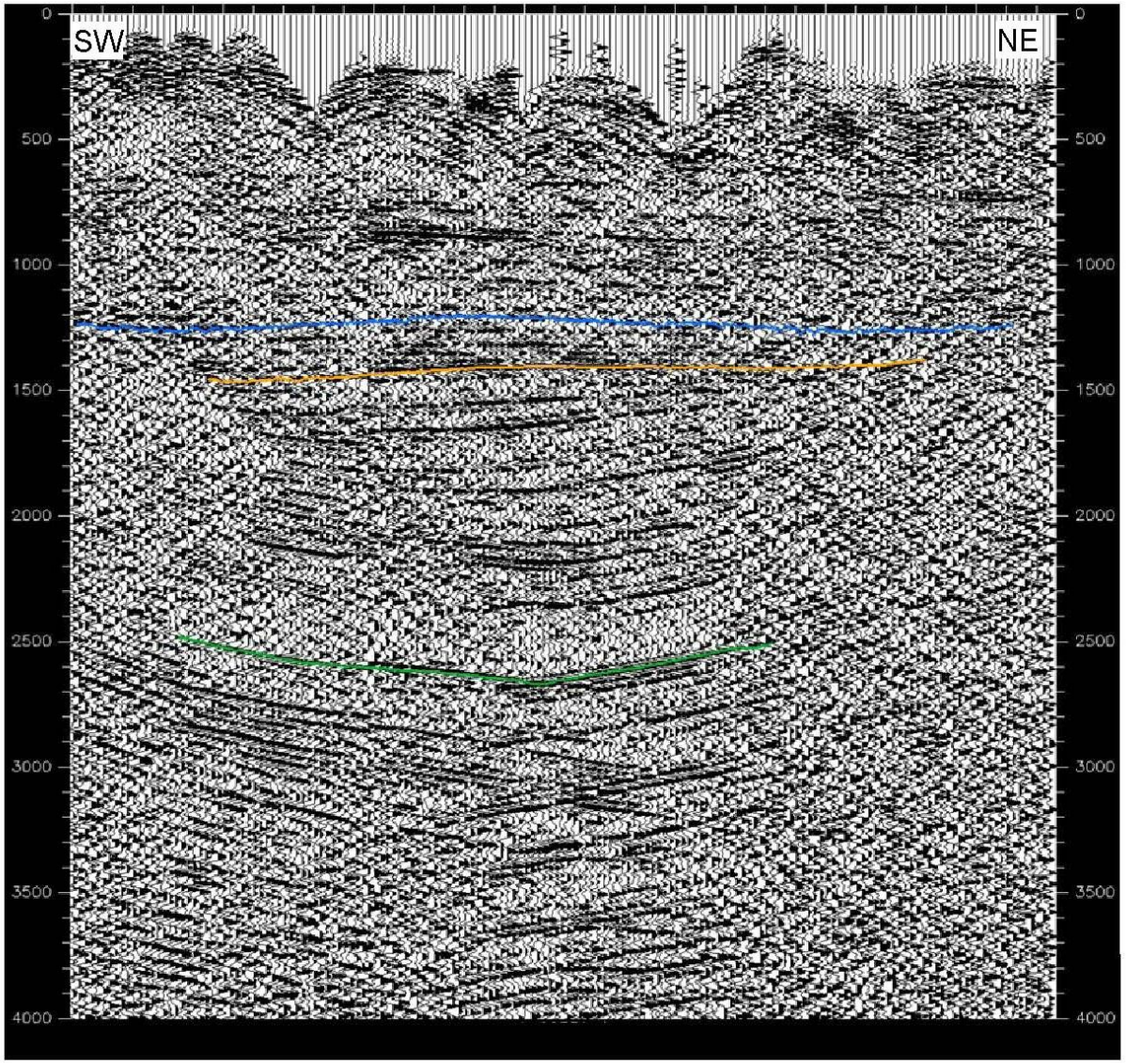

Figure 36 – Seismic cross section taken in line from the decimated receiver volume before flex binning has been applied. The horizons are shown by the blue (1), orange (2), and green (3) lines.

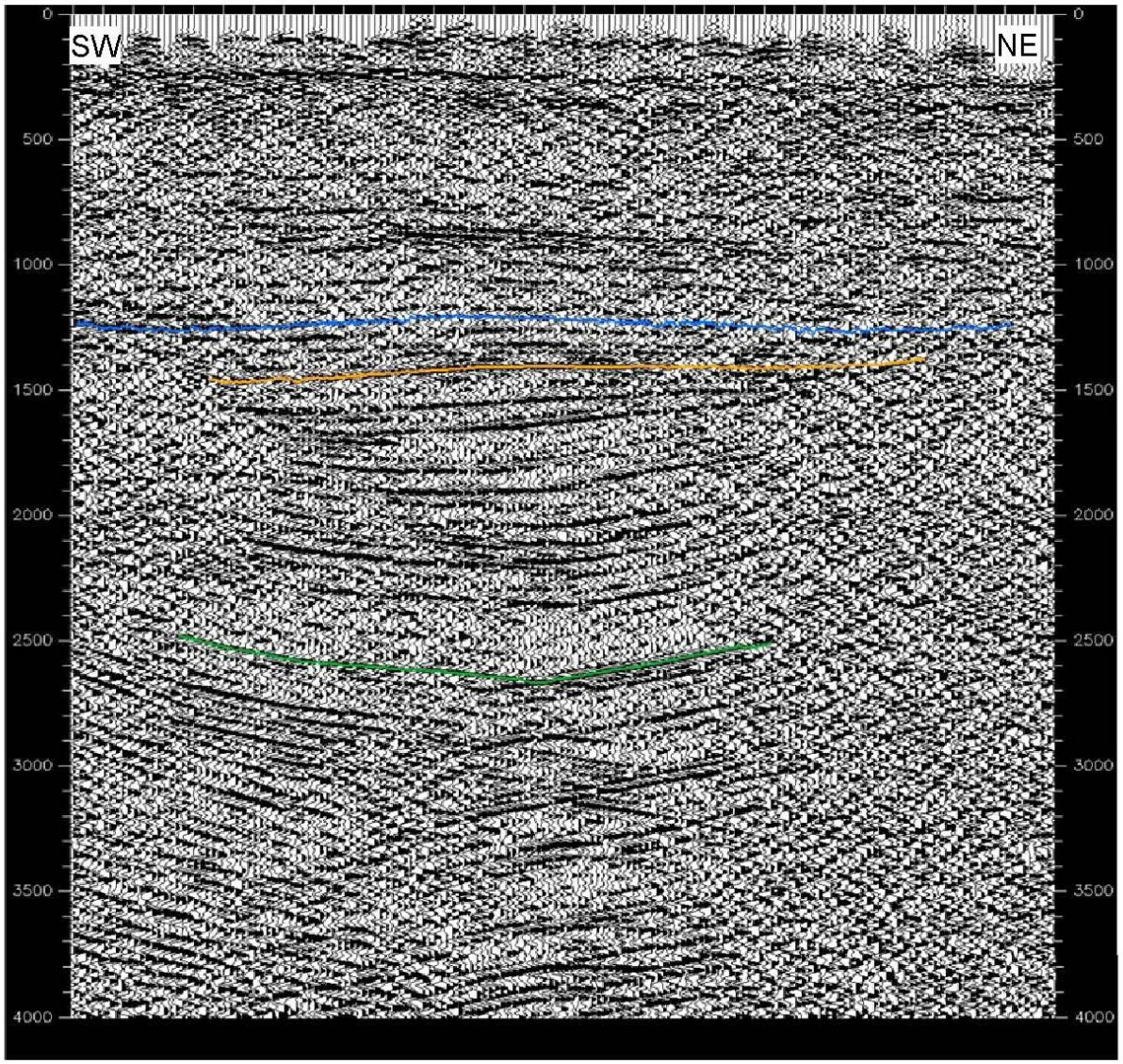

Figure 37 – Seismic cross section taken in line from the decimated receiver volume after flex binning has been applied. The horizons are shown by the blue (1), orange (2), and green (3) lines.

decimation, when every other shot and/or receiver is taken out, unevenness develops in the fold distribution, especially when the bin size remains the same. This problem can occur without decimation due to irregular subsurface topography, though it was not observed in the reference volume. To compensate for the "checkerboard" effect from areas of alternating high and low fold, flex binning is used to expand to nearby traces that are duplicated in empty bins. Only the decimated receiver volume was used as an example to show the effects of flex binning. Comparing Figure 36 and Figure 37 demonstrates how flex binning results in better, more accurate final images. Focusing on the shallower sections from 100 ms through 2500 ms, a more interpretable image results after the process has taken place. However, when looking in the deeper section to the left of the diffractions, the flexed version actually loses coherency of reflectors which may indicate that flex binning does not always increase interpretability.

The cross line direction images show drastic improvement through the use of flex binning (Compare Figure 38 and 39). There is little interpretable data until below 600 ms when flex binning is not used (Figure 38). There is also a consistently noisy area visible throughout the recorded section. When flex binning is used (Figure 39), the result is a better image, where horizons can be tracked across the entire length of the section.

In this study flex binning also helped avoid false time structures. For example, Figure 40 shows a time slice at 2900 ms for the decimated receiver volume before (a) and after (b) flex binning was applied. In the non-flexed version (Figure 40a) there is break in the amplitude which could be interpreted as a fault. However, the flex binned version

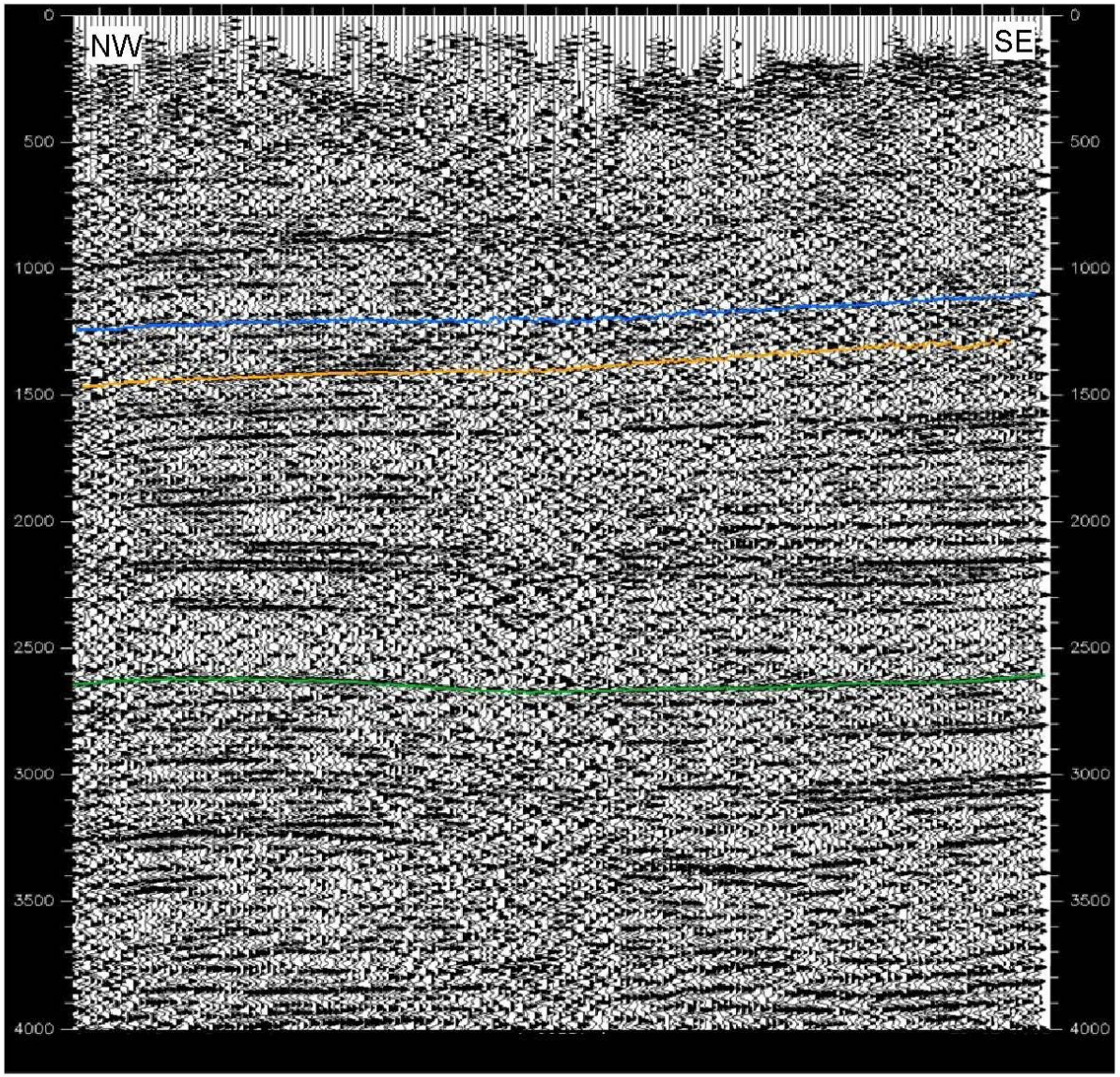

Figure 38 – Seismic cross section taken in line from the decimated receiver volume before flex binning has been applied. The horizons are shown by the blue (1), orange (2), and green (3) lines.

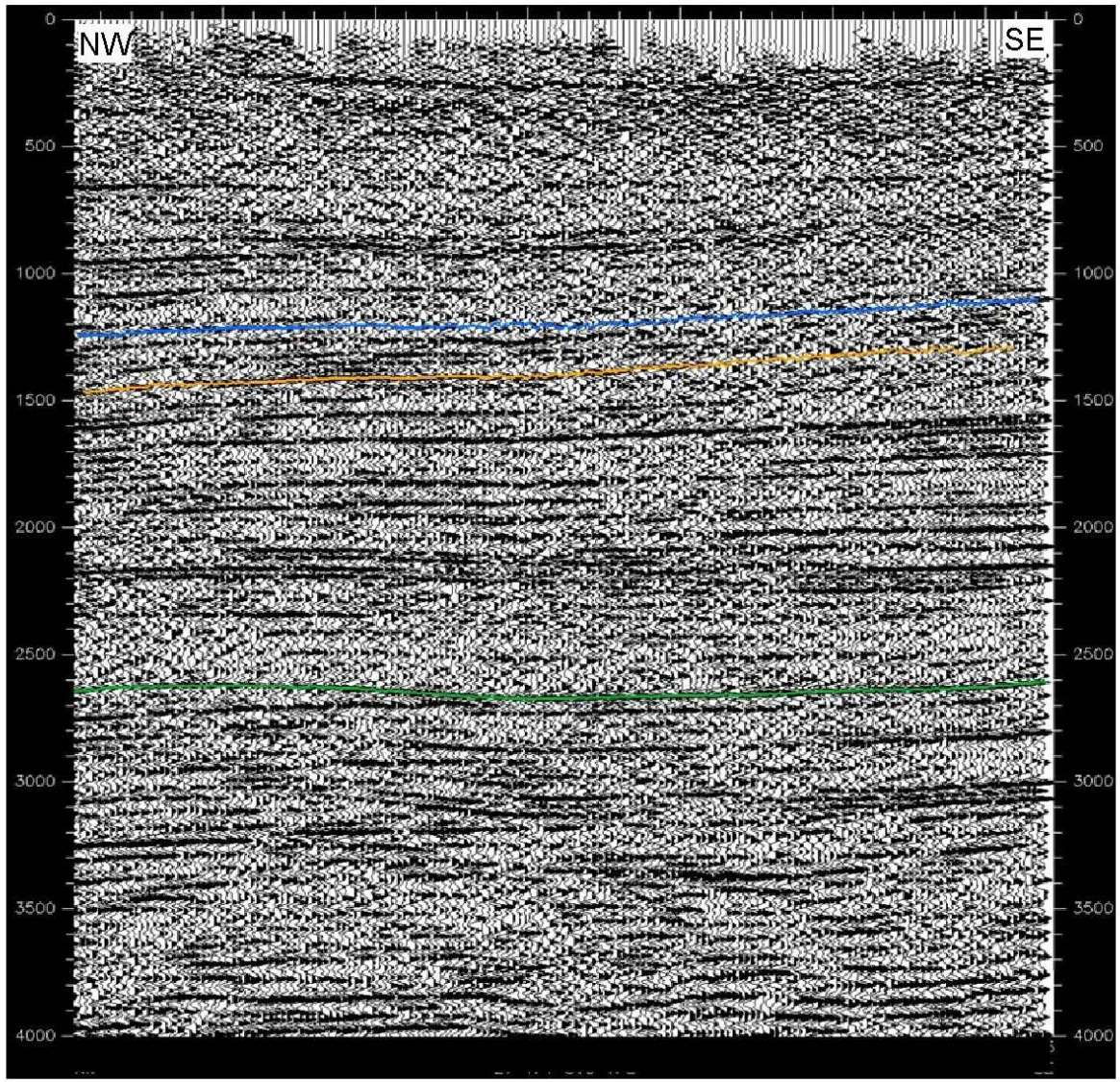

Figure 39 – Seismic cross section taken cross line from the decimated receiver volume after flex binning has been applied. The horizons are shown by the blue (1), orange (2), and green (3) lines.

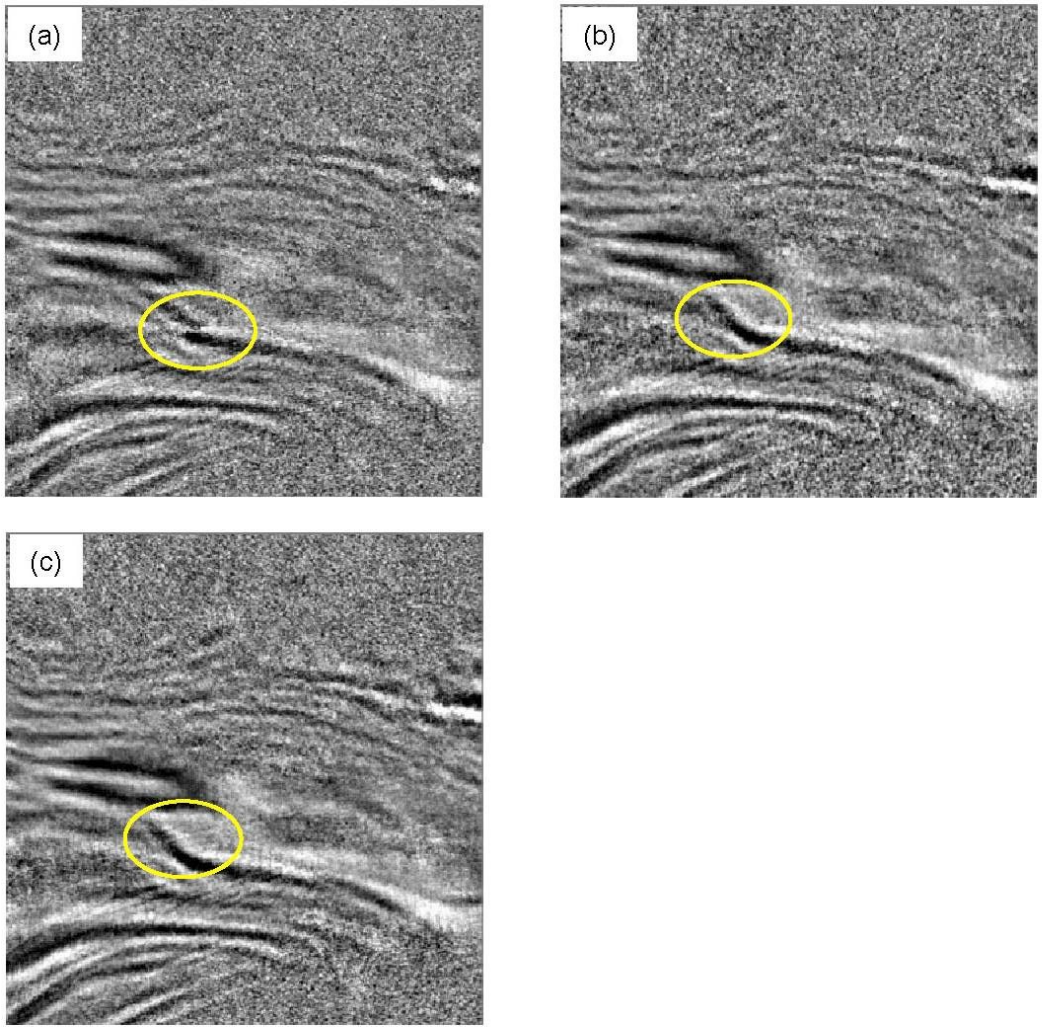

Figure 40 – Time slices taken at 2900 ms for the (a) decimated receiver volume before flex binning, (b) decimated receiver after flex binning, and (c) reference volumes. The circle denotes the potential fault created in the decimated receiver volume without flex binning.

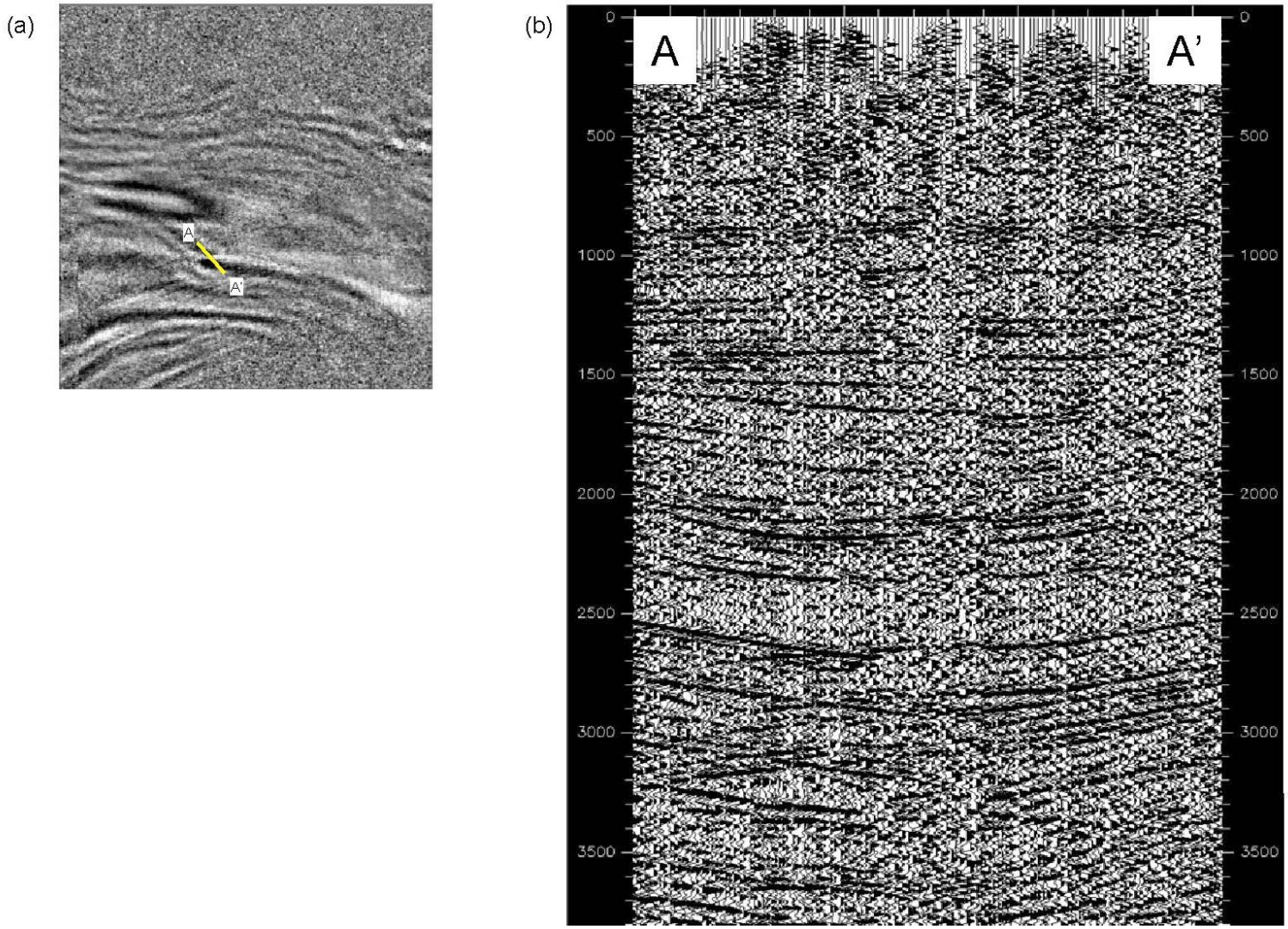

Figure 41 – Time slice (a) taken at 2900 ms from the decimated receiver volume before flex binning. Seismic cross section (b) taken from A – A' in (a).

does not have this feature nor does the reference volume (Figure 40c). A cross-section was then extracted through the area of interest on the decimated receiver, non-flexed image (Figure 41). The cut reflector in cross-section shows a shift in time that resembles the throw of a fault. In order to confirm if the feature was artificial or geology, the reference volume was evaluated. Within the reference volume no evidence suggested a fault in this area of the section. Though it is not clear how this feature would have changed through migration of the data.

Empirical Observations – Time slices

Time slices are a plan view of the whole volume corresponding to a single time. The light and dark areas reflect changes in amplitude signal. These figures provide another perspective on the image quality. Again observation alone will serve as the main method of comparison for the four volumes. These visual comparisons are just as important as quantitative analyses because they show how the interpretation capability changes. Three separate times slices from each volume were chosen to show the difference in image quality in the shallow, medium, and deep sections. These sections were taken at 1000, 3500, and 4800 ms.

The first time slice is at 1000 ms (Figure 42). This time was selected because it is in the low fold section, due to muting, and is expected to be very responsive to the effects of decimation. The lower right corner of the slice for the reference volume (Figure 43a) is very defined compared to the decimated versions (Figure 43b-d). In the decimated shot (Figure 43c) and decimated receiver (Figure 43b) volumes the amplitudes are not as

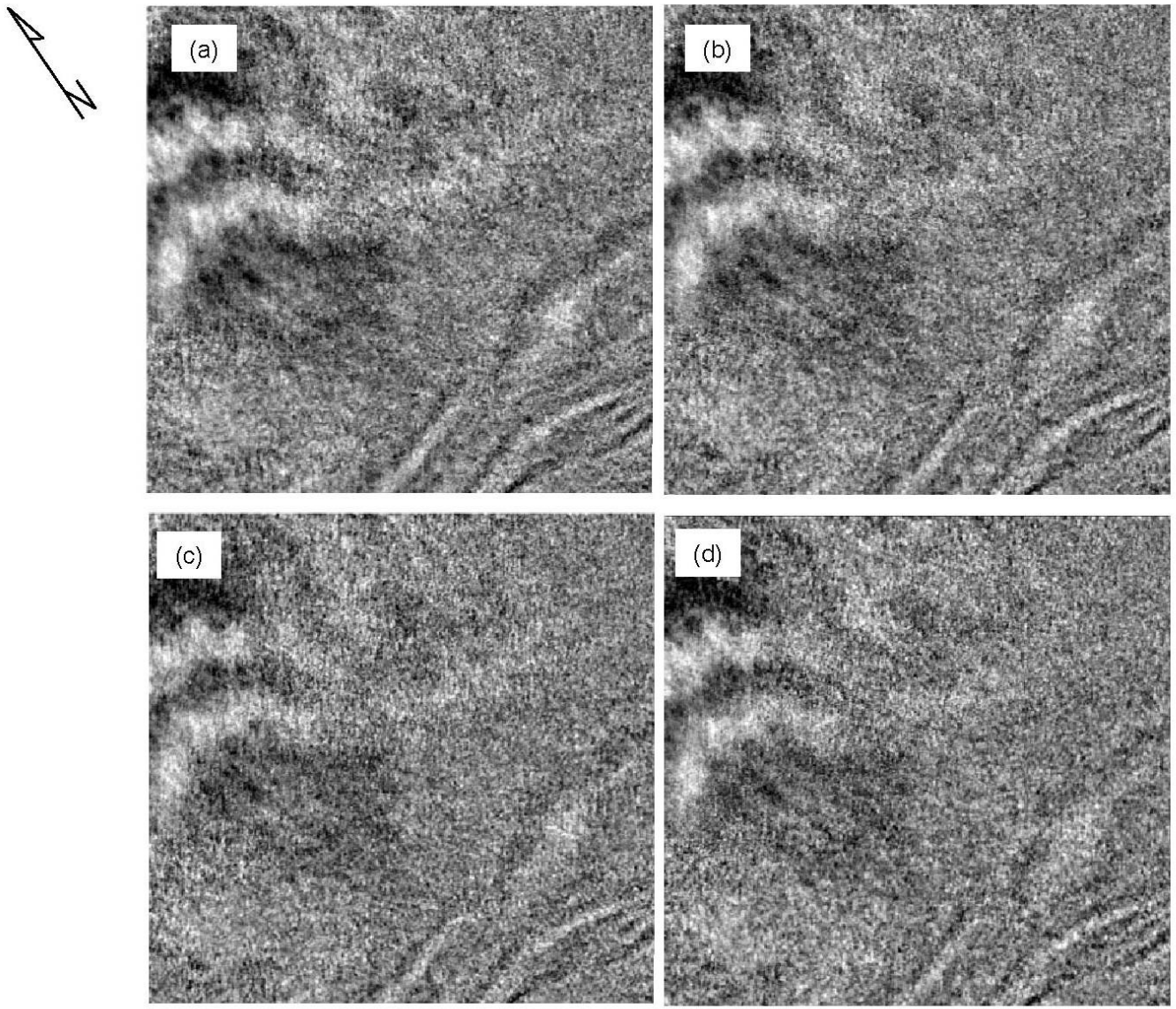

Figure 42 – Time slices taken at 1000 ms for the (a) reference volume, (b) decimated receiver volume, (c) decimated shot volume, and (d) decimated shot and receiver volume.

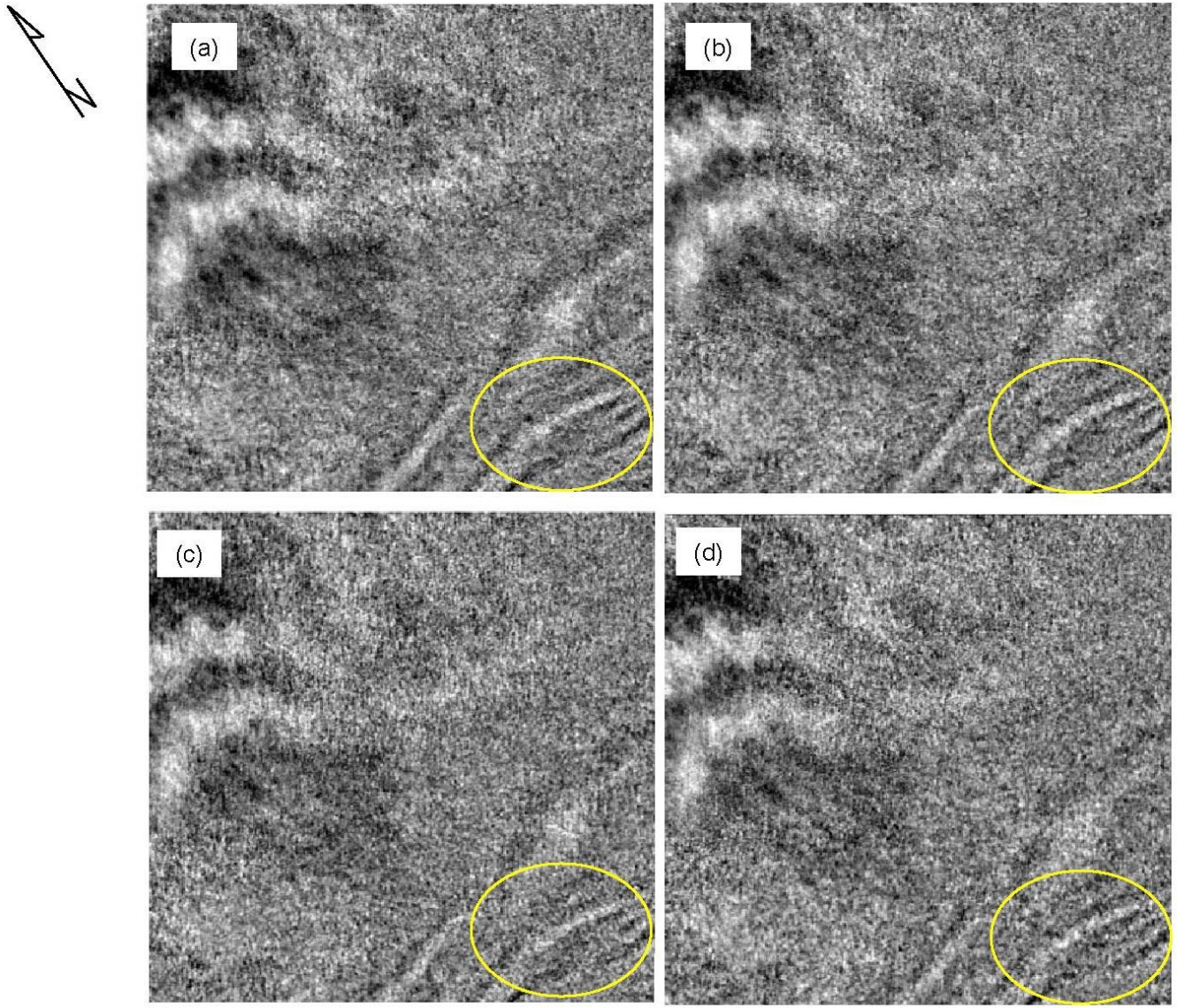

Figure 43 – Time slices with interpretation taken at 1000 ms for the (a) reference volume, (b) decimated receiver volume, (c) decimated shot volume, and (d) decimated shot and receiver volume.

sharp. Additionally, the decimated shot volume does not exhibit contrasting amplitudes that are as clear as in the decimated receiver volume. The overall image for the decimated shot and receiver volume appears fuzzy in comparison to the other volumes from the reduction of sampled traces. However the difference in image quality for the decimated shot and decimated receiver volumes only appear degraded in the lower right corner when compared to the reference volume.

At the mid-level depth of 3500 ms (Figure 44) the fold should not be controlled by muting or anything other than the differences in acquisition design. The images for all four volumes appear overall very similar. It can still be shown that degradation has taken place through a more intensive investigation to compare. Figure 45 shows the same time slices with significant differences in quality indicated between the reference and decimated volumes. Image distortion is worst in the decimated shot and receiver volume (Figure 45d). The decimated shot (Figure 45c) and decimated receiver (Figure 45b) volumes have a more subtle contrast compared to the reference volume. Of the two, the quality is more degraded in the decimated shot volume.

In the deepest time slice at 4800 ms (Figure 46), conflicting coherent reflectors appear to cross one another. This is an effect that results from the lack of migration. These are diffractions that occur in structurally complex regions and are misplaced from their point of origin. Though the diffracted waves are misplaced it is still recorded energy that is compared to the reference volume. In Figure 47 duplicate time slices have again been annotated to show certain areas of interest. This time slice shows some of the most

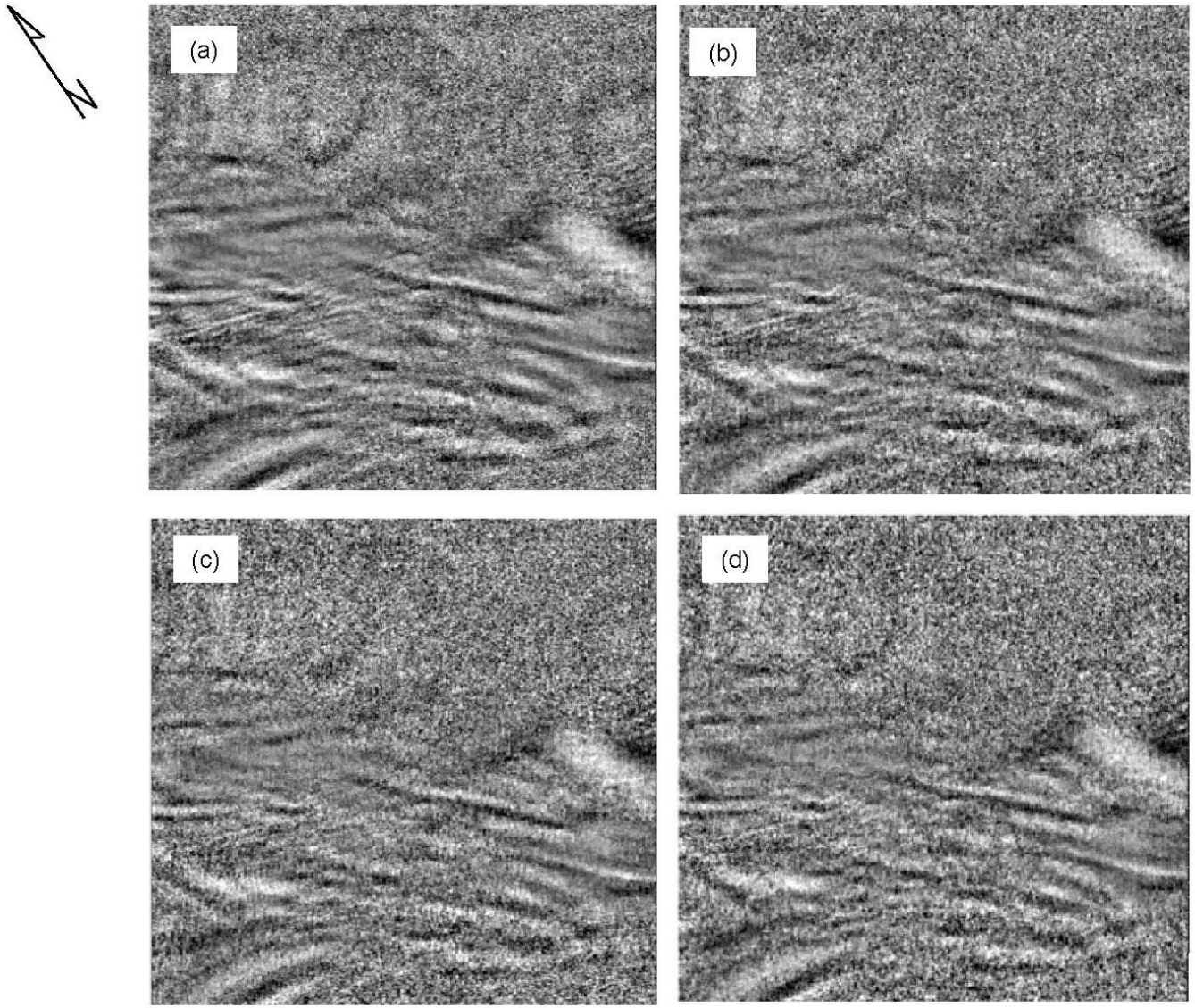

Figure 44 – Time slices taken at 3500 ms for the (a) reference volume, (b) decimated receiver volume, (c) decimated shot volume, and (d) decimated shot and receiver volume.

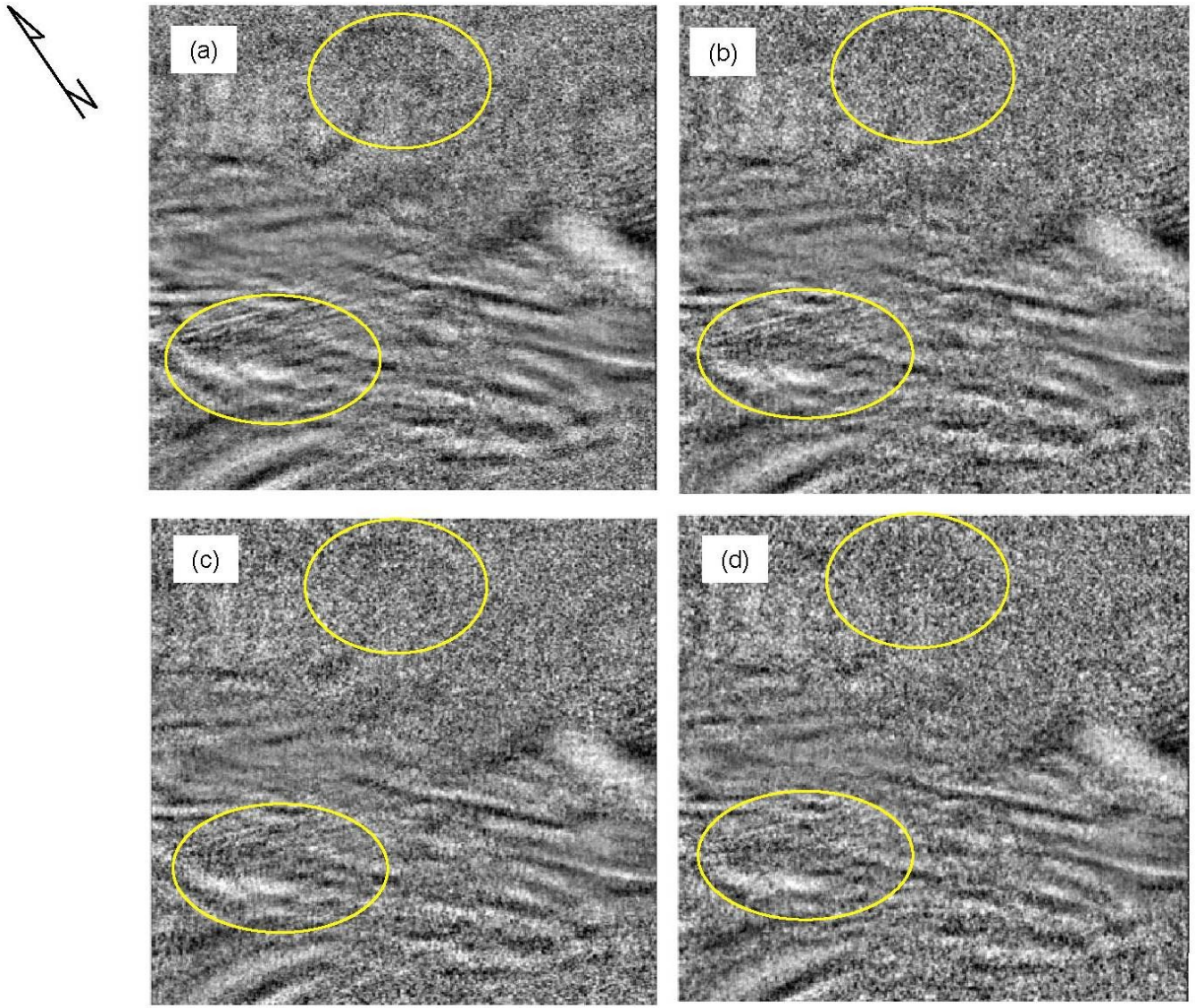

Figure 45 – Time slices with interpretation taken at 3500 ms for the (a) reference volume, (b) decimated receiver volume, (c) decimated shot volume, and (d) decimated shot and receiver volume.

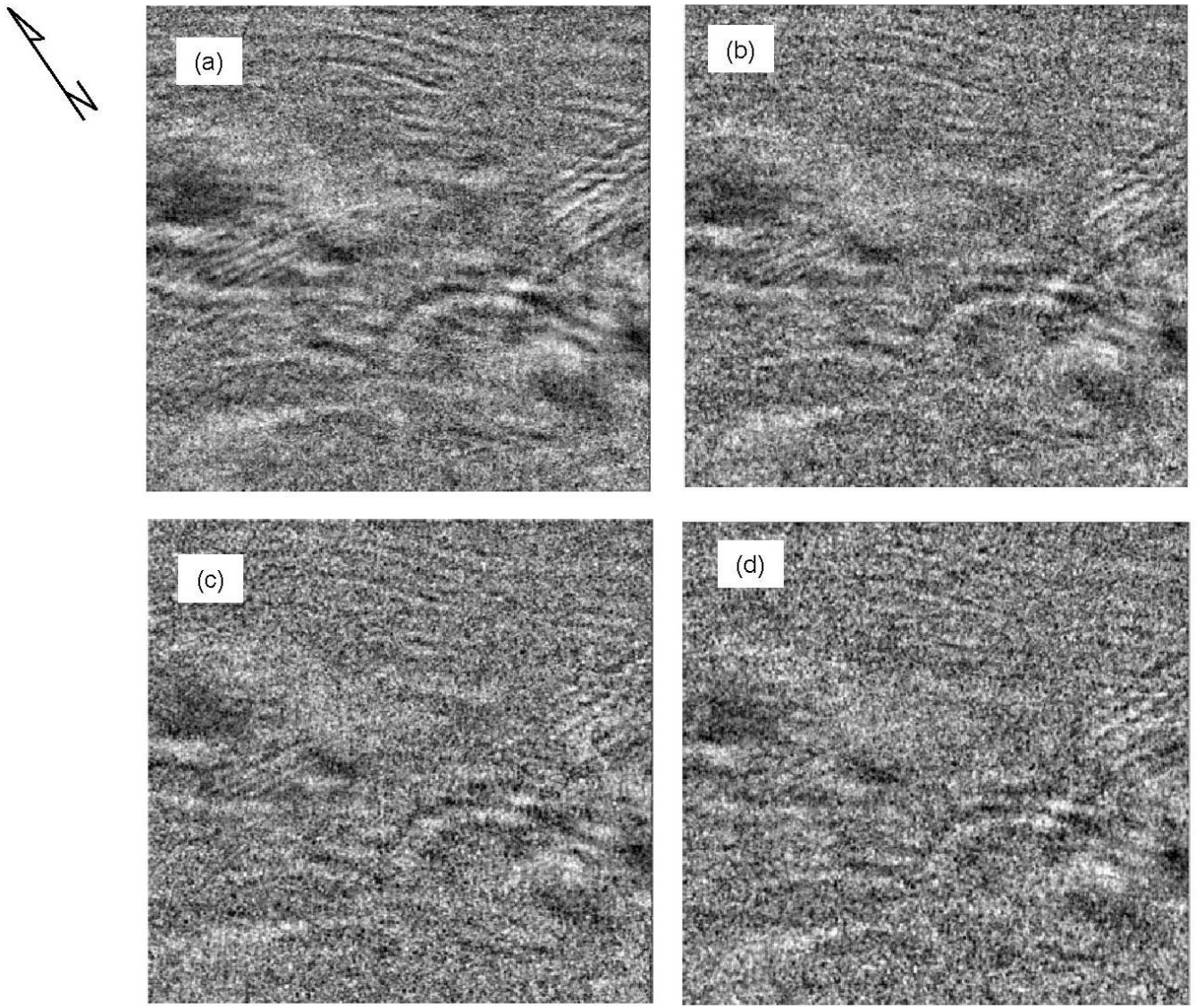

Figure 46 – Time slices taken at 4800 ms for the (a) reference volume, (b) decimated receiver volume, (c) decimated shot volume, and (d) decimated shot and receiver volume.

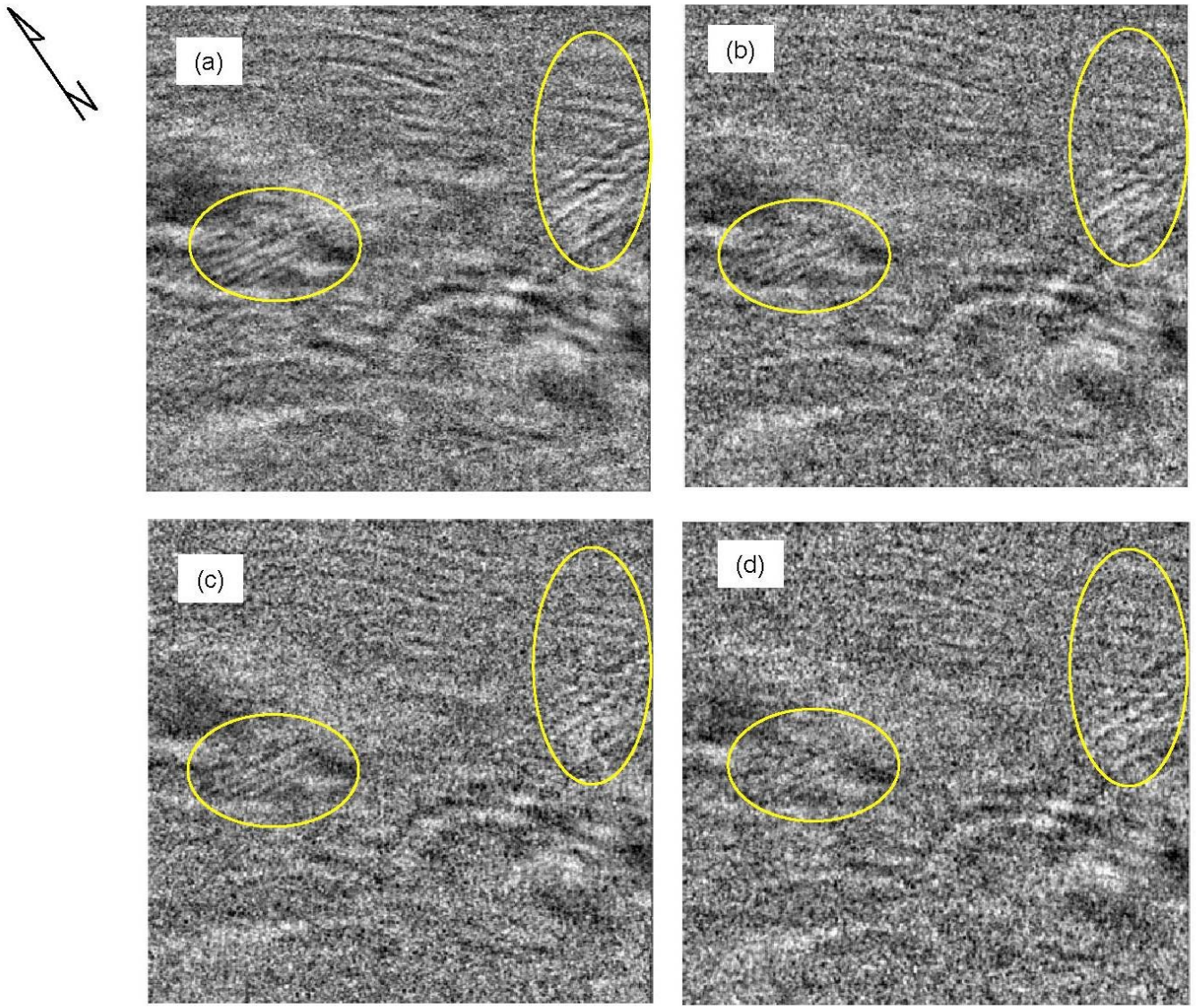

Figure 47 – Time slices with interpretation taken at 4800 ms for the (a) reference volume, (b) decimated receiver volume, (c) decimated shot volume, and (d) decimated shot and receiver volume.

obvious differences in clear, continuous energy recorded by the reference volume compared to others. The reference volume gives a much better image than the next best volume. That next best volume appears to be the decimated receiver which still maintains some difficult reflection areas. In comparison of the decimated shot to the decimated shot and receiver there is not much difference that is easily observed. However focusing on the left central area there is a certain group of diffractions that seem to be better recorded by the decimated shot volume.

The time slices overall appear to have replicated the reference volume. However, with intensive comparison of decimated volumes there are noteworthy differences in the image quality relative to the reference volume. These subtle and drastic differences are largely created by the decreased fold. As the trace density has reduced so to has the image quality within the decimated volumes.

Difference Volumes

The next method of comparison was done by creating difference volumes. This process is an empirical method but also capable to quantitatively compare volumes. This part of the comparison is only briefly discussed as it is neither reasonable nor necessary to quantify each reflector. Rather the visual magnitude displayed in the figures allows for easier comparisons of the volumes. Difference volumes are created by subtracting amplitudes of each trace in one survey from the same trace in another survey. This can be very difficult when the number of traces changes between the surveys, such as is usually the case in decimation. However, this difficulty was avoided by keeping the bin sizes the same and using flex binning to keep the same number of traces in each volume.

After subtraction of two initial volumes, a number of different patterns can be observed. If the difference volume has coherent reflectors this indicates that one volume has more signal than the other. The strength of the amplitude on the difference volume is a measure of the difference in signal strength. Another pattern that can be observed is many random amplitudes that are considered noise. Subtracting noise from a survey with signal or noise, can result in a difference volume of only noisy traces and/or some faint coherent reflectors. Thus, if too much noise is present in one survey, no coherent energy may be visible regardless of its strength in the other volume. The last major pattern that is relevant to the following figures are difference traces that approach zero. In the following figures this is represented by a medium gray tone color. When this occurs it indicates that the two input volumes are very similar.

The first difference volume to be calculated was the decimated receiver subtracted from the reference volume. Figure 48 shows an in line section while Figure 49 displays the cross line section. On the in-line section there is some evidence of coherent energy in the shallow section from 200 – 1000 ms (Figure 48). Faint banded, coherent energy is observed around 1350 ms. Below 2500 ms several distinct reflectors exist down to 3500 ms. On the cross-line section (Figure 49) the same features can be observed. There is more difference between the two volumes in the shallow section than in the deeper section. The reference volume had larger amplitudes than the decimated receiver volume

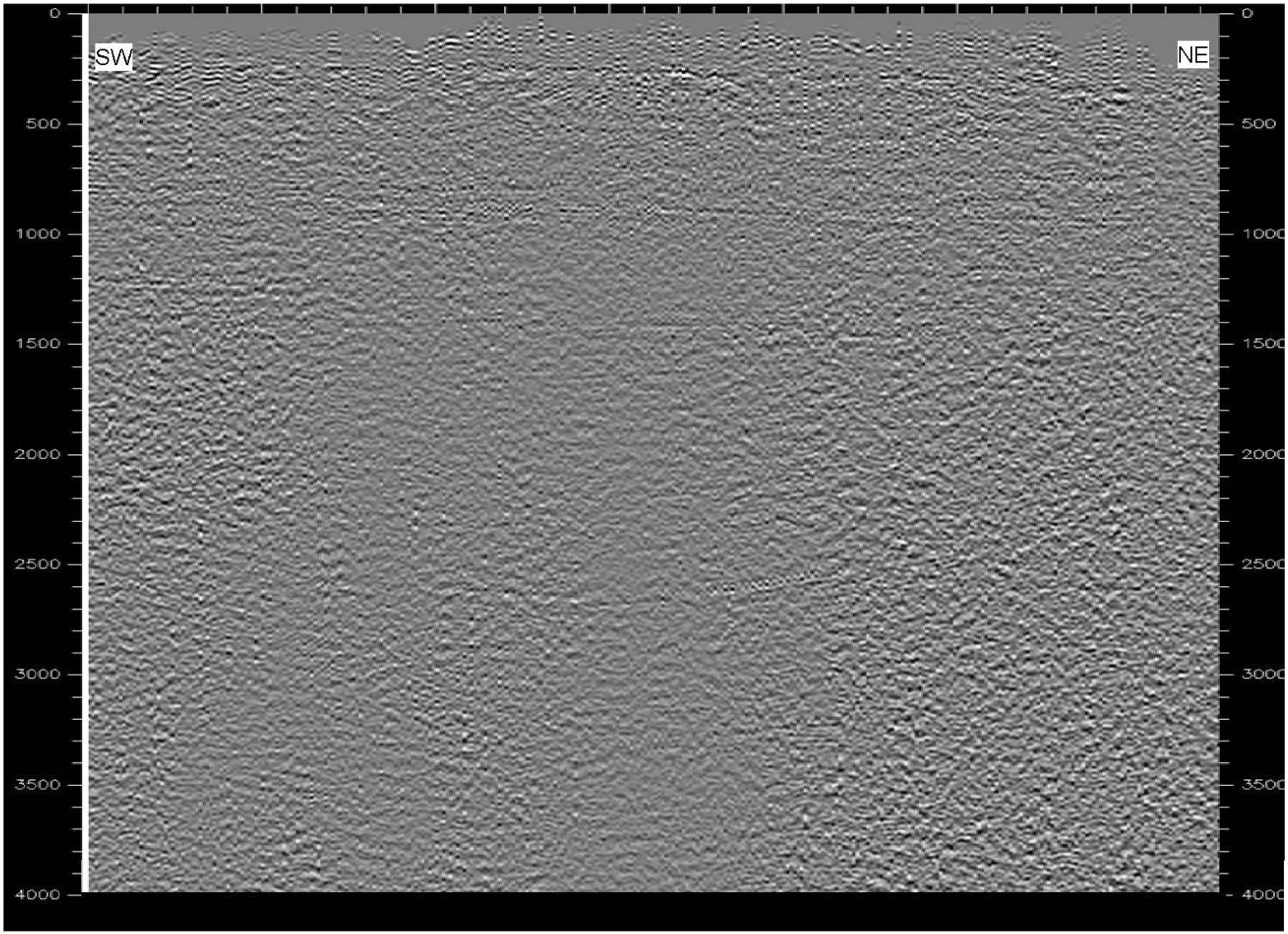

Figure 48 – Volume difference section taken in the in line direction. The decimated receiver volume was subtracted from the reference volume.

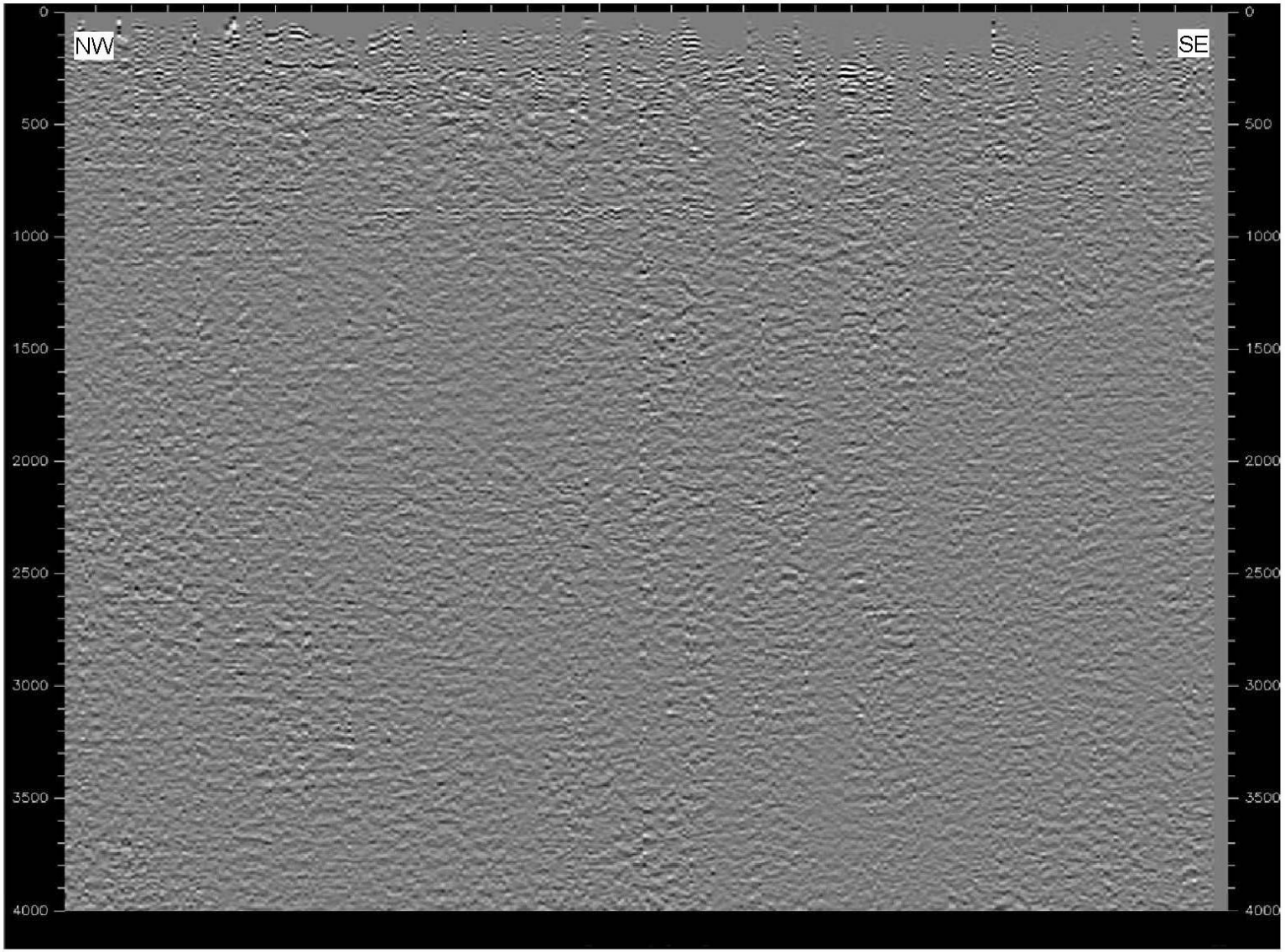

Figure 49 – Volume difference section taken in the cross line direction. The decimated receiver volume was subtracted from the reference volume.

when readings were taken along a coherent reflector. This results from the higher fold and signal to noise ratios in the reference volume. This type of confirmation was only conducted on coherent signal because in areas of noise amplitudes vary in a random fashion and do not represent which volume contains more signal.

The next difference volume was calculated between the decimated shot and reference volumes. In Figure 50, taken on the in line, the same set of coherent reflectors are present as the lighter and darker continuous lines that were observed in the previous difference volume. At 250 ms a very prominent reflector is shown and the section of 700 – 1000 ms also represents a difference in recorded signal. Deeper in the section to 1400 ms a coherent reflector is noted that was not previously observed in the reference and decimated receiver volume. A series of these reflectors can be seen down to roughly 2300 ms. In the range of 2500 – 3500 ms, layers are again present that were witnessed in the earlier difference volume. Observing the cross line section (Figure 51) there appears to be considerable differences in the amount of signal recorded. The central area looks slightly noisy but to the left many reflectors can easily be distinguished. Again the reference volume was confirmed to have the higher energy relative to the decimated version.

This process gives the ability to make a direct comparison of the decimated shot to the decimated receiver volume. The in line difference section in Figure 52 shows multiple reflectors can be seen that were present in the other difference comparisons which proves the fact that significant differences in recorded signal exist. This was also

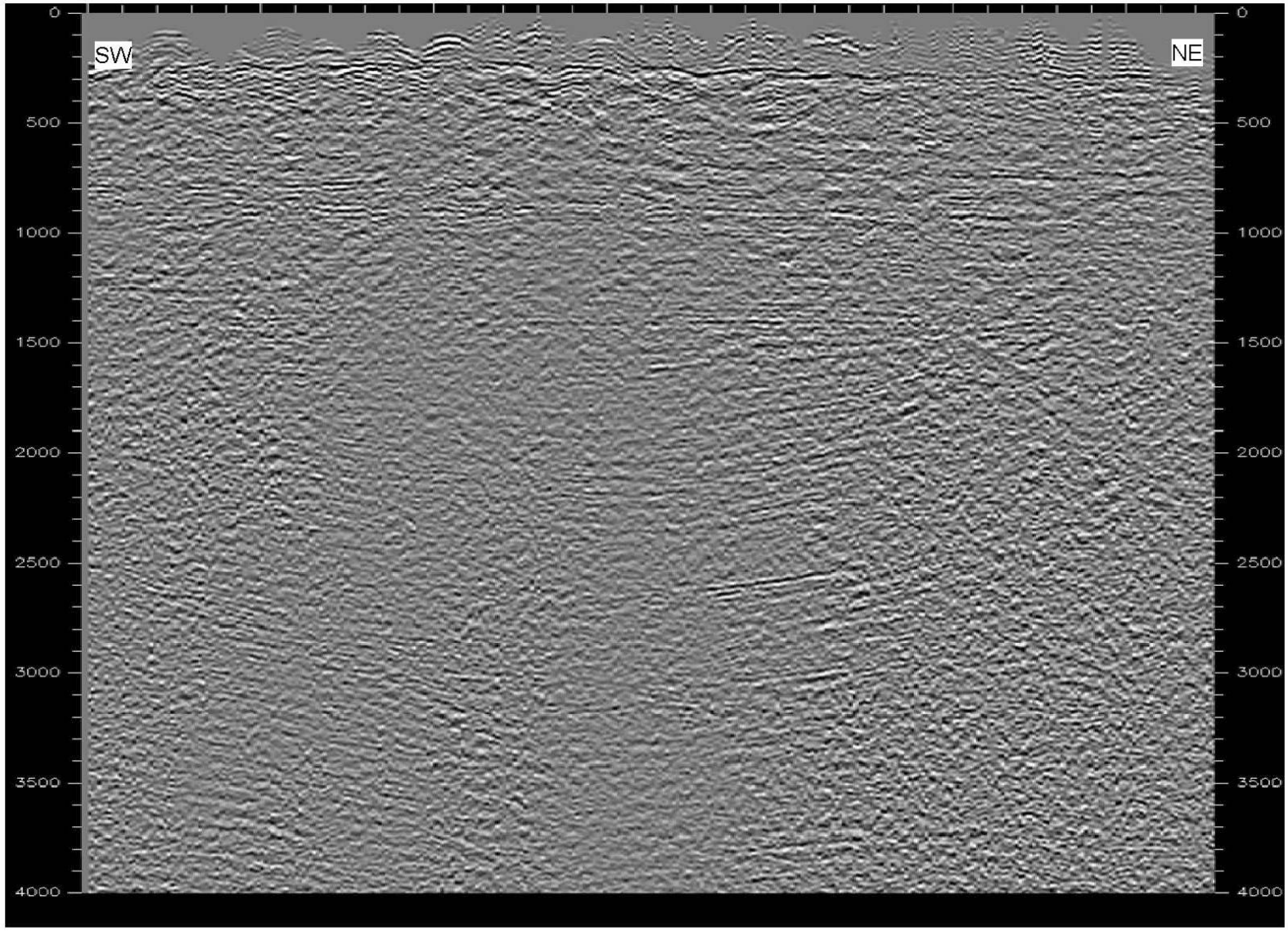

Figure 50 – Volume difference section taken in the in line direction. The decimated shot volume was subtracted from the reference volume.

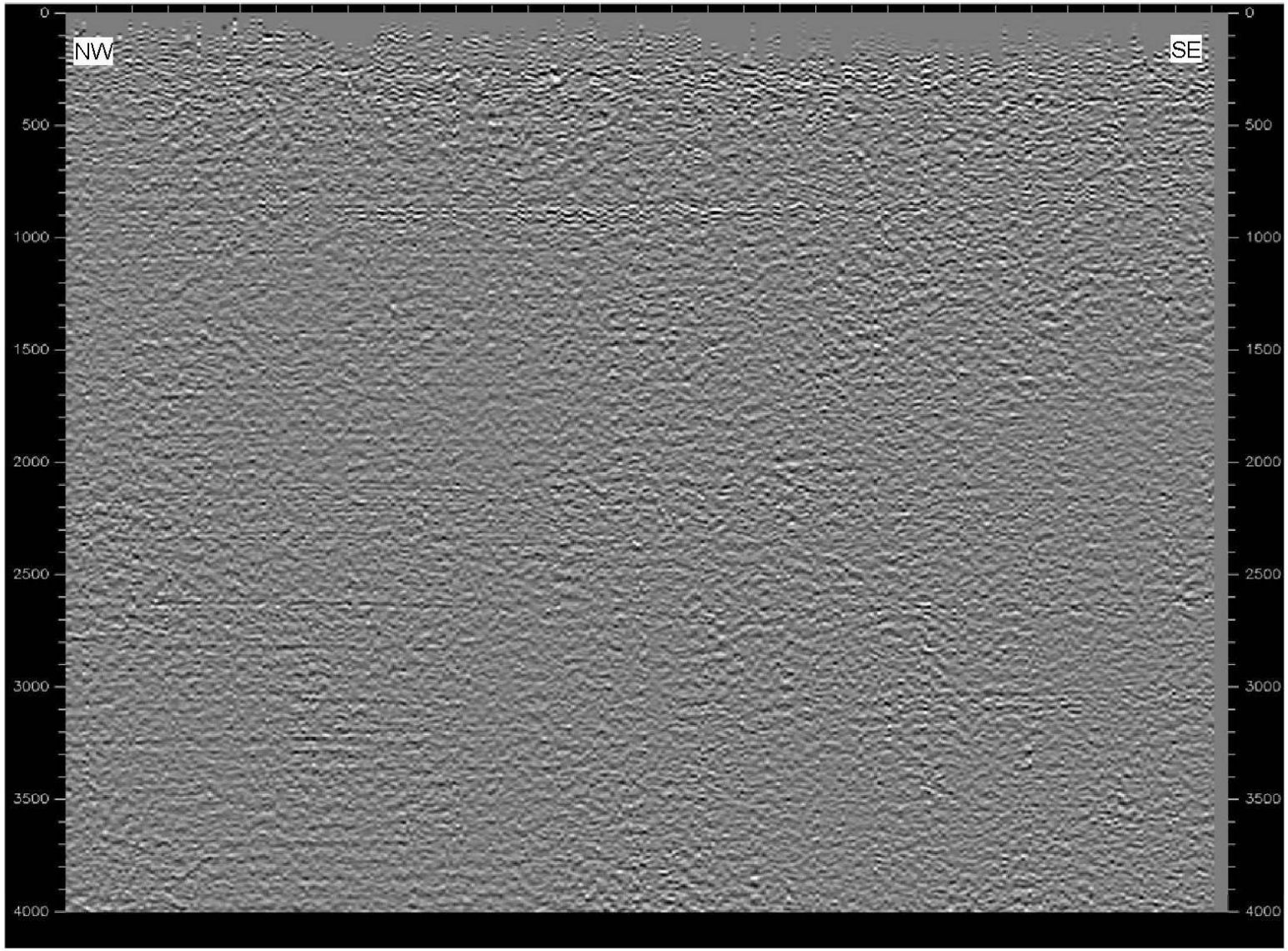

Figure 51 – Volume difference section taken in the cross line direction. The decimated shot volume was subtracted from the reference volume.

displayed by the cross line section (Figure 53) where distinct differences are present, however coherent reflectors are not as prominent. To confirm which volume contained more signal a comparison of the amplitudes had to be made in each individual volume. From that comparison it is confirmed that more signal exists in the decimated receiver than in the decimated shot volume. In regards to the image quality the decimated shot volume is more affected by decimation than is the decimated receiver volume.

Analyzing the difference volume for the reference and decimated shot and receiver volume, did not show any surprises (Figure 54 and 55). The same reflectors were present throughout the image, however some of the reflectors in the in line section appeared less continuous than in earlier difference volumes. It was expected that this difference volume would show the most difference in signal due to the increased reduction of samples in the decimated shot and receiver volume. This is interpreted to be a result of the fact that more random noise is imbedded in the decimated shot and receiver volume. Thus the noise did not allow coherent energy to remain visible across the survey. The cross-line section does show the extensive continuous reflectors that we expected to see based on the increased reduction of traces used in the decimated shot and receiver volume.

Amplitude Maps

In order to compare amplitude distribution differences between volumes a group of horizons were picked on each section and an amplitude map was constructed. Observing the spatial distribution of amplitude anomalies is very important based on the

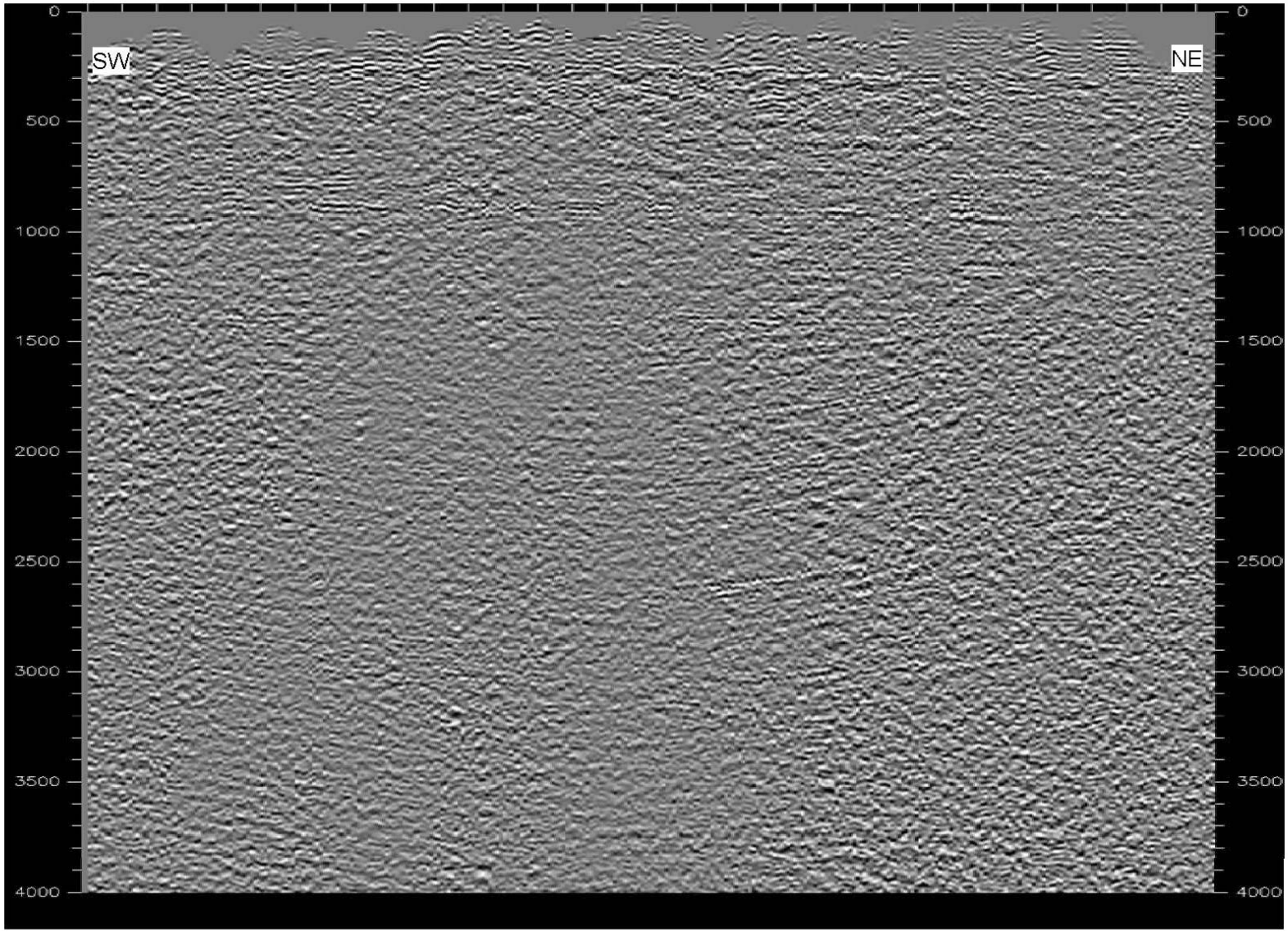

Figure 52 – Volume difference section taken in the in line direction. The decimated receiver volume was subtracted from the decimated shot volume.

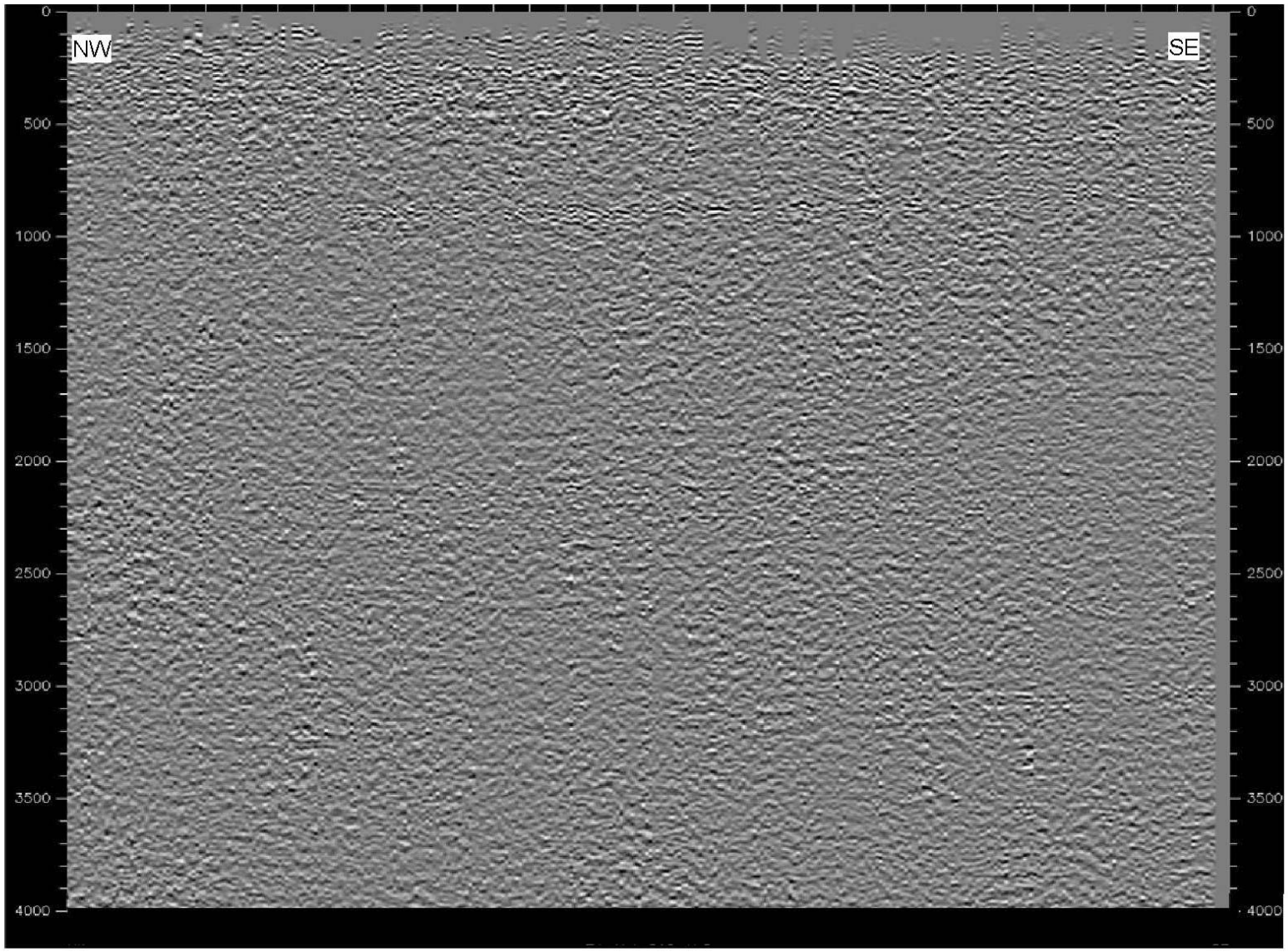

Figure 53 – Volume difference section taken in the cross line direction. The decimated receiver volume was subtracted from the decimated shot volume.

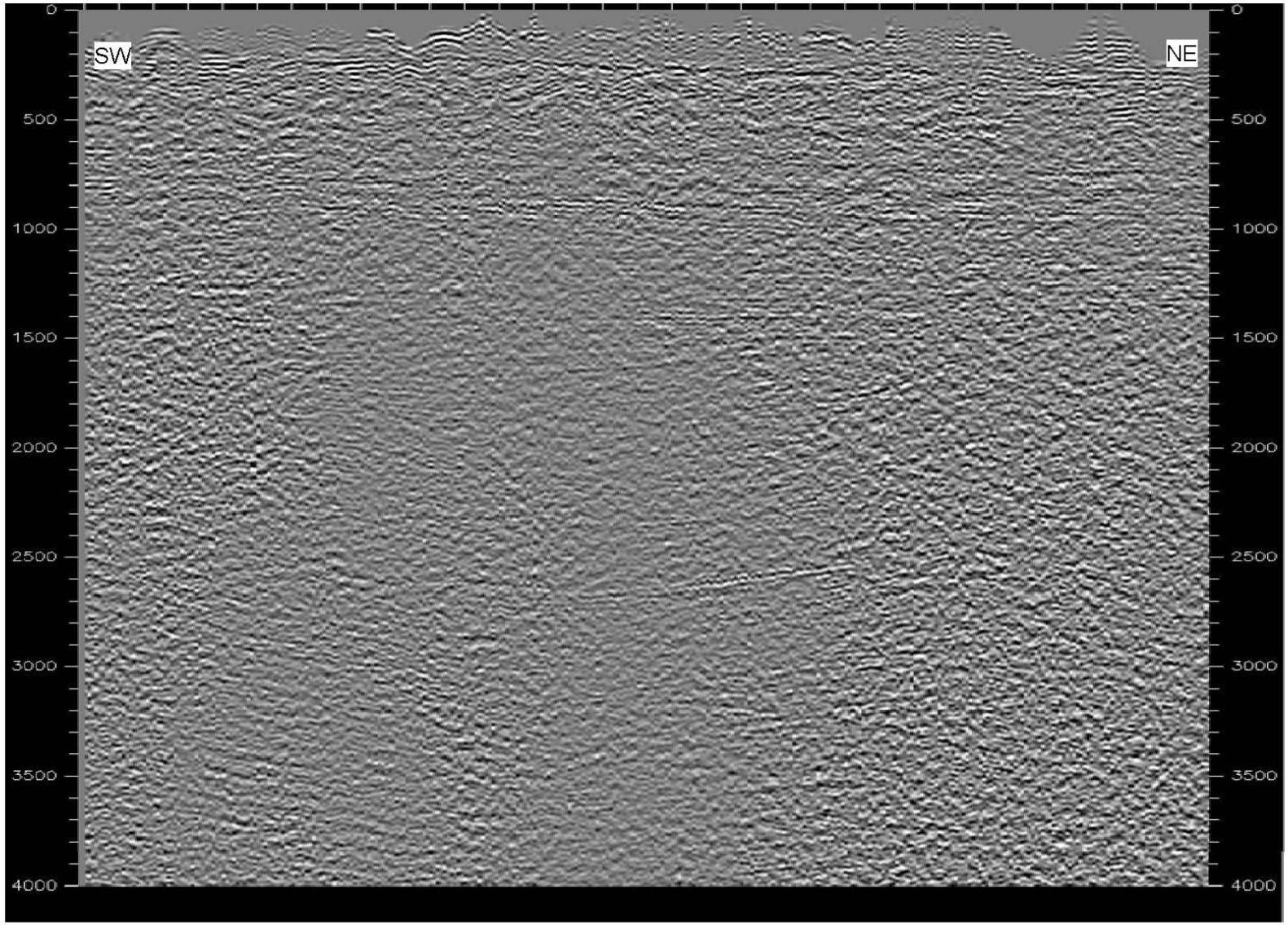

Figure 54 – Volume difference section taken in the in line direction. The decimated shot and receiver volume was subtracted from the reference volume.

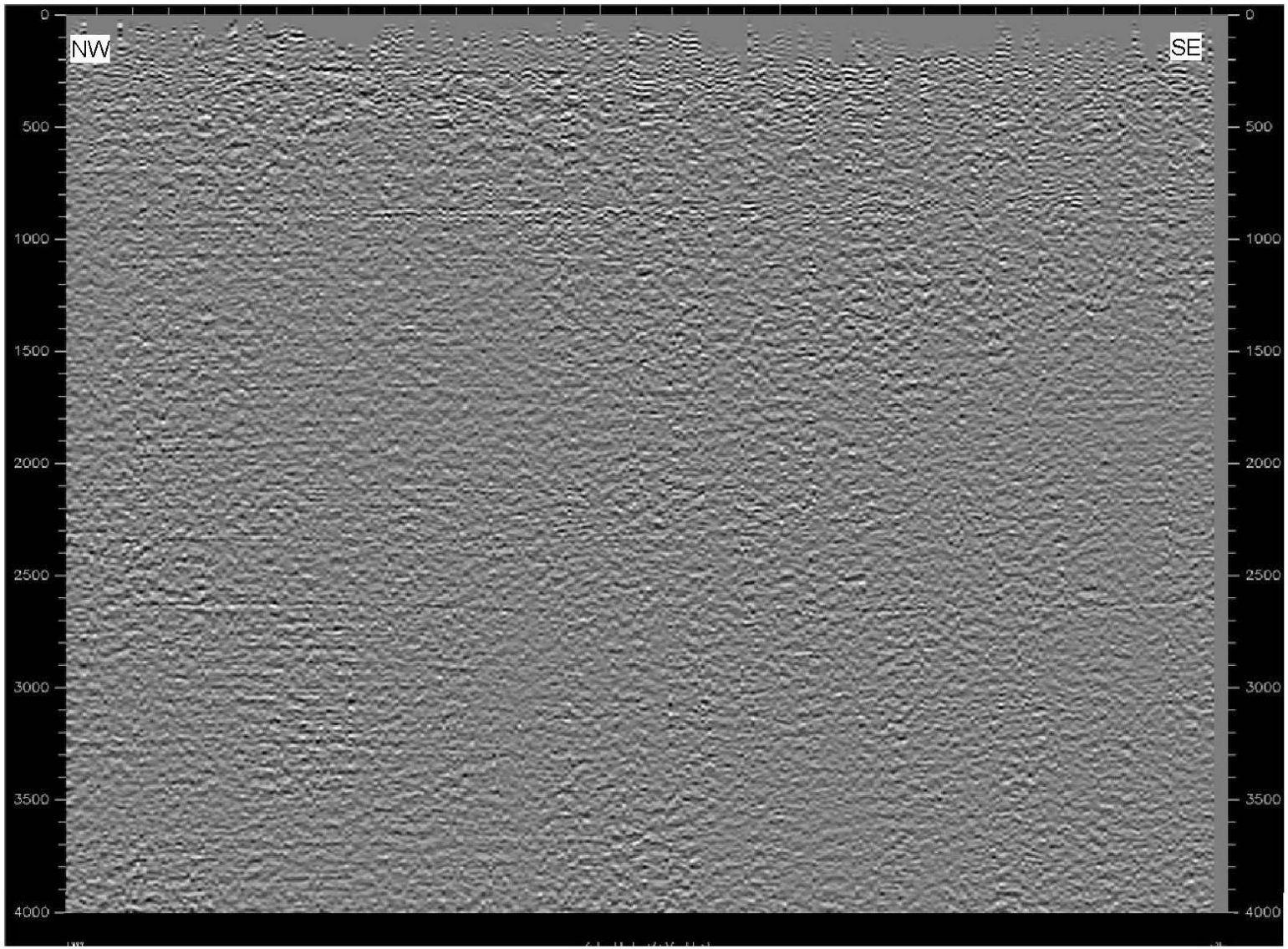

Figure 55 – Volume difference section taken in the cross line direction. The decimated shot and receiver volume was subtracted from the reference volume.

attribute's economic impact. Commonly amplitude maps are used to assist the guidance of exploration and development of petroleum fields. If the spatial distribution of an anomaly changed with decimation, it could affect recommendations for proposed well placement. Therefore, the main concern within this method of comparison is the anomaly location and not the quantitative differences. Since there are several variables involved in the creation of an amplitude map, control had to be obtained. The first thing that was eliminated was the difference in interpretation, so that a volume could not be favored over another. To do this, the reference volume was used to pick the horizons because of its signal quality, coherency and continuity, was found to the best in the previously compared methods. That same horizon was used on the other volumes so that in areas of difficult interpretation it was already determined where the reflector should arrive. The next major variable to control is the ZAP function. The ZAP function is part of Landmark's interpretation software, and is a process that allows the computer to populate lines between the interpreters's picked lines. To try and limit its variability a finer set of picked seismic lines, compared to typical line interpretation intervals, used every fifth line. Additionally, the parameters within the process remained the same for each volume. The last control implemented was the use of three horizons so that one could not be considered erroneous.

The first horizon was selected at approximately 1200 ms. This choice was made due to the shallow depth and its lack of complex structure. Figure 56 shows the amplitude maps for all the volumes. The incompleteness of the populated horizon stands out at first glance. This was believed to occur because of restrained parameters in the program and changes in the coherency of the reflector, so the program was unable to

complete the pick after a defined uncertainty is reached. This is a better situation than when the uncertainty control in ZAP is left open and the picks become very erratic. Since the picks were limited to the horizon of interest, this incompleteness was believed to be acceptable. Looking past that issue, a fair judgment can be made based strictly on the amplitude anomaly distribution. In this study the term 'anomaly' is referring only to patches that contrast in amplitude value to surrounding areas. In analyzing the reference volume amplitude map it looks as though the anomalous amplitudes are well defined and isolated. The decimated receiver amplitude map appears to maintain most of the same features; however the isolation of the anomalies has become slightly blurred or spread out. This same issue is seen in the decimated shot version however the larger problem is the fact that the relative intensity of the anomalies has not closely matched the reference volume. The last volume of decimated shot and receiver actually seems to capture the relative intensity changes seen in the amplitude map for the reference volume. However the sharpness of the isolated areas seems to have become the most distorted out of all the tested volumes.

Another shallow horizon was mapped around 1500 ms. This horizon was selected because it is a strong coherent reflector that was visible throughout both the reference and decimated volumes. Where as the first horizon at 1200 ms had many changes throughout the survey as well as reduced visibility in the decimated volumes compared to the

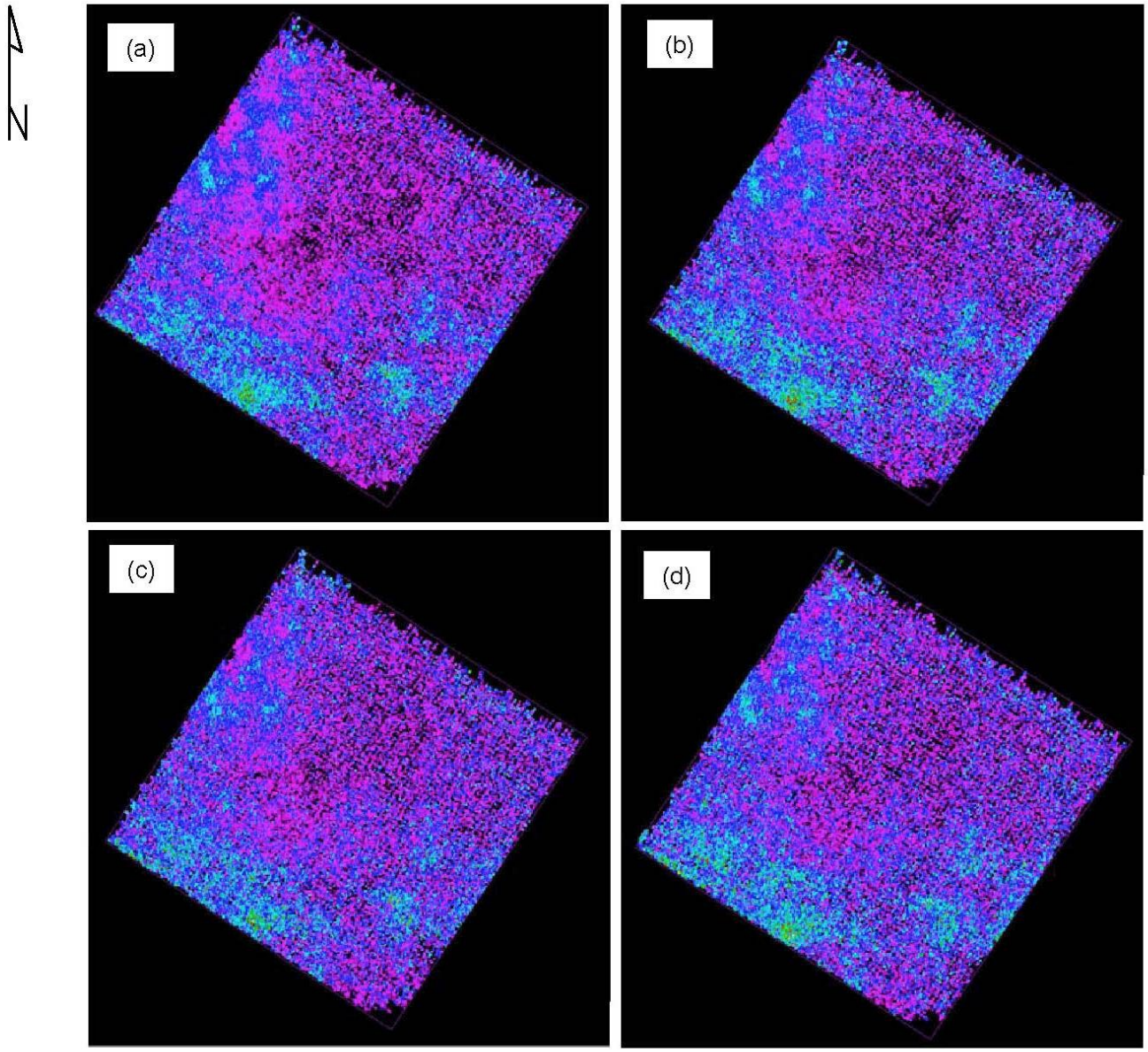

Figure 56 - Amplitude map extracted from Horizon 1 using the (a) reference volume, (b) decimated receiver, (c) decimated shot, and (d) decimated shot and receiver.

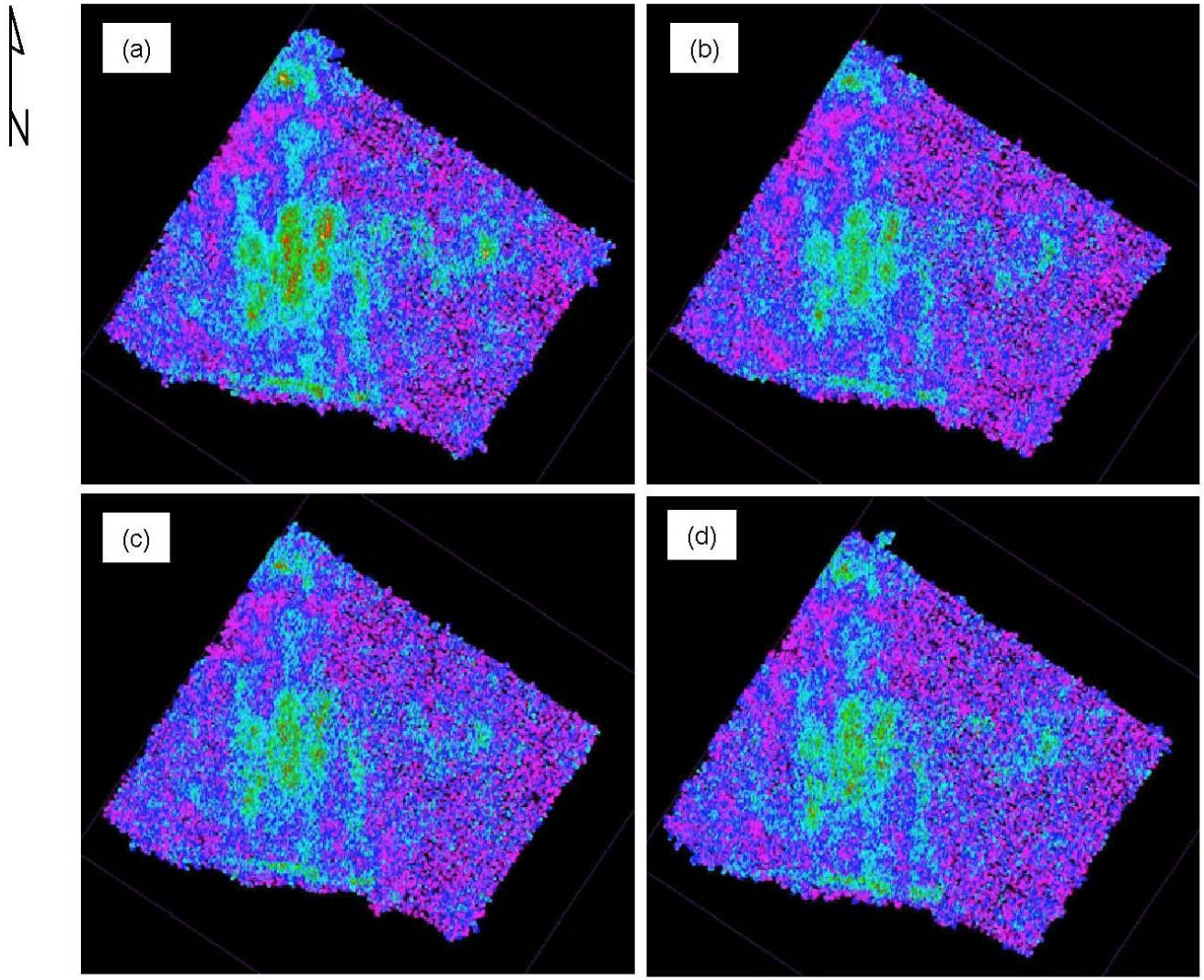

Figure 57 - Amplitude map extracted from Horizon 2 using the (a) reference volume, (b) decimated receiver, (c) decimated shot, and (d) decimated shot and receiver.

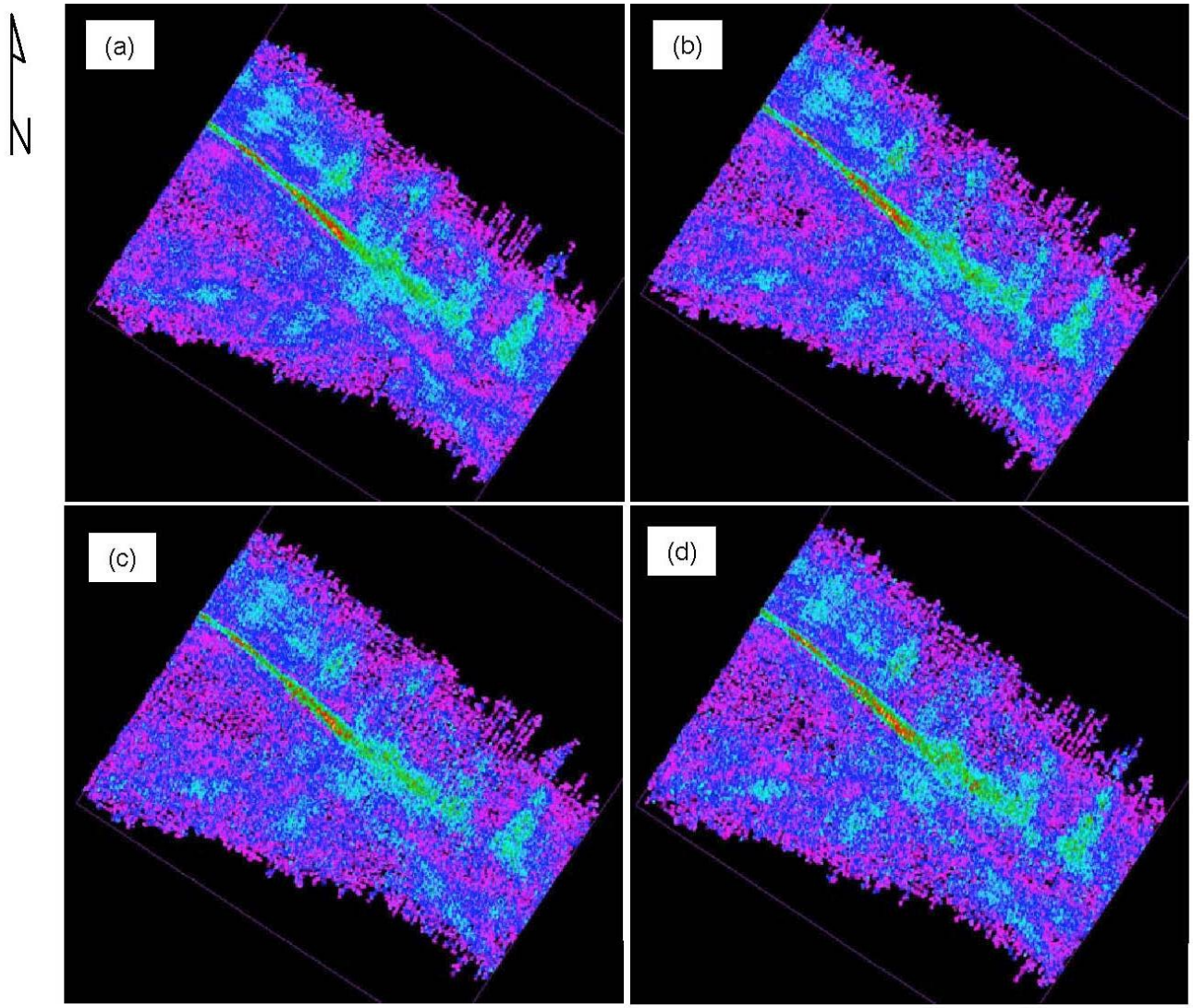

Figure 58 – Amplitude map extracted from Horizon 3 using the (a) reference volume, (b) decimated receiver, (c) decimated shot, and (d) decimated shot and receiver.

reference volume. Structural complexity in this part of the section is still relatively simple as can be seen in Plate 1. In Figure 57, the reference volume shows three central anomalies with a few others located to the North, East, and South. After observing the decimated versions in the figure it seems that each one has accurately placed the anomaly in its correct spatial locality. However it also appears as though each volume failed to match the relative intensity and magnitude of the anomalies. It does not seem strikingly obvious as to which of the decimated versions is the best but the decimated shot and receiver looks the most blurred.

The last horizon of interest is deeper in the section at roughly 2600 ms (Figure 58). This horizon marks the limit below which everything else is strongly affected by the lack of migration. It is located in a synclinal feature and experiences a "bow tie effect" time structure on the seismic cross section. In the figure a strong linear anomaly is seen trending northwest – southeast. This again is related to the "bow tie" time structure where two diffraction waves intersect and combine amplitudes. In regards to the reference volume the anomalies seem very well defined. When comparing the decimated receiver volume it has mimicked the reference image very well. One notable change for this volume is in the diffraction merger or anomaly where the magnitude seems slightly more extensive. The decimated shot on the other hand did not retain the clarity, magnitude, or relative intensity of the anomalies. The decimated shot and receiver shows good relative intensity and magnitude but did not keep the same clarity of the anomalous areas.

Synthetic Tie

As is always the case, the most important aspect of a seismic survey is the ability to tie into the geology. Without this tie, there is no value to the seismic data that has been collected. Within the decimated section there are two wells that should allow for an attempt at tying the seismic, however, since the data is not migrated only one well that had a sonic and was deep enough could be used. Figures 59-66 show the sonic log from the well compared to each decimated volume. The best to place to begin the tie is Horizon 3 which has a bold reflection. Looking at the figure the reference volume appears slightly off but matches very well. In each of the decimated versions the tie seems to have areas of significant difficulty compared to the reference volume. It did not seem obvious as to which decimated volume was the best thus the only comparison to be made is that the reference volume proved superior in matching the well at this point. In order to determine which decimated volume match the best a scaled copy was printed out of both the seismic line and synthetic seismogram. Each reflector that matched was counted and the final tally was used to compare volumes. The decimated receiver volume matched more events and did the other decimated volumes. The decimated shot and receiver matched the fewest number of reflectors.

Another way of displaying the matchability of the synthetic to the seismic data is shown in Figure 67. Track 4, which is the center wiggle trace plot, shows the synthetic seismogram. In track 3, seismic traces have been extracted from the reference volume and show that a fair tie is possible. This is proven by the strong reflection signal that is created from horizon three that matches very well. Other reflectors from the reference volume are also seen to match with the synthetic seismogram. However in comparison to the traces displayed in track 5 the tie is not very good. Track 5 shows the reference

volume after migration has taken place and shows that the ability to tie the seismic data with the synthetic seismogram is greatly improved through the use of migration. This indicates that even though the strong reflectors were able to tie in earlier displays (Figures 59 – 66), the ability to match the synthetic data would be better tested after the process of migration for all volumes.

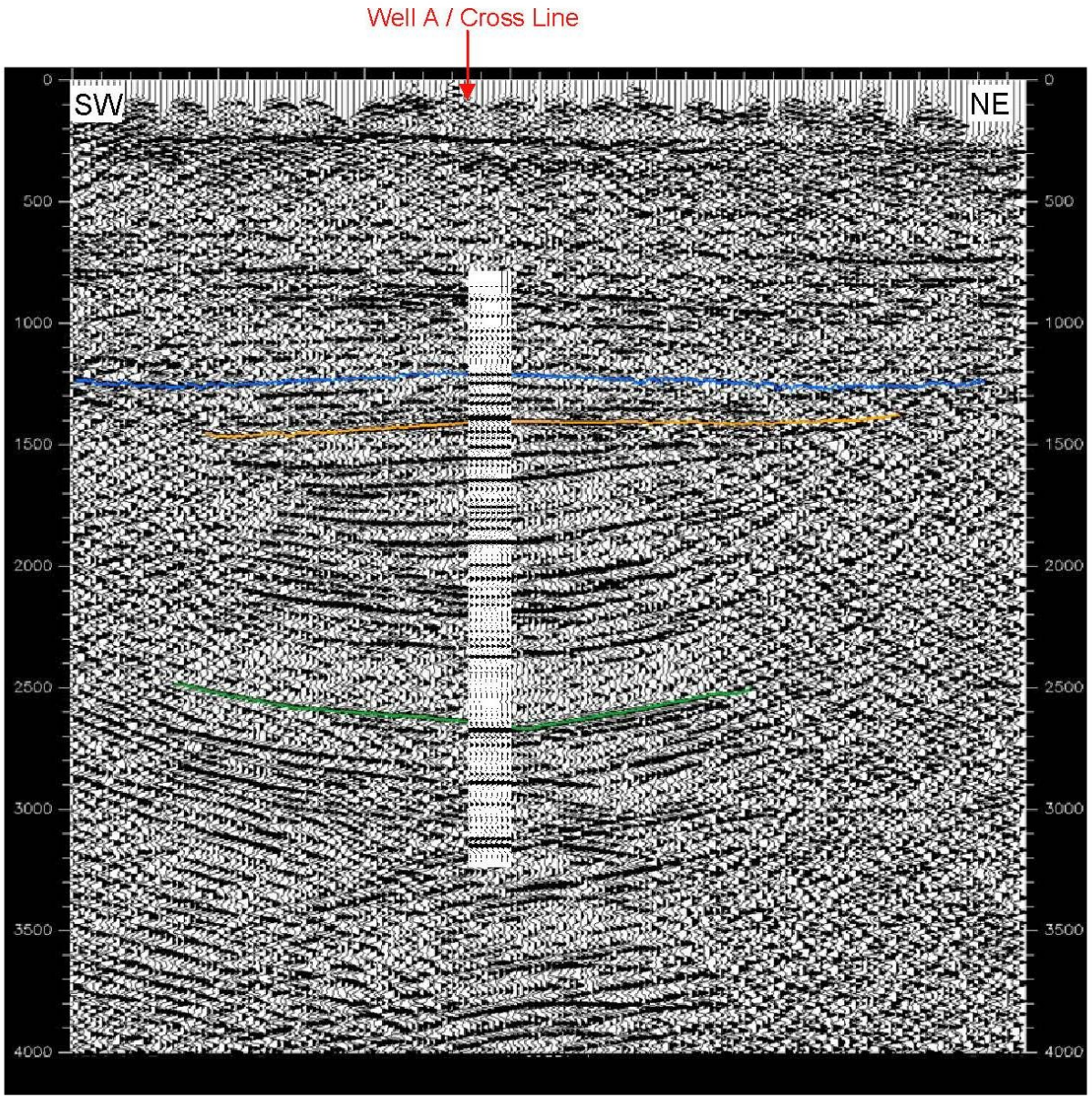

Figure 59 – Seismic cross section taken in the in line direction from the reference volume. The synthetic seismogram from Well A is overlaid. The horizons are shown by the blue (1), orange (2), and green (3) lines.

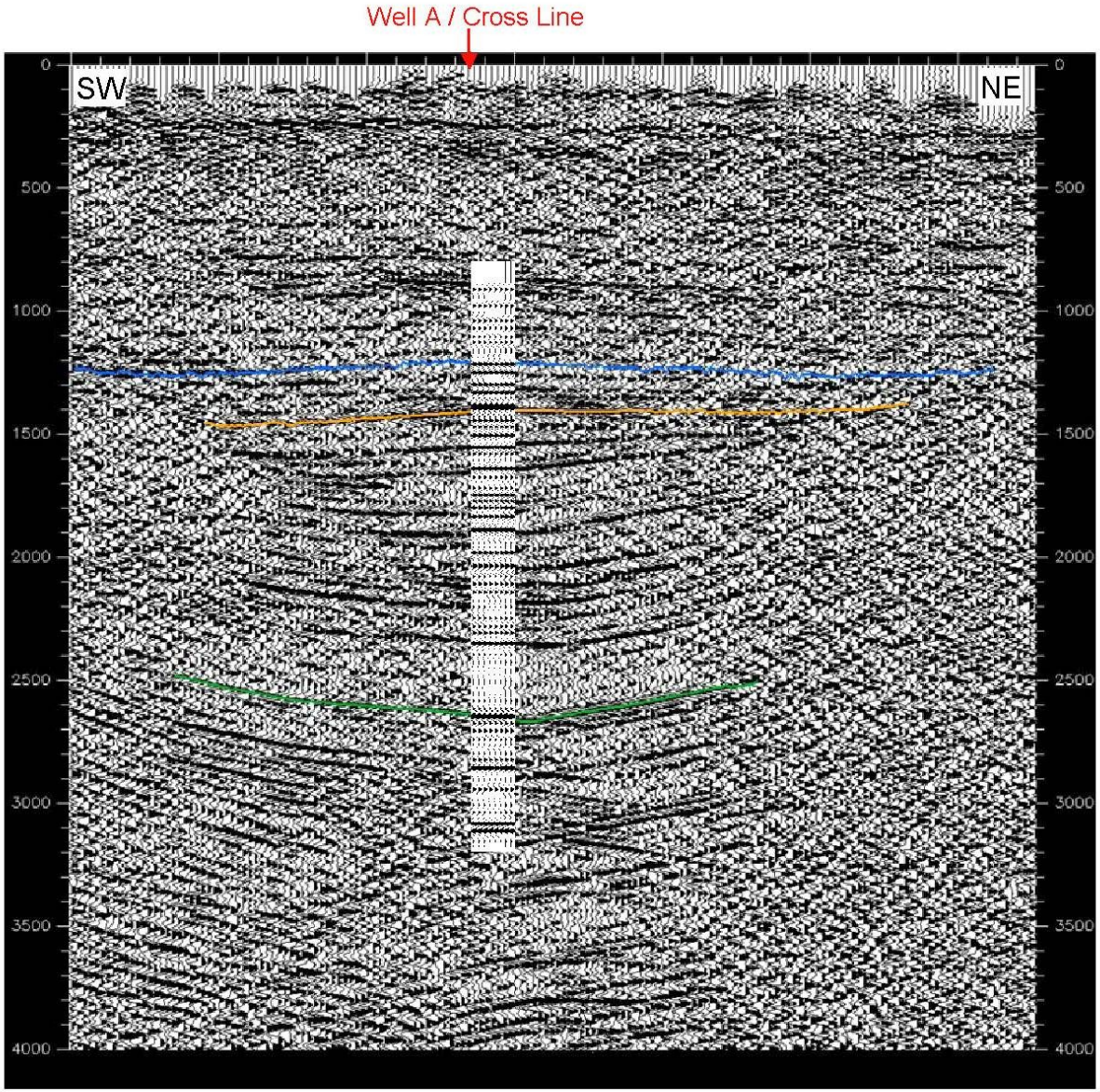

Figure 60 – Seismic cross section taken in the in line direction from the decimated receiver volume. The synthetic seismogram from Well A is overlaid. The horizons are shown by the blue (1), orange (2), and green (3) lines.

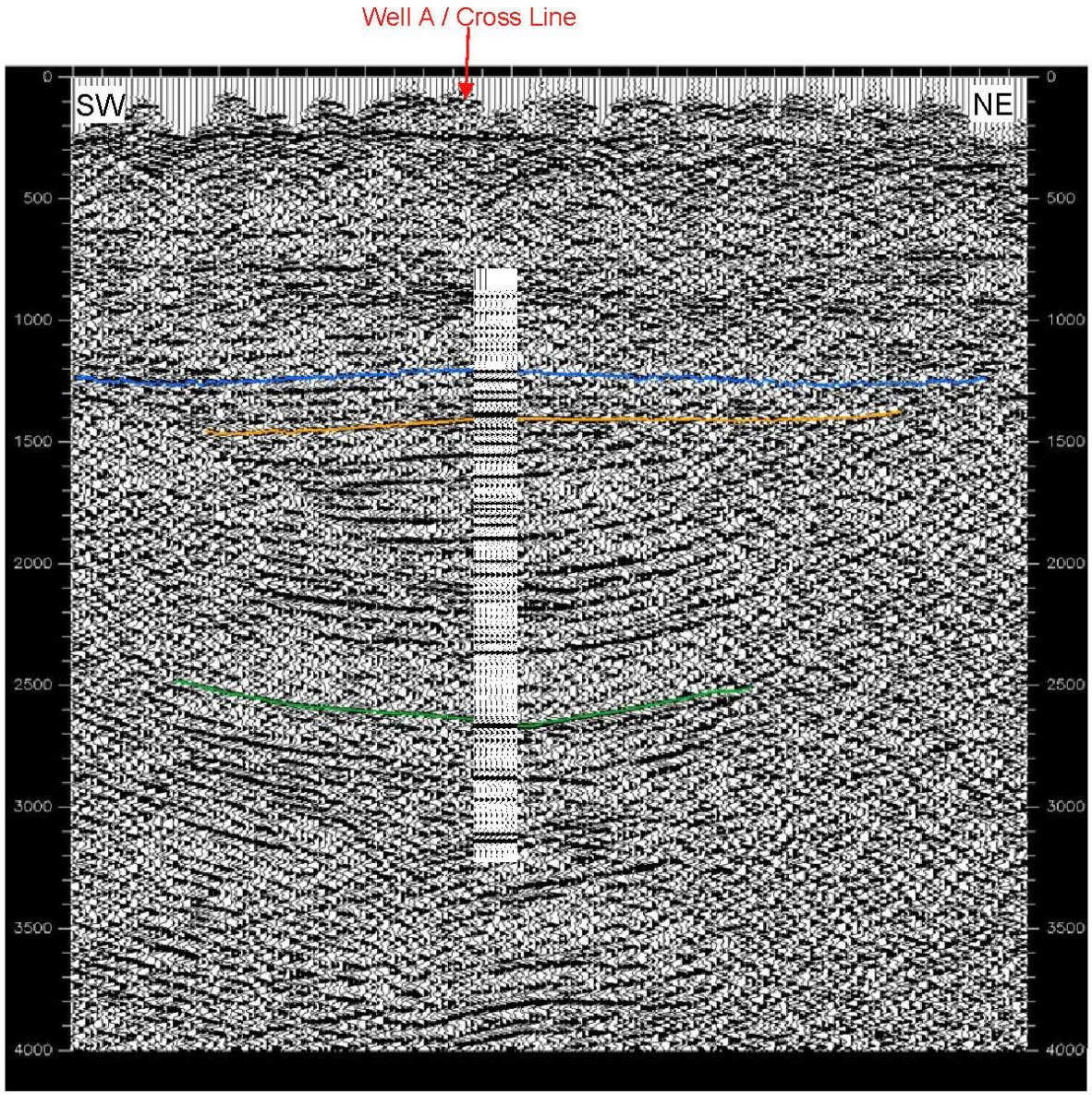

Figure 61 – Seismic cross section taken in the in line direction from the decimated shot volume. The synthetic seismogram from Well A is overlaid. The horizons are shown by the blue (1), orange (2), and green (3) lines.

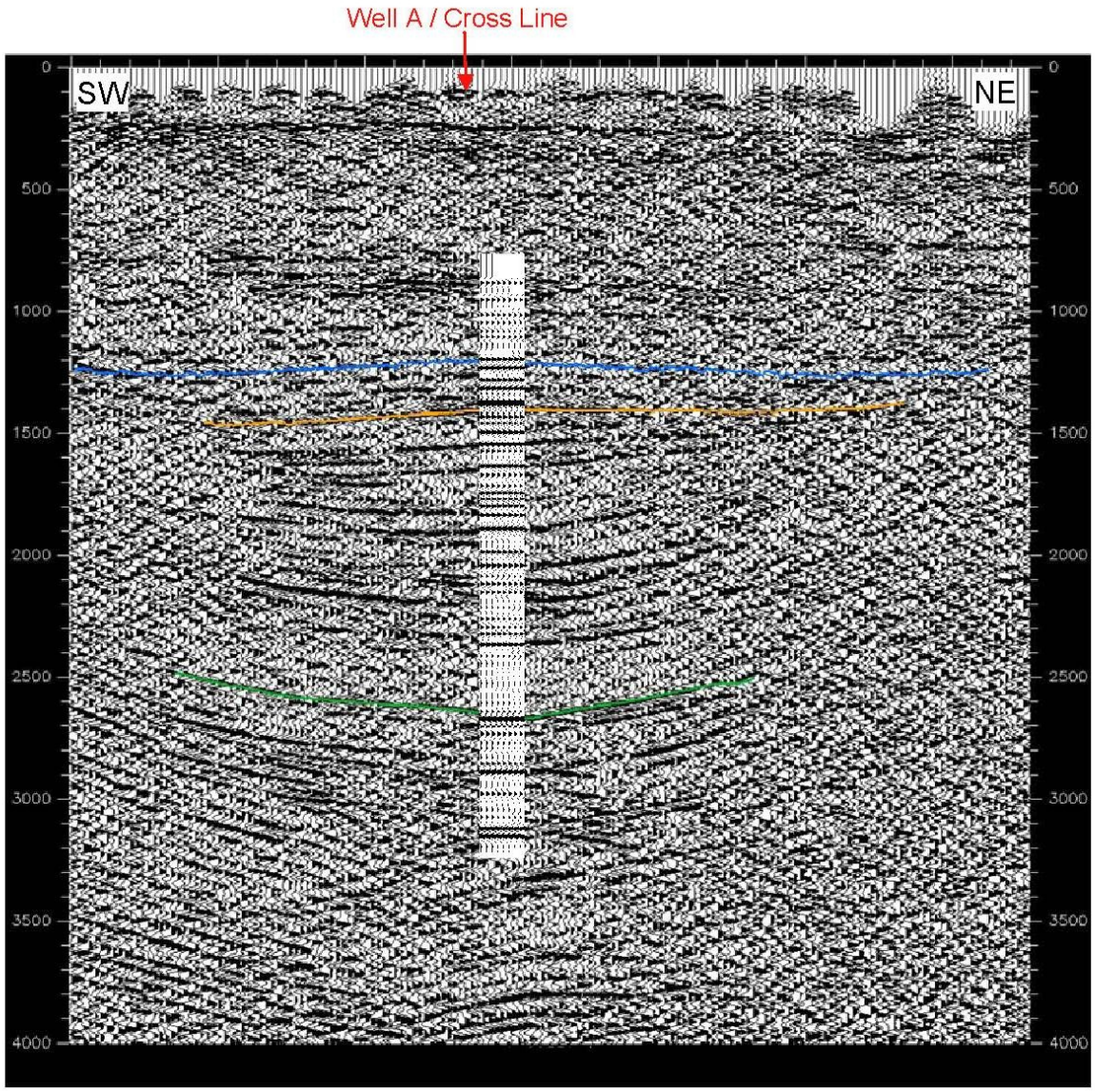

Figure 62 – Seismic cross section taken in the in line direction from the decimated shot and receiver volume. The synthetic seismogram from Well A is overlaid. The horizons are shown by the blue (1), orange (2), and green (3) lines.

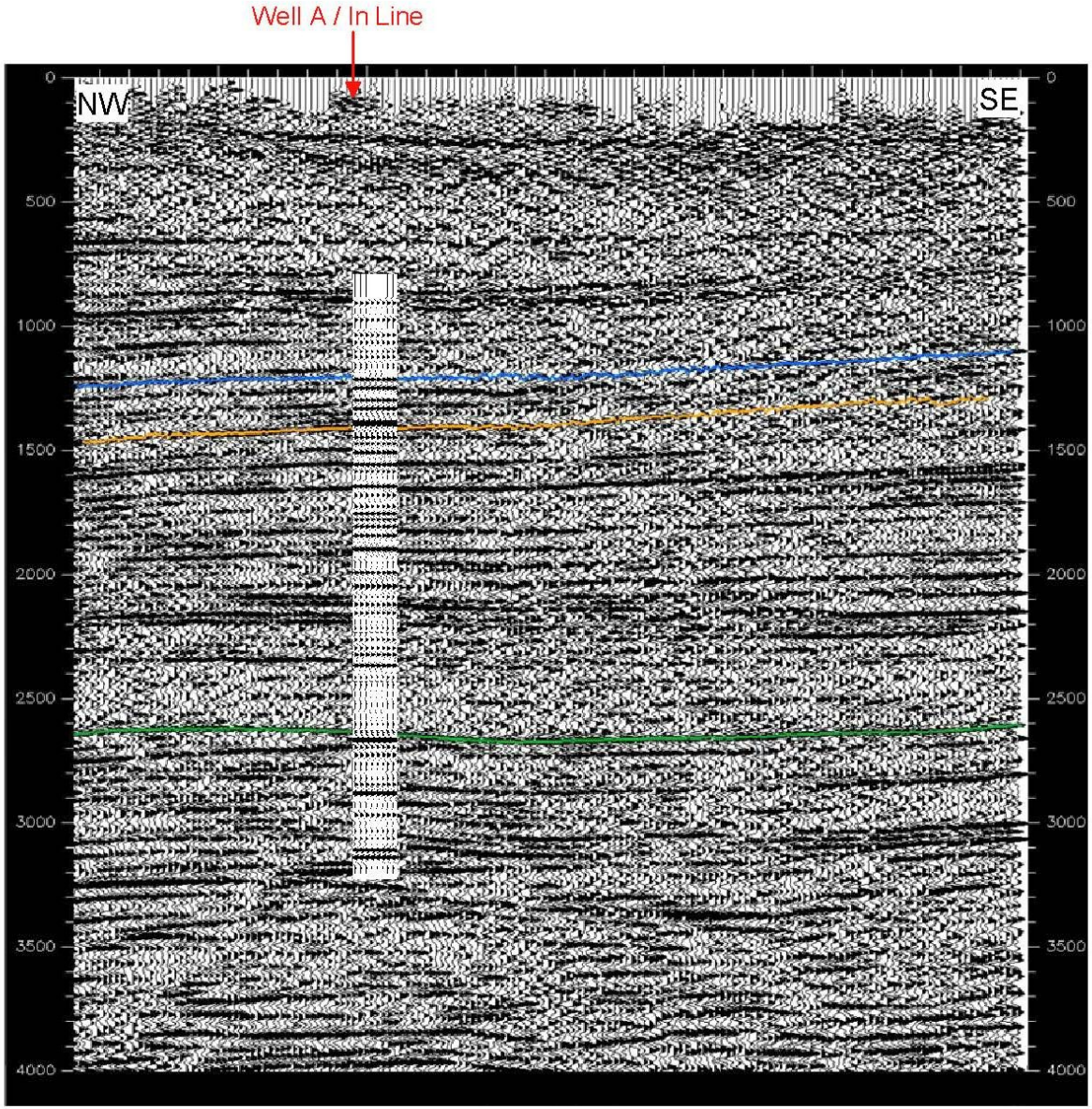

Figure 63 – Seismic cross section taken in the cross line direction from the reference volume. The synthetic seismogram from Well A is overlaid. The horizons are shown by the blue (1), orange (2), and green (3) lines.

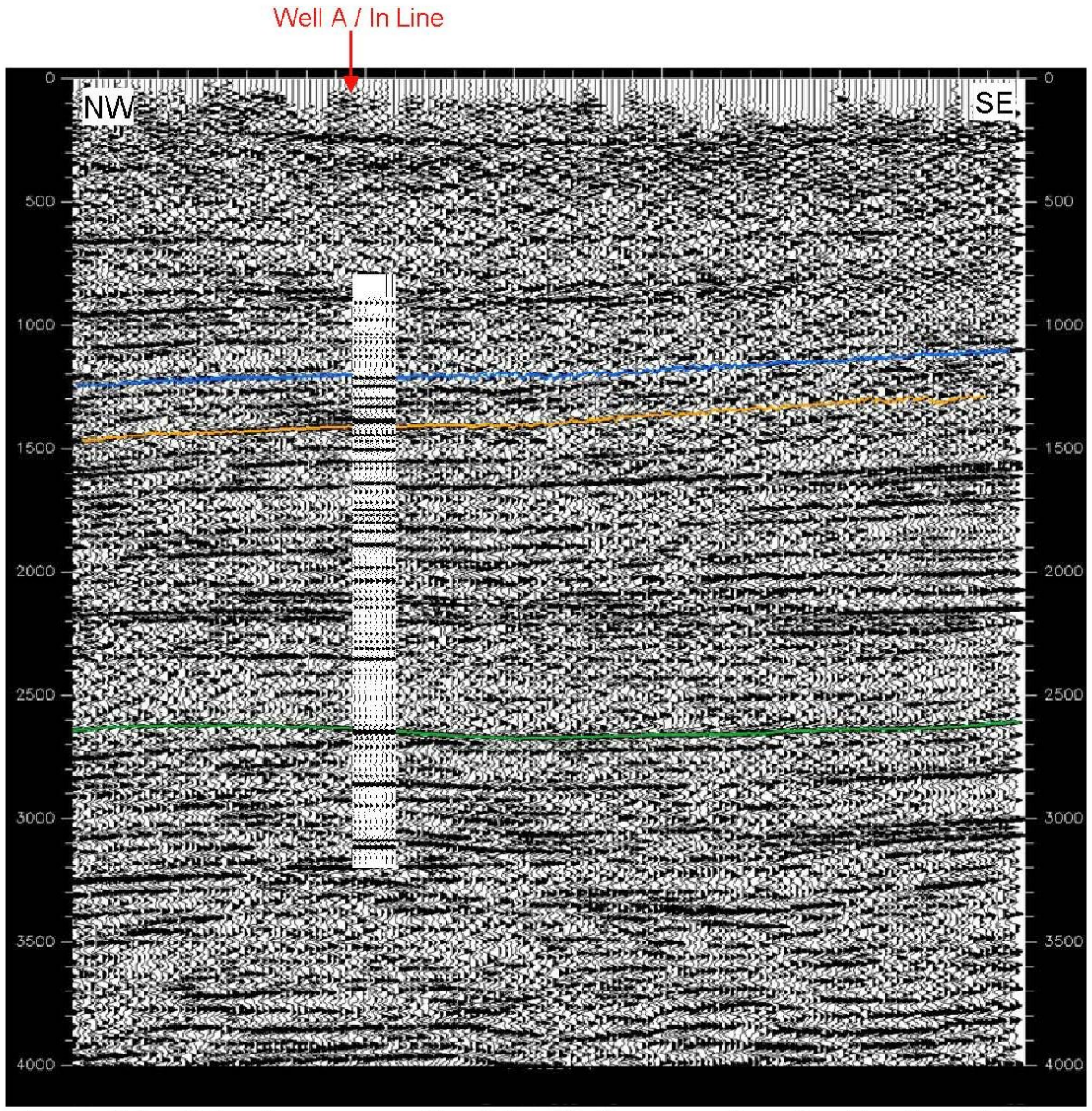

Figure 64 – Seismic cross section taken in the cross line direction from the decimated receiver volume. The synthetic seismogram from Well A is overlaid. The horizons are shown by the blue (1), orange (2), and green (3) lines.

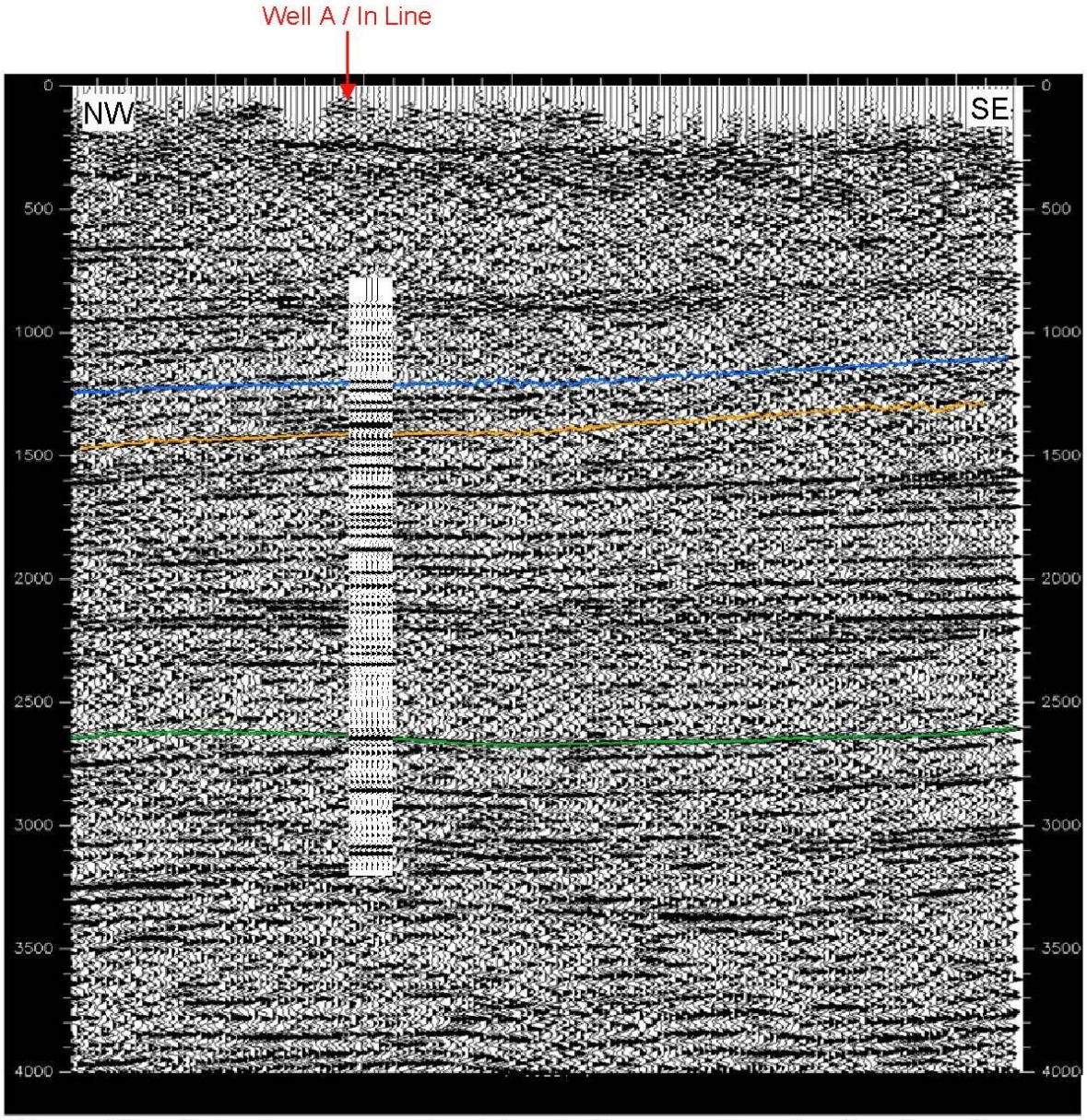

Figure 65 – Seismic cross section taken in the cross line direction from the decimated shot volume. The synthetic seismogram from Well A is overlaid. The horizons are shown by the blue (1), orange (2), and green (3) lines.

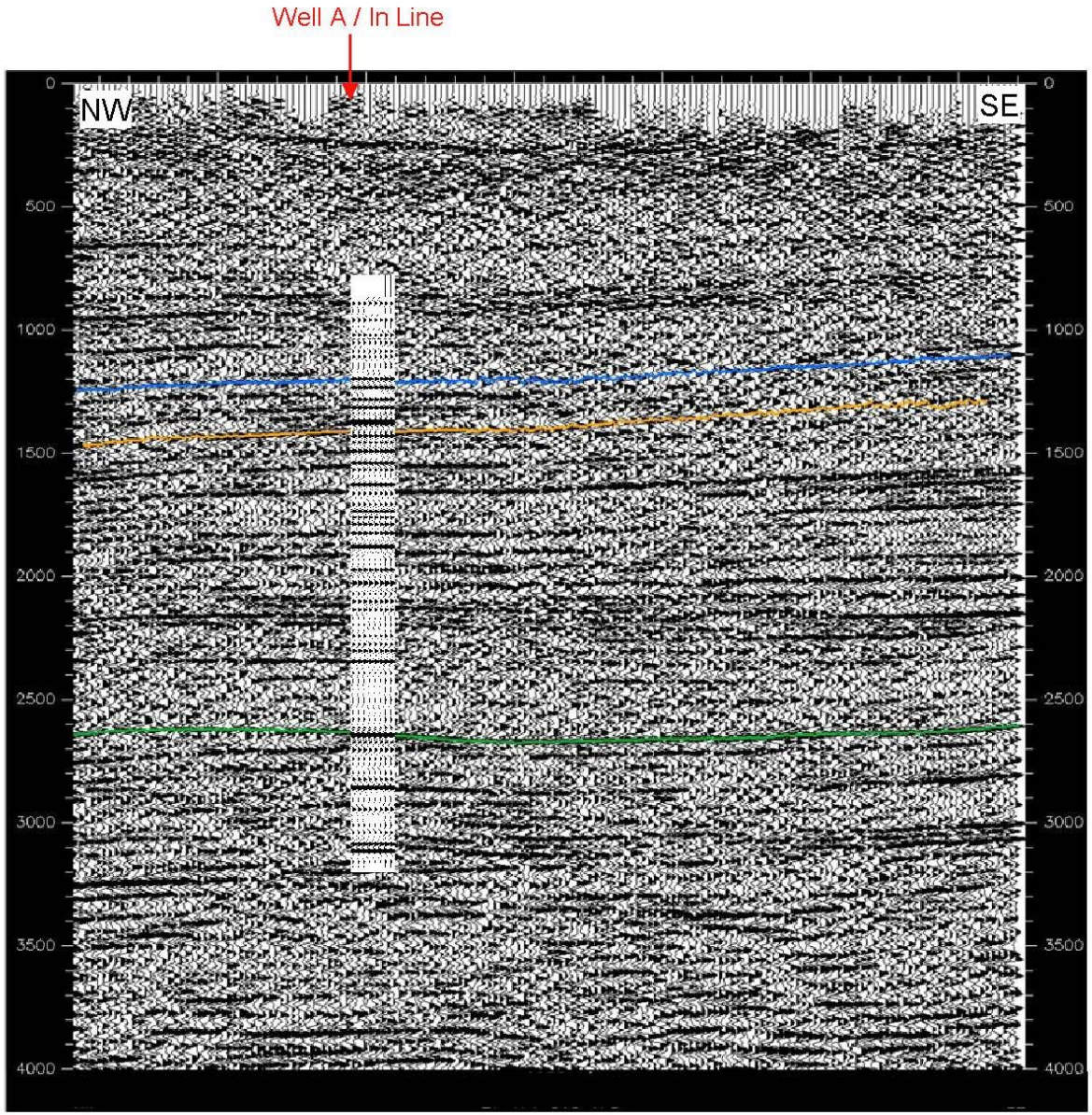

Figure 66 – Seismic cross section taken in the cross line direction from the decimated shot and receiver volume. The synthetic seismogram from Well A is overlaid. The horizons are shown by the blue (1), orange (2), and green (3) lines.

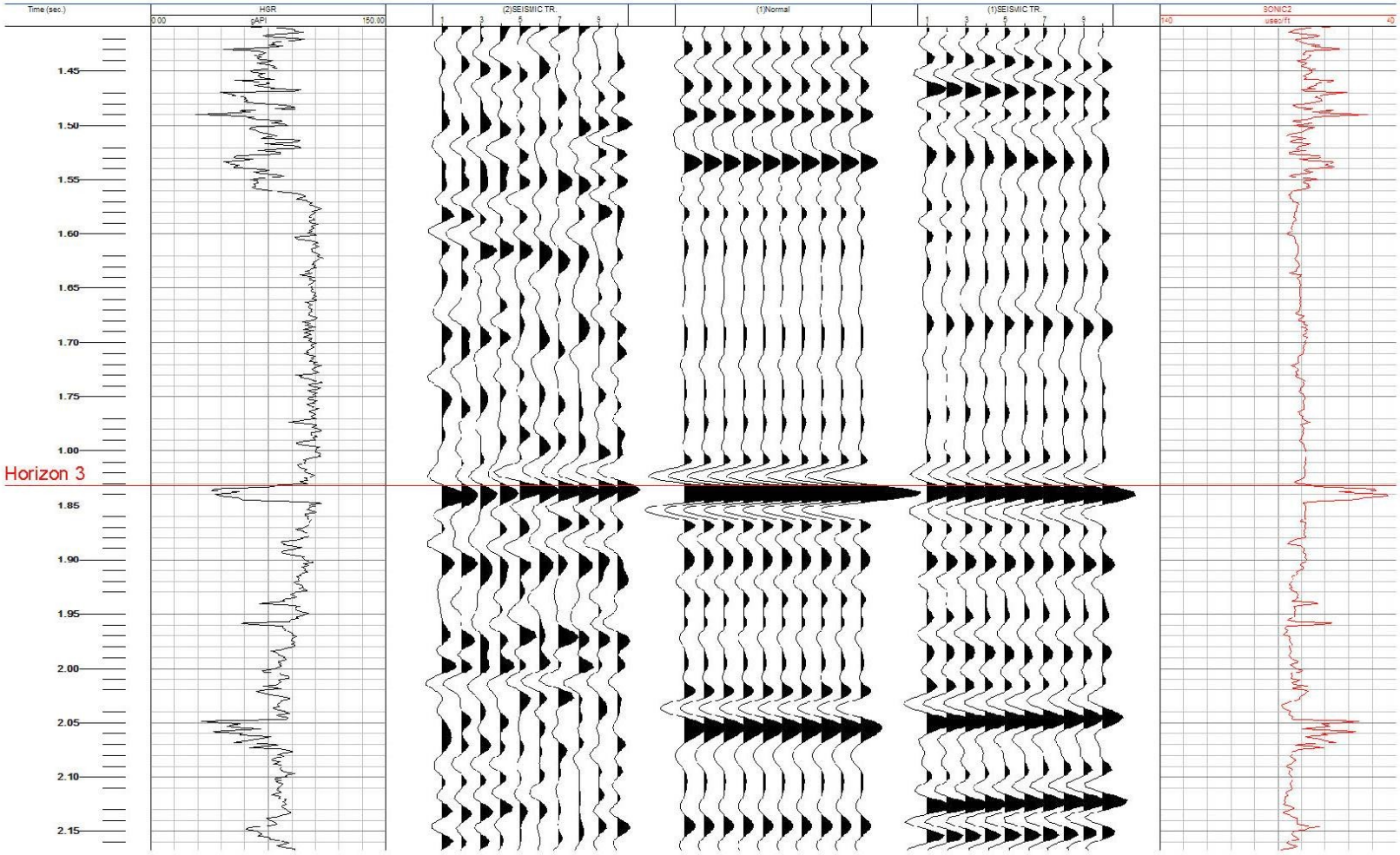

Figure 67 – The synthetic seismogram (Track 4, center trace) is compared to the reference volume traces before migration (Track 3, left trace) and after migration (Track 5, right trace). Horizon 3 is also denoted to give reference where the enlargement is from.

CHAPTER VI

CONCLUSIONS

Based on the results of this study several conclusions were reached that should only be applied to the mountain front area. Since acquisition design is reliant on the geology, it is not certain how these tests would have responded in a different geological setting.

1. Removing every other shot and/or receiver group while keeping bin size constant resulted in irregular fold distribution. This uneven distribution has the ability to create artifacts within the data.
2. Flex binning can be a viable option to distribute fold across the data, however it creates a smearing affect that can degrade certain areas of the data.
3. Residual statics were seen to play a vital role in the interpretation capability. The danger of using a correlation window in the muted section with a low signal to noise ratio was shown. With the incorrect solution, not only did the resolution suffer but false structures were created.
4. Though a different correlation window was used for the decimated shot from the other decimated volumes, the correct solution was obtained.

5. After the application of residual static corrections the decimated volumes matched the reference volume in temporal placement.
6. The semblance plots used in velocity analysis were shown to slightly change with decimation. The decimated shot volume and decimated receiver volume plots looked markedly similar. While the decimated shot and receiver volume appeared more distorted it still provided an accurate set of coherent zones to pick. The constant velocity stacks made up for any differences seen in the semblance plots and resulted in the same velocity model for all volumes.
7. Empirically the image was seen to be considerably degraded in areas while others were unaffected by decimation. Consistent degradation took place in the shallow sections where longer offsets had not contributed. Overall the decimated receiver performed the best. The next best volume was the decimated shot while the decimated shot and receiver performed the worst in comparison to the reference volume as expected.
8. Using several time slices to compare the data set again showed the decimated receiver volume to have better quality compared to the other decimated versions. Decimated shot volume followed close in image quality with the decimated shot and receiver volume showing the most degradation.
9. Difference volumes in the study confirmed that the decimated receiver volume maintained the closest similarity to the reference volume. The

decimated shot and receiver volume recorded the most difference in recorded signal compared to the reference volume.

10. Amplitude maps were shown to vary significantly with no preference in decimated volumes. None of the volumes consistently performed better than the other.
11. The synthetic tie proved to be difficult in unmigrated sections but overall seemed to favor the decimated receiver volume more than the decimated shot volume. The decimated shot and receiver volume was only able to tie on certain reflectors but it is believed that migration would increase all the volumes abilities to match the synthetic.

Future Investigations

Results concerning the final image in this study are taken with some degree of uncertainty due to the fact that migration has not been performed. Assumptions were made that the decimated volumes should record energy the same way as the reference volume. This may be true but severe difficulties were seen with attempting to tie even the reference version without migration. It is not clear whether the same amount of difference would exist between the reference and decimated volumes after migration.

This work could also be extended by changing the bin size to the natural spacing created by the station intervals. By allowing the bin size to retain its natural shape, the fold would have been maintained. Knowingly the lateral resolution would have decreased but the amount is unknown.

Finally if the tests were to be conducted in a different area it is recommended to avoid merged projects as its affect on the study is also unclear. It did however create an

artificial high fold band that would not be seen in normal acquisition. Since this area was essentially double the designed fold, decimation may have only reduced the fold to what was initially required. Thus, degradation observed was potentially not as drastic as what should have been seen.

REFERENCES

Asquith, G. and Krygowski, D., 2004, Basic Well Log Analysis 2nd Edition; American Association of Petroleum Geologists Methods in Exploration Series, No. 16.

Bouska, J., 1995, Cut to the quick: investigating the effects of reduced surface sampling in 3D data acquisition: Ann. Mtg. of the Can. Society of Exploration. Geophysicists., Expanded Abstracts, 181–182.

Bouska, J., T. Lyon, R. Johnston, D. Buddery, D. Howe, M. Mueller, L. Thomsen, D. Ebrom, 2004, Acquisition Design of the First Four Component 3D Ocean Bottom Seismic in the Caspian: 74th Annual International Meeting, SEG, Expanded Abstracts, 23, 49–52.

Bouska, J., Howie, J., Nolte, B., Johnston, R., Alexandra, R,. and Walters, R., 2005, Azeri 4C Time-Lapse Design Using 3D 4C OBS imaging Decimation Tests: Presented at SEG 2005 Annual Meeting.

Boyd, D. T. 2002b, Oklahoma Natural Gas: Past, Present, and Future: Oklahoma Geology Notes, v. 62, no. 4, p. 143–155.

Brown, A. R., 1991, Interpretation of Three-Dimensional Seismic Data, Third Edition: AAPG Memoir 42, American Association of Petroleum Geologists.

Cooper, N. M., 1995, 3D Seismic Acquisition Design and Quality Control: Presented by Mustagh Resources.

Cordsen, A., Galbraith, M., Peirce, J. , 2000, Planning Land 3-D Seismic Surveys; Geophysical Developments 9, Society of Exploration Geophysicists.

Energy Information Administration, 2003, U.S. and Global Petroleum Information: Accessed December 2004 at h*ttp://www.eia.doe.gov/pub/oil_gas/natural_gas/data_publications/ \crude_oil_natural_gas_reserves/current/pdf/ch3.pdf*

Evans, J.L., 1979, Major Structural and Stratigraphic Features of the Anadarko Basin, *in* Pennsylvanian Sandstones of the Mid-Continent: Tulsa Geological Society Special Publication 1, p. 97-113.

Google Earth. 2007. < http://earth.google.com/>

Ham , W. E., and Wilson, J. L., 1967, Paleozoic Epeirogeny and Orogeny in the Central United States: American Journal of Science, v. 265, p 332-407.

Krey, Th. C., 1987, Attenuation of Random Noise by 2-D and 3-D CDP Stacking and Kirchhoff Migration: Geophys. Prosp., 35, 135 –147.

Johnson, K. S., Amsden, T. W., Denison, R. E., Dutton, S. P., Goldstein, A. G., Rascoe, B., Jr., Sutherland, P. K., and Thompson, C. M., 1988, Southern Midcontinent region, *in* Sloss, L. L. (ed), Sedimentary cover—North American Craton, U.S.: Geological Society of America, The Geology of North America, v. D-2, p. 307-359. {Re-printed in 1989 as Oklahoma geological Survey Special Publication 89-2.}

Johnson, K. S. and Cardott, B. J., 1992, Geologic Framework and Hydrocarbon Source Rocks of Oklahoma: Oklahoma Geological Survey Circular v. 93, p. 21-37.

Johnson, K. S., Northcutt, R. A., Hinshaw, G. C., Hines, K. E., 2001, Geology and Petroleum Reservoirs in Pennsylvanian and Permian Rocks of Oklahoma: Oklahoma Geological Survey Circular 104. p. 1-19.

Lansley, R. M. 2004, CMP Fold: A Meaningless Number?, The Leading Edge v. 23 p. 1038-1041.

Lu, L., Chen, J. J., Bell, L., and Lara, R., 1996, 3D Flex Binning and DMO: Society of Exploration Geophysicists, Expanded Abstracts 15.

Lyon, T., J. Bouska, R. Johnston, M. Mueller, L. Thomsen, 2004, Reducing Structural Uncertainty on the Azeri Field Using Ocean Bottom Seismic: Offshore Azerbaijan: 74th Annual International Meeting, SEG, Expanded Abstracts, 468–471.

Nolte, B., R. Clarke, R. Read, 2004, Decimation Tests Using Vahall Ocean-Bottom-Cable data: 74th Annual International Meeting, SEG, Expanded Abstracts, 45–48.

Marsden, D., 1993, Static Corrections-A Review, Part I, The Leading Edge v. 12, p. 43-49.

Marsden, D., 1993, Static Corrections-A Review, Part II, The Leading Edge v. 12, p. 115-120.

Marsden, D., 1993, Static Corrections-A Review, Part III, The Leading Edge v. 12, p. 210-216.

Nolte, B., Brandsberg-Dahl, S., Clarke, R., and Read, R., 2004. Decimation Tests Using Valhall Ocean-Bottom-Cable Data: Presented at SEG International Exposition and 74th Annual Meeting.

Rider, M., 2002, The Geological Interpretation of Well Logs 2nd ed. Rider-French Consulting Ltd.

Sheriff, R. E., 1991, Encyclopedic Dictionary of Exploration Geophysics, 3rd ed.: Soc. Exploration. Geophysicists.

Spitzer, R., Nitsche, F. O., Green, A. G., and Horstmeyer, H., 1998, High-resolution 3D Seismic Survey Applying Effective Acquisition and New Processing Strategies: Society of Exploration of Geophysicists, Expanded Abstracts 20.

Wombell, R., Mason, M., Wallbank, T., Jack, I., Allen, T., Watts, G., 1999, Sparse 3D Land and Transition Zone Acquisition: Decimation and Interpolation Trails: European Association of Geoscientists & Engineers.

Yilmaz, O., 2001, Seismic Data Analysis: Society of Exploration Geophysicists.

PLATE 1 - IN LINE SEISMIC SECTION

Horizon 1
Horizon 2
Horizon 3

(A) Reference Volume
(B) Decimated Receiver Volume
(C) Decimated Shot Volume
(D) Decimated Shot and Receiver Volume

(A)

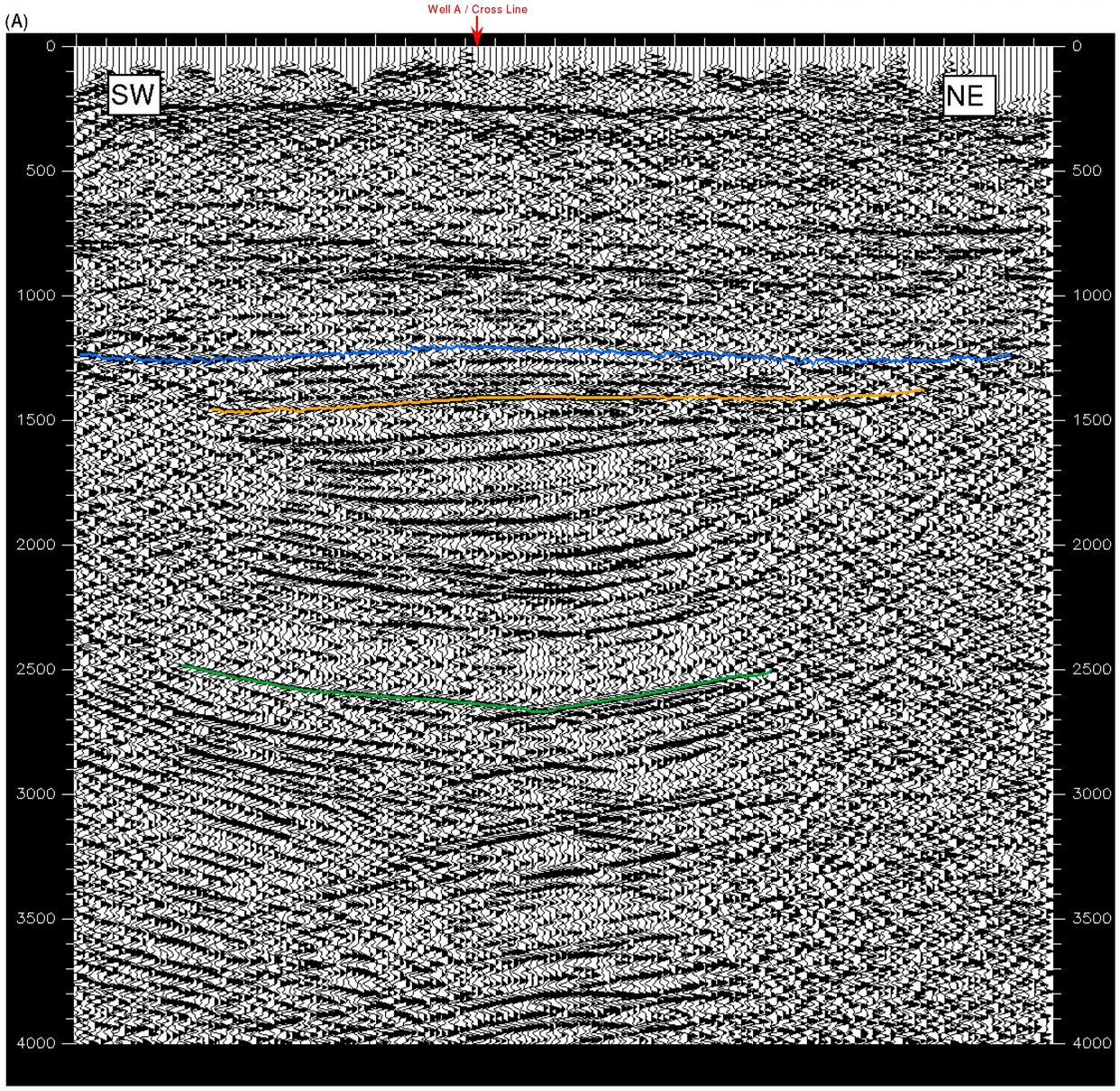

(B)

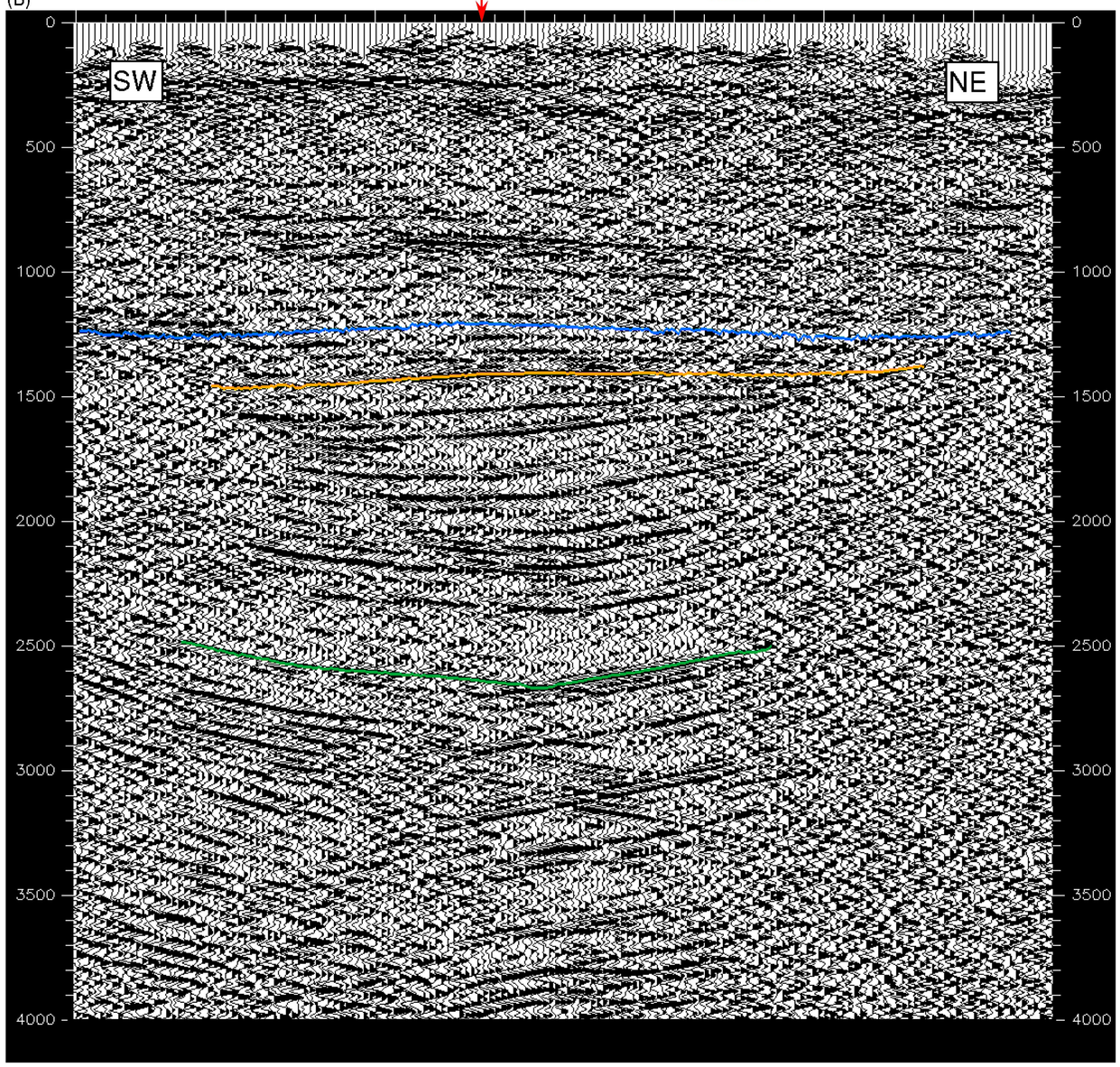

(C)

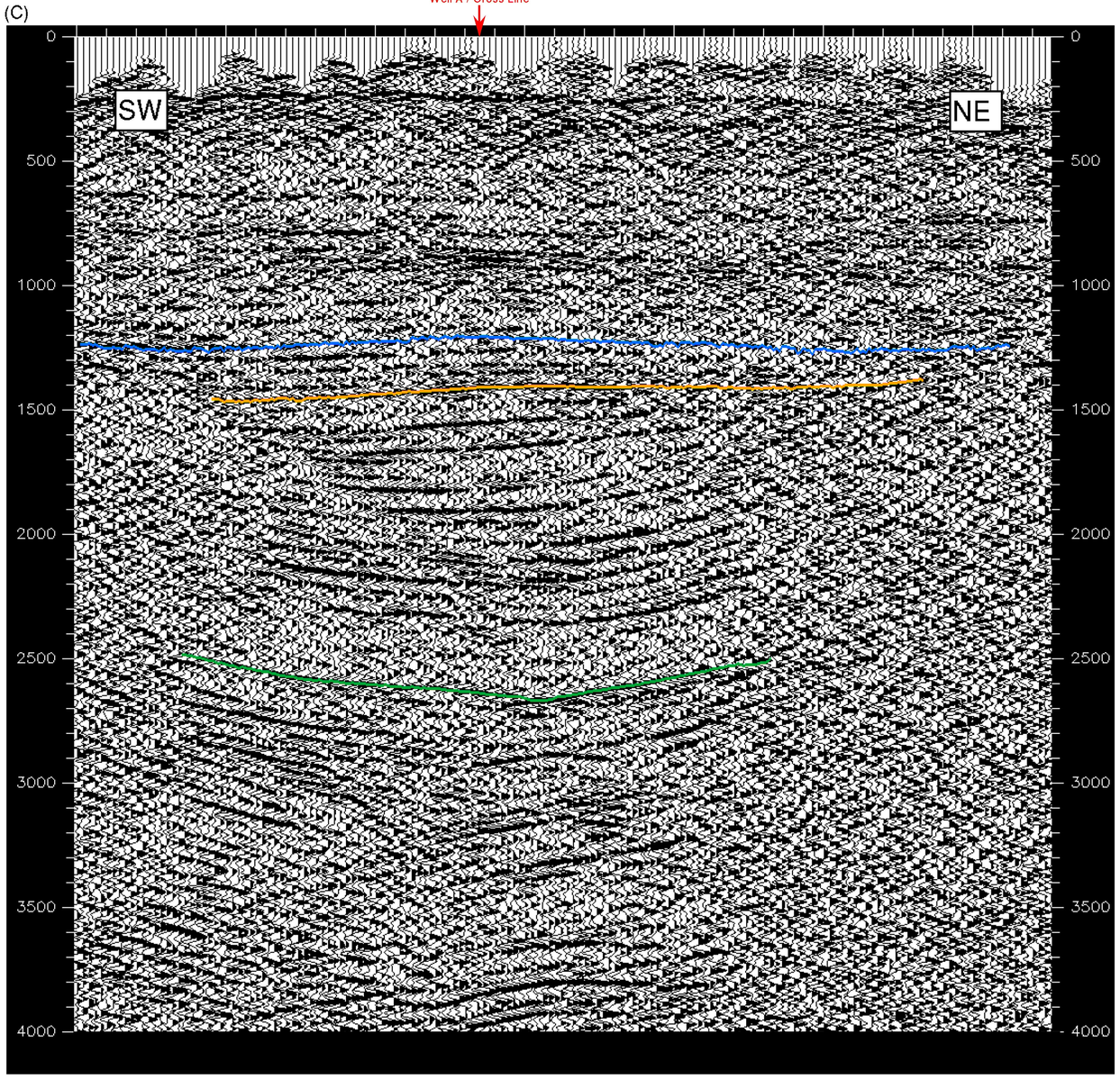

(D)

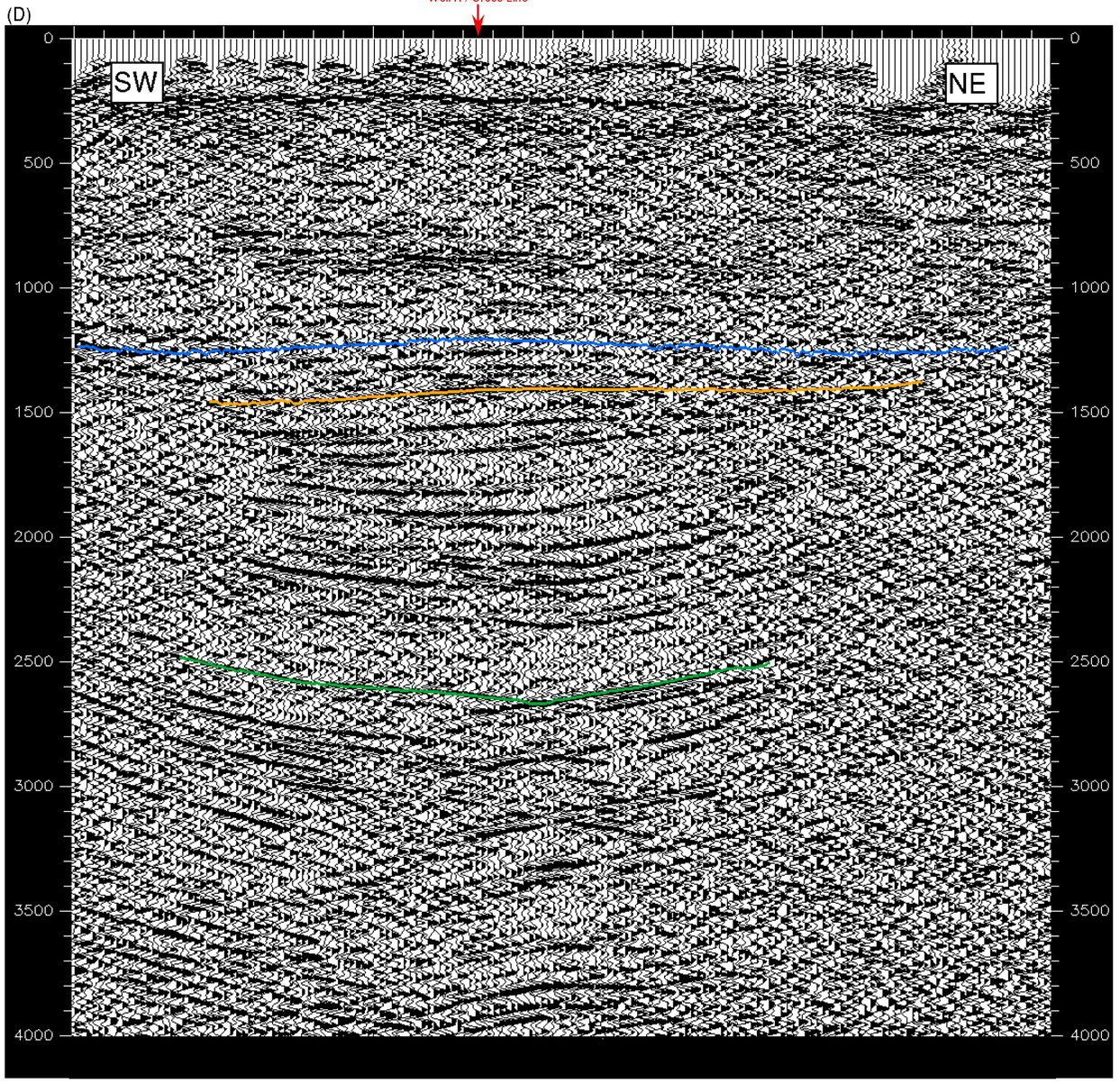

PLATE 2 - CROSS LINE SEISMIC SECTION

Horizon 1
Horizon 2
Horizon 3

(A) Reference Volume
(B) Decimated Receiver Volume
(C) Decimated Shot Volume
(D) Decimated Shot and Receiver Volum

(A)

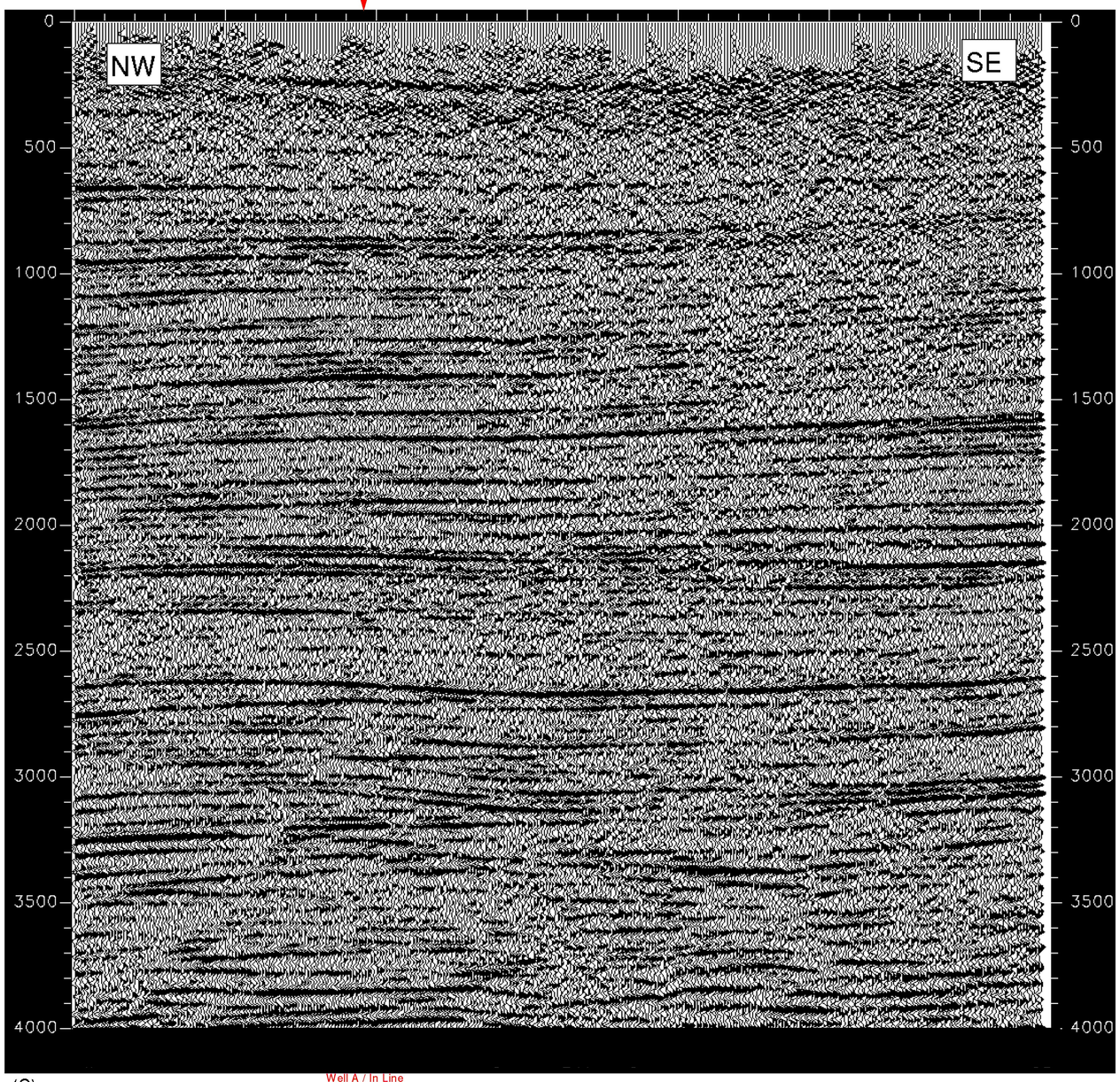

(B)

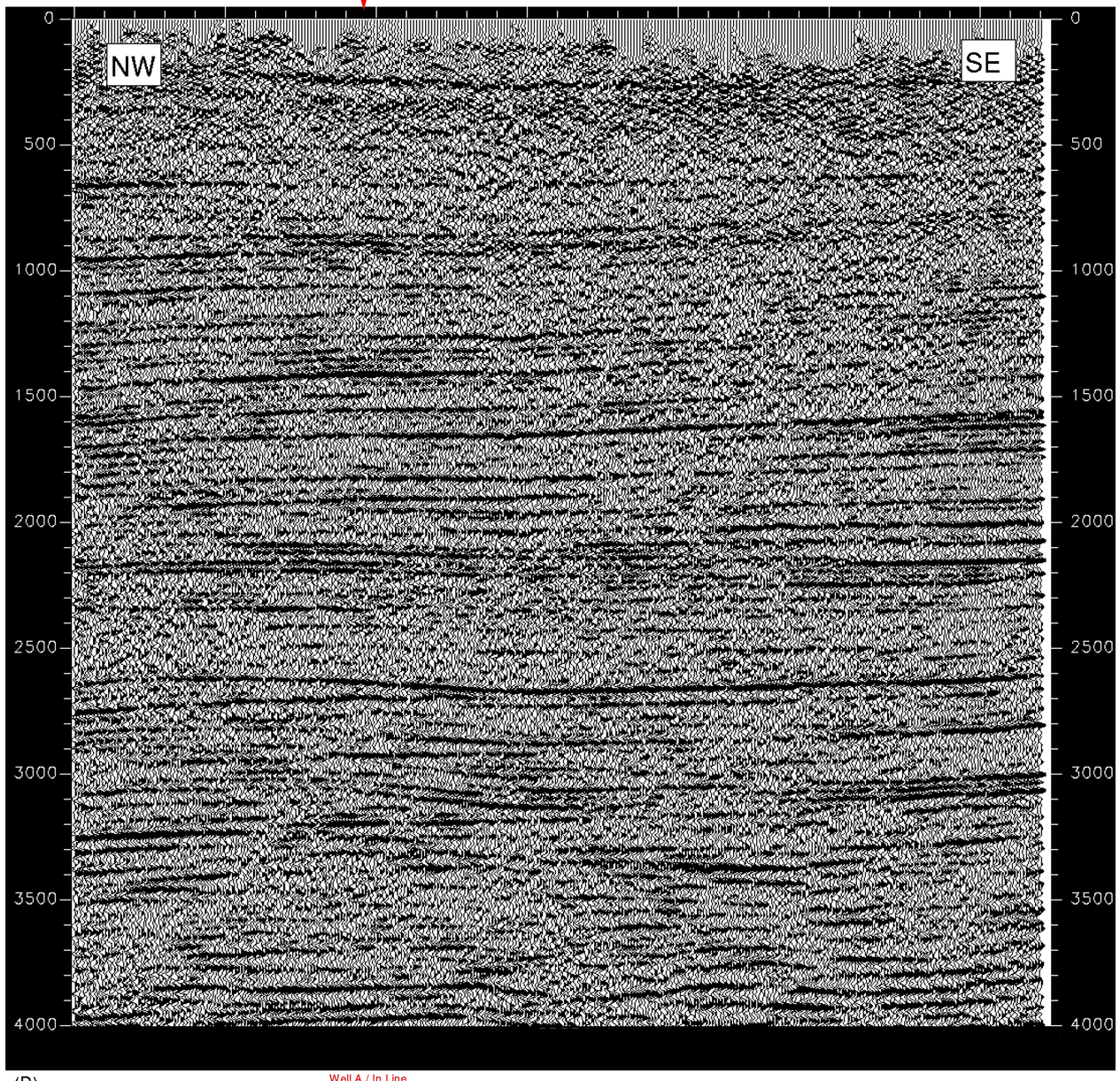

(C)

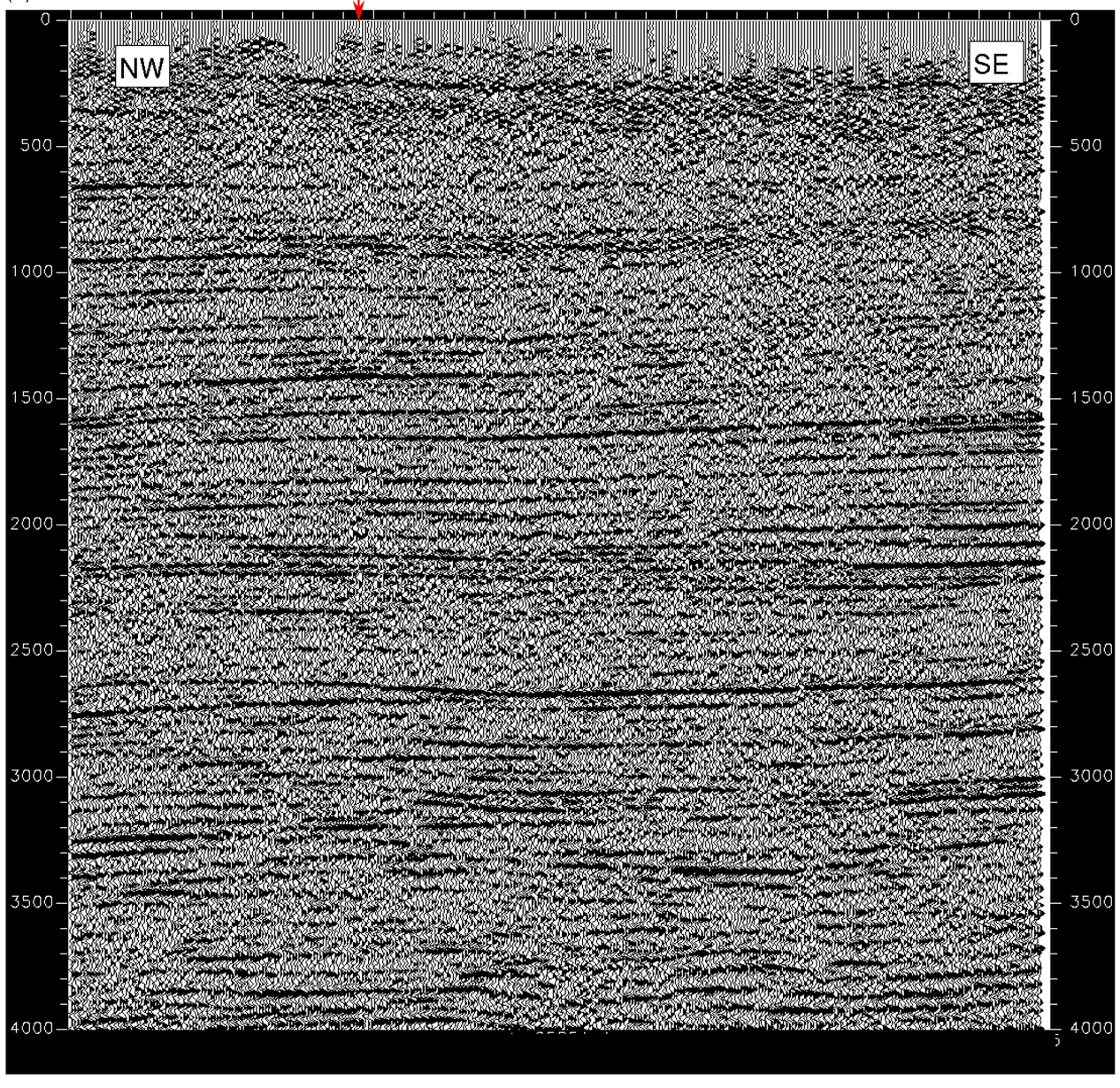

(D)

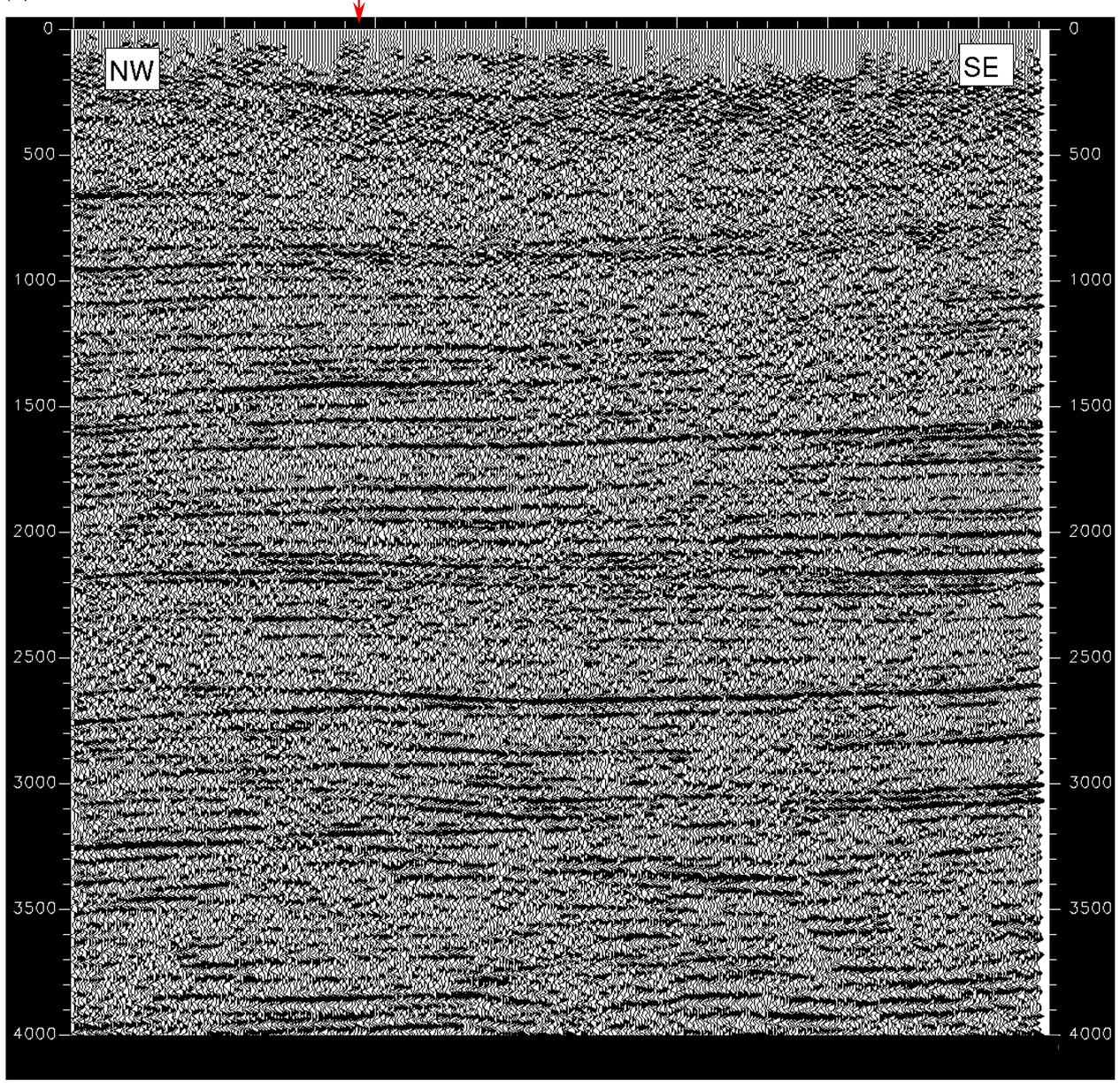

VITA

Eric Matthew Gerding

Candidate for the Degree of

Master of Science

Thesis: DECIMATION TESTING OF HIGH DENSITY SEISMIC DATA FOR THE WICHITA MOUNTAIN FRONT AREA

Major Field: Geology

Biographical:

Education: Graduated from McNicholas High School, Cincinnati, Ohio in June 1999. Graduated from Wright State University, Dayton, Ohio with a Bachelors of Science degree in Geology in March 2004. Completed requirements for the Master of Science degree with a major in Geology at Oklahoma State University in May, 2007.

Experience at Oklahoma State University:
Geology Teaching Assistant 2005-2007
Geology Technical Lab Assistant 2006-2007
Oklahoma State University Geology Students (OSUGS)

Work Experience:
Devon Energy Corp., Intern
Mid-Continent Central Division May 2006 - March 2007

Devon Energy Corp., Geophysicist
Mid-Continent Central Division April 2007 - Present

Professional Memberships:
Society of Exploration Geophysicists (SEG)
Association of American Petroleum Geologists (AAPG)

Name: Eric M. Gerding Date of Degree: May, 2007

Institution: Oklahoma State University Location: Stillwater, Oklahoma

Title of Study: DECIMATION TESTING OF HIGH DENSITY SEISMIC DATA FOR THE WICHITA MOUNTAIN FRONT AREA

Pages in Study: 121 Candidate for the Degree of Master of Science

Major Field: Geology

Scope and Method of Study: Several decimation tests were conducted on an originally high trace density survey. This was conducted to assess the capability of lowering collection costs by reducing the field effort. Decimation volumes were created for one-half source, one-half receiver, and one-half source and receiver. Each volume was subjected to a series of tests to show the amount of degradation of the data. Comparisons were made in the processing stage as well as the final image.

Findings and Conclusions: All findings in this study are cautioned to be location specific, meaning that results may not hold true in other locations. While maintaining the bin size the reduction of traces in a systematic pattern resulted in an irregular distribution of fold. Flex binning was found to be necessary to improve resolution and eliminate potential false structures. In the area of processing, which included velocity analysis and residual statics, decimation performed very well. However residual statics for the decimated receiver and decimated shot and receiver required a slightly different correlation window to arrive at the correct solution. Empirical comparisons of seismic cross sections and time slices showed that the clarity of certain reflectors was considerably compromised in all decimated volumes. Difference volumes provided a better look at the amount of signal that was sacrificed through decimation. The decimated receiver appeared to be the most similar to the reference volume while the decimate shot and receiver showed the most contrast. Comparison of the amplitude maps had varying results. None of the decimated volumes repeatedly reproduced the reference amplitude maps. The final comparison of the synthetic tie to each volume seemed to favor the decimated receiver more than the other decimated volumes. Nearly all volumes tied on several of the distinct reflectors but struggled with others. This test would have been better served on a set of migrated volumes that were unavailable. Overall the decimated receiver seemed to come the closest to replicating the reference volume in every tests, but even signs of degradation were still evident.

ADVISER'S APPROVAL: Dr. Surinder Sahai